Geoscience Laser Altimeter System (GLAS)

Algorithm Theoretical Basis Document
Version 3.0

GLAS ATMOSPHERIC DATA PRODUCTS

Prepared by:

Steve Palm[1], William Hart, Dennis Hlavka
Science Systems and Applications, Inc.
Lanham, MD

James Spinhirne
NASA Goddard Space Flight Center
Greenbelt, MD

July 1999

Corresponding Address: Code 912, Goddard Space Flight Center, Greenbelt, MD 20771
Email: spp@virl.gsfc.nasa.gov

Table of Contents

1 Introduction

Scheduled for launch in mid 2001, the Geoscience Laser Altimeter System (GLAS) is an atmospheric lidar in addition to a surface altimeter. GLAS will provide high resolution measurements of global topography with special emphasis on the determination of the temporal changes of ice sheet mass over Antarctica and Greenland. These measurements, obtained continuously for a period of 10 to 15 years, will enable scientists to determine whether the ice sheets are growing or shrinking which has implications for climate change. The atmospheric objectives of GLAS are the global laser profiling of atmospheric aerosols and clouds. Knowledge of the height, coverage and thickness of cloud layers is essential in modeling the radiative fluxes at the surface and within the atmosphere. Clouds frequently occur in multi-layer systems on many spatial scales. Satellite based radiometers and imagers do an excellent job of viewing the cloud tops, but are limited in their ability to distinguish multi-level cloud formations and determine the true vertical distribution of clouds. Passive remote sensors also tend to underestimate the fraction of optically thin clouds, while overestimating the percent of broken, optically thick clouds. Recent sensitivity studies using calculations based on ISCCP (International Satellite Cloud Climatology Project) data indicate that the largest uncertainty in long wave radiative flux at the surface is caused by the lack of knowledge of the amount of cloud overlap or multi-layering (Wielicki et al. 1996).

Anthropogenic aerosol is also known to have important implications for the earth's radiative balance. Both direct (scattering and absorption of sunlight) and indirect (changing of cloud radiative properties) forcing by mainly sulfate aerosols has recently been shown to cause net regional cooling (IPCC, 1994). With current passive sensors, our ability to map the amount and extent of global aerosol is limited. Passive sensing provides essentially no information on vertical distribution an there are formidable analysis problems, especially over land. GLAS will significantly enhance our ability to measure atmospheric aerosol, both natural and anthropogenic. This has implications for improving climate models by providing better knowledge of the anthropogenic direct aerosol forcing, which at this point can only be estimated from sulfate source models.

The primary atmospheric science goal of the GLAS cloud and aerosol measurement is to determine the radiative forcing and vertically resolved atmospheric heating rate due to cloud and aerosol by directly observing the vertical structure and magnitude of cloud and aerosol parameters that are important for the radiative balance of the earth-atmosphere system, but which are ambiguous or impossible to obtain from existing or planned passive remote sensors. A further goal is to directly measure the height of atmospheric transition layers (inversions) which are important for dynamics and mixing, the planetary boundary layer and lifting condensation level. Towards these goals, the various level 2 data products which will be generated on the GLAS ground processing system are:

1. GLA07 - Profiles of calibrated cloud and aerosol attenuated backscatter cross section
2. GLA08 - Planetary Boundary Layer (PBL) height
3. GLA08 - Elevated tropospheric aerosol layer height
4. GLA09 - Cloud top (and bottom when possible) heights

5. GLA10 – Attenuation-corrected backscatter cross section for clouds and aerosol layers
6. GLA10 - Cloud and aerosol extinction cross sections
7. GLA11 - Thin cloud and aerosol layer optical depth

The intent of this document is limited to a description of the theoretical basis and the approach that is to be pursued in developing processing algorithms for the GLAS level 1 and 2 atmospheric data products. The actual development of the algorithms will involve modeling and testing over the next two years. We anticipate subsequent revision(s) of the GLAS atmospheric products ATBD as we collectively continue to code these algorithms and exercise them on various simulated GLAS data sets. The level 1 and 2 products described are those that will be produced by real time processing of data. The basis for the initial approach is described. More sophisticated approaches and improvements from post processing are to be developed. To date almost all resources that have been available for the development of algorithms for atmospheric products have gone into the development of comprehensive, bit level, simulation of GLAS data as a tool for instrument design studies (Spinhirne and Palm, 1997) and calculations of multiple scattering effects on surface ranging (Duda et al. , 1999a and b). The level 1 and 2 data products only involve data input from the GLAS instrument and other ancillary information that is available in real time, such as atmospheric temperature profiles. Level 3 products and improvement of level 2 products from post processing will involve measurements and retrievals from other satellites and models. The further research for these will be described in section IX.

To begin, we will first review some of the prior lidar work which is pertinent to the GLAS data products discussed here, before presenting the details of the individual algorithms in section 3. Section 4 discusses the practical applications and implementation issues of each algorithm including examples of output. Section 5 briefly addresses multiple scattering induced ranging error and section 6 lists a number of possible browse products which can be used to monitor the algorithm output. Section 7 discusses the algorithm development plan with section 8 providing details on the pre and post launch validation plan. Finally, section 9 touches on ideas for future research.

2 Overview and Background

2.1 History

The purpose of this document is to develop and present a detailed description of the algorithm theoretical basis for each of the GLAS data products. Most of the expertise for this endeavor is the result of many years work with aircraft and ground-based lidar systems. Each of the authors have had many years experience designing and coding algorithms for the retrieval of atmospheric parameters from lidar data. The Cloud and Aerosol Lidar System (CALS), which flies on the NASA ER-2 high altitude aircraft, has been employed in many field experiments around the world and algorithms have been developed to analyze these data for a number of atmospheric parameters. CALS data have been analyzed for cloud top height, thin cloud optical depth, cirrus cloud emittance (Spinhirne and Hart, 1990) and boundary layer depth (Palm and Spinhirne, 1987, 1998). Work by others also demonstrate the utility of lidar for deriving cloud optical properties, especially when combined with passive, multispectral radiometric observations (Platt et al, 1980; Spinhirne

and Hart, 1990). We believe the methods developed to analyze CALS data can be adapted for use with GLAS data and will produce the best atmospheric data products possible.

2.2 Description of GLAS Atmospheric Channel Data

The atmospheric channel of GLAS will provide a record of the vertical structure of backscatter intensity from the ground to a height of about 40 km with 76.8 meter vertical resolution. Two channels will be employed, the Nd:Yag fundamental wavelength of 1064 nm and the frequency doubled 532 nm wavelength in the visible portion of the spectrum (green channel). The green channel will be the primary atmospheric signal, using a photon counting detector and will be for the detection of thin cirrus, elevated aerosol and haze layers and the planetary boundary layer. When the densest clouds are encountered, the 532 channel will saturate but will still provide an accurate measure of the height of the cloud tops. In this instance, the IR channel can then be used directly or as a way of estimating what the data from the green channel would have been had it not saturated.
The basic equation which describes the atmospheric return signal p(z) is the standard lidar equation

$$(2.1) \qquad p(z) = \frac{CE\beta(z)T^2(z)}{r^2} + p_b + p_d$$

where $\beta(z)$ is the total atmospheric backscatter cross section at an altitude z, T(z) is the transmission from the top of the atmosphere to altitude z, r is the range from the spacecraft to the altitude z, E is the transmitted laser pulse energy and C is a dimensional constant referred to as the calibration constant. There are two range independent background terms, p_b from scattered solar radiation and p_d for any detector dark signal. In the case where p would be the signal in watts returned to the receiver detector, the calibration constant is given as

$$(2.2) \qquad C=cAT_s/2$$

where c is the light speed constant , A the area of the receiver and T_s the optical transmission of the receiver system.
For the GLAS 532 nm atmospheric channel the signal will be acquired as the photo-electron count rate from the detector n(z). In this case the calibration constant will be given as

$$(2.3) \qquad C=AT_s\lambda q/2h$$

where λ is the wavelength, q is the photon detection probability or quantum efficiency, and h is the Plank constant. The background radiance signal in terms of photo-electron count rate will be

$$(2.4) \qquad n_b=AT_sI_b\Omega\Delta/hc$$

where I_b is the background radiance and Ω is the receiver solid angle and Δ is the optical bandwidth. The additional background signal will be any detector dark photo-electron count rate n_d.

The 1064 um detector for GLAS is the same silicon APD detector that will be used for the surface return signal although a separate lower speed A/D signal acquisition will be used. The signal in this case is a voltage from the detector amplifier V(z). The calibration constant will be

(2.5) $C=AT_s crg_v/2$

where r is the detector responsivity in amps/watt, and g_v is the voltage gain of the detector preamplifier. The detector background signal will be $i_d g_v$ where i_d is the detector dark current.
The accuracy of the received GLAS atmospheric signals will be limited by the fundamental probability, or signal shot noise of the signal. For the case of the 532 nm photon counting signal, the noise factor is given by Poisson statistic. The signal to noise ratio will then be given by

(2.6) $$S/N = \frac{n(z)}{\sqrt{n(z) + n_b + n_d}}$$

Where n(z) is the number of photons detected by the lidar at range z. In the case where the signal is voltage derived from a detected current the basic signal to noise will be:

(2.7) $$S/N = \frac{i_s}{\sqrt{2\Delta f(i_s + i_b + i_d)e}}$$

where i_s is the detector current produced by the backscattered signal, i_b is the detector current produced by background ambient light i_d is the detector dark current, Δf is the system electronic bandwidth, and e is electron charge. The signal noise defines the degree to which the lidar data may be usefully applied.

2.3 Instrument Description

The GLAS atmospheric measurements will be obtained from the 590 km polar orbiting platform both day and night using two separate channels. The 532 nm, photon counting channel will be the most sensitive and will provide the highest quality data obtaining both aerosol and cloud returns. This channel will employ an etalon filter which will be actively tuned to the laser frequency, providing a very tight bandpass filter of about 30 picometers. This, together with a very narrow (150 μr) receiver field of view (FOV), will enable high quality daytime measurements even over bright background scenes. There are 8 separate photon counting detectors for this channel which will significantly increase the available dynamic range while providing some degree of redundancy in the case of detector failure. The 1064 nm channel will use an Avalanche Photo Diode (APD) detector with a much wider (0.1 nm) bandpass filter and FOV (475 μr). The sensitivity of the 1064 channel will be limited by the inherent detector noise. It will, however, provide sufficient signal to noise to profile optically thick clouds and will be used to supplement the 532 channel when and if it becomes saturated. The 1064 data will not be used to retrieve atmospheric parameters since the signal to noise ratio of the 532 channel will be much better. The only exception to this would be in the case of problems or complete failure of the 532 channel, at which point the 1064 channel data

would be used for cloud height retrieval. Table I lists the major GLAS system parameters which ultimately affect system performance and data quality.

GLAS will carry three identical and redundant 40 Hz, solid state Nd:YAG lasers onboard, each with an expected lifetime of about 2.5 billion shots, or approximately 2 years of continuous operation. If a laser malfunctions, or simply comes to the end of its normal lifetime, switching to one of the other lasers is straightforward. The laser will transmit short (5 nanosecond) pulses of laser light (in the nadir direction) that will produce a footprint 70 meters wide upon striking the surface, and each footprint will be about 175 meters apart. The backscattered light from atmospheric clouds, aerosols and molecules will be digitized at 1.953 MHz, yielding a vertical resolution of 76.8 meters. The horizontal resolution will be a function of height. For the lowest 10 km, each backscattered laser pulse will be stored. Between 10 and 20 km, 8 shots will be summed, producing a horizontal resolution of 5Hz or 1.4 kilometers. For the upper half of the profile (20-40 km), which is entirely within the stratosphere, 40 shots will be summed, providing a horizontal resolution of about 7.5 kilometers. This approach was adopted for a number of reasons. First, the atmospheric processes of interest have more variability and smaller scales in the lower troposphere (particularly the boundary layer) than in the mid and upper troposphere. Second, the amount of molecular and aerosol scattering in the upper troposphere and stratosphere is so small that summing multiple shots is required to obtain a non zero result. Lastly, this approach will help to reduce the amount of data that has to be stored on board the spacecraft and transmitted to the ground.

Table I. GLAS System Parameters

Parameter	532 Channel	1064 Channel
Orbit Altitude	590 km	590 km
Laser Energy	36 mJ	73 mJ
Laser Divergence	110 μ rad	110 μ rad
Laser Repetition Rate	40 Hz	40 Hz
Effective Telescope Diameter	98 cm	98 cm
Receiver Field of View	150 μ rad	475 μ rad
Detector Quantum Efficiency	60 %	35 %
Detector Dark Current	3.0×10^{-16} A	50.0×10^{-12} A
RMS Detector Noise	0.0	2.0×10^{-11}
Electrical Bandwidth	1.953×10^{6}	1.953×10^{6}
Optical Filter Bandwidth	0.030 nm	0.100 nm
Total Optical Transmission	30 %	30 %

3 GLAS Atmospheric Algorithms

This section will address in detail the structure and content of the six algorithms which comprise the level 1A, 1B and level 2 GLAS atmospheric data products. A theoretical description will be given for each algorithm followed by error quantification and a description of the confidence (quality) flags which attempt to assign a confidence level to the quality of the algorithm output. Section 4 will discuss the issues related to the practical application and implementation of the algorithms.

3.1 Normalized Lidar Signal (GLA02)

3.1.1 *Theoretical Description*

The normalized lidar signal is a level 1A data product which applies the fundamental corrections and normalizations to the raw data as well as providing an estimate of the height of the first cloud top and/or the bin location of the ground return. Additionally, it will flag each 532 nm channel bin which has reached saturation so that it may be corrected in later processing. The algorithm applies range and laser energy normalizations, computes and subtracts out the ambient background signal, and performs dead time correction to the photon counting (532 nm) channel. The dead time correction is performed by using a look-up table which contains a dead time corrected value for each possible output from the photon counting channel (sum of 8 individual photon counting detectors). The raw (not dead time corrected) signal from the photon counting channel will range from zero to about 100 photons per bin (0.512 microsecond). Thus, the lookup table need have only 100 or so entries. The exact content of the lookup table will be determined by careful laboratory calibration procedures prior to launch. In the case of the 1064 channel, the digital counts that are output from the analog to digital converter must first be converted back to a voltage using a lookup table which has been calibrated and tested in the laboratory. The background subtraction, energy and range corrections are then applied to the data.

The basic output of GLA02 is the generation of what we call normalized lidar signal (P'(z)). From (2.1) we first subtract the background, then multiply by the square of the range from the lidar receiver to the return bin (R^2) and divide by the laser energy (E). Here, we have combined the detector dark current (P_d) and the ambient background light (P_b) into one background term (B). We must also perform dead time correction on the raw photon counts (for the 532 channel) and convert from digital counts to volts via a lookup table for the 1064 channel. The equations that describe this are:

(3.1.1) $$P'_{532}(z) = C_{532}\beta_{532}(z)T^{2}{}_{532} = (DC[S_{532}(z)] - DC[B_{532}])R^2 / E_{532}$$

(3.1.2) $$P'_{1064}(z) = C_{1064}\beta_{1064}(z)T^{2}{}_{1064} = (DA[S_{1064}(z)/G] - DA[B_{1064}/G])R^2 / E_{1064}$$

where $S_{532}(z)$ and $S_{1064}(z)$ are the raw signal from the 532 photon counting channel and 1064 photo diode channel, respectively and G is the 1064 programmable gain amplifier setting (which should be a multiplicative factor such as 1, 2, 4 or 8). The range from the spacecraft to the return bin (R) should be in kilometers and the laser energy (E) should be in Joules. DC and DA denote the dead time correction lookup table and the digital to analog conversion table respectively, as described above. At this time, these tables are undefined. The values for these tables will be determined from careful laboratory measurements which will likely be completed in FY99 or FY00. The background signal (B) for the two channels is computed for each laser shot from time integrated measurements of the background intensity at two separate times relative to laser fire. The first is prior to the laser beam reaching the atmosphere (about 70 km altitude), and the second is after the beam strikes the Earth (-5 km). The two background measurements for each channel will be stored as two byte values and must be normalized before use in equations 3.1.1 and 3.1.2. Letting T_b equal the background integration time in microseconds, and I_{532} and I_{1064} the integrated background signal for T_b microseconds, the background values to be used in equations 3.1.1 and 3.1.2 are:

(3.1.3) $$B_{532} = I_{532} / (1.953 T_b)$$

(3.1.4) $$B_{1064} = I_{1064} / (1.953 T_b)$$

The background will be computed in this manner for the two integration periods. Although it is not definite, most likely the second of the two background measurements will be used in equations 3.1.1 and 3.1.2. However, it is possible that the average of the two measurements would be used. The profiles defined by 3.1.1 and 3.1.2 will have the same format as the raw input data. This means that from –1 to 10 km altitude, both the 532 and 1064 channels will be 40 Hz, between 10 and 20 km the profiles will be at 5 Hz, and between 20 and 40 km we have only 532 data at 1 Hz. The background computation as described above will be performed at 40, 5 and 1 Hz (the 5 and 1 Hz backgrounds are computed by averaging the 40 Hz background measurements) for the 532 channel and at 40 and 5 Hz for the 1064 channel and stored as part of the GLA02 output.

Listed below are a number of other parameters which will be calculated by the GLA02 algorithm:

1. 532 channel saturation flag for the 3 segments, -1 to 10 km (40 Hz), 10 to 20 km (5 Hz) and 20 to 40 km (1 Hz)
2. Predicted height of first cloud top (5 Hz)
3. Ground return peak signal and bin location (5 Hz)

The photon counting channel will at times become saturated by strong signals from very dense clouds. When this occurs, the data are no longer valid. Therefore, it is important to be able to recognize and flag this condition so that we can apply a correction in later data processing. The 532 channel saturation flag will take the form of a profile (SF(z)) and will have a one-to-one correspondence with the 532 channel return signal bins. Each bin of the 532 channel will be checked against a maximum value (L_s) above which the signal will be considered saturated. This value will be determined in the laboratory and will likely be about 80 counts per bin (or 156 photons per microsecond, prior to dead time correction). This is shown as:

$$SF(z) = 0 \quad \text{FOR} \quad S_{532}(z) < L_s$$
$$SF(z) = 1 \quad \text{FOR} \quad S_{532}(z) \geq L_s$$

The predicted height of first cloud top (above local ground) is computed from the raw 532 signal (S_{532}) by simply searching downward in the profile (starting at 20 km altitude) for two consecutive bins which have a signal value greater than a threshold value. The search continues to about 500 meters above the ground so that the ground return itself is not mistaken for a cloud. Extensive GLAS atmospheric channel simulations run at Goddard Space Flight Center have determined that a representative cloud threshold is about 10 photons per bin (assuming the background calculated by equation 3.1.3 has been subtracted out). The return bin to stop the search is easily calculated, since the data acquired is based on the spacecraft position and an onboard Digital Elevation Map (DEM). Based on the DEM, GLAS will acquire data from 40 km above the ground to 1 km below the ground. Since the last bin of the lowest layer is 1 km below the ground, the bin corresponding to 500 meters above ground would be 20 bins above this last bin. In similar fashion, the height of the cloud is calculated from the bin number, assuming that the last bin is 1 km below the local ground level. The cloud search is not intended to be exhaustive or the most sensitive. It is only meant to provide a means of detecting the first fairly dense cloud encountered. It will certainly not be capable of detecting thin cirrus. This will be done in later processing (GLA09). The cloud height thus defined will be in kilometers above the local ground surface.

The ground search is performed much like the cloud search but begins at 500 m above the ground and continues to the end of the data (the –1 to 10 km profile). This amounts to searching the last 20 bins of the lowest layer (532 channel). The signal is searched downward until one bin exceeds a preset threshold value. This threshold is much larger than the threshold for cloud detection and was determined through simulation to be about 50 raw photons per bin. Once the ground is detected, the maximum of that bin and the following 3 is stored as the 'ground return peak signal'. Generally the maximum signal will be the first bin that exceeds the threshold value but may be one of the next 1 to 3 bins.

Parameters which will be read in by the algorithm and passed through as part of the output include but are not limited to:

1. Location of waveform peak (from altimeter channel)
2. 532 laser transmit energy
3. 1064 laser transmit energy
4. 1064 programmable gain amplifier setting (1 Hz)
5. Etalon filter settings (532 channel only)

3.1.2 *Error Quantification*

In this section we will try to first identify the main sources of error in the computation of normalized lidar signal and then attempt to quantify their magnitudes. Referring to equations 3.1.1 and 3.1.2, the main sources of error stem from incorrect knowledge of the laser energy (E) and inaccurate dead time correction factors for the 532 channel, and digital to analog conversion factors for the 1064 channel. The laser energy will be estimated by splitting off a small portion of the beam and

sending it to an energy measuring device. The total energy of the beam transmitted to the atmosphere is then computed from this measurement. Generally, this approach to measuring the laser energy is accurate only to about 5 percent. The other major error in computing the normalized signal is the inaccuracy of the dead time correction table. This is much harder to characterize and has the added problem of changing with time. As the photon counting detectors age, and are exposed to continuous radiation in the space environment, their response characteristics, as well as the amount of detector dark current, will change. This in turn affects the dead time correction table. It is hoped that the detector change with time can be quantified by using 'calibration targets' – places where the return signal should not change with time. Examples of this are the upper troposphere or lower stratosphere where, barring strong volcanic eruptions, known backscatter cross section with time should prevail. Additionally, certain areas of the Earth's surface (providing that the atmospheric conditions are nearly the same) should give the same ground signal independent of time. This would be true over the ocean surface or desert areas where the surface albedo does not change appreciably. It may be possible to use such 'targets' to keep track of detector changes.

Other factors affecting data quality are laser performance, boresite accuracy and, in the case of the 532 channel, how well the etalon filter is tuned to the laser frequency. We anticipate that occasionally, the laser footprint (spot on the ground) will drift from the telescope field of view. This will cause loss of signal until a boresiting procedure can be run to re-align the system (via an onboard software procedure). Likewise, signal loss will occur if the etalon filter is not tuned to the laser frequency. There should be some measure of the etalon tuning stored in the GLAS data stream, but the specifics of this are uncertain at this time. In the next section we will develop a set of confidence flags which are intended to provide a measure of data quality.

3.1.3 Confidence Flags

Confidence flags are meant to give an indication of data quality and our confidence that the data are at a level where all science objectives can be met. As mentioned above, there will be circumstances where the caliber of the data is reduced due to a variety of causes. A useful measure of the data quality can be obtained in a number of ways. The simplest and most straightforward is to integrate the entire signal from 20 km to the end of the profile and compute the average signal and standard deviation. The average and standard deviation should fall within known limits if the data are good. Another approach is to develop a histogram of the lidar return. If the signal were pure background noise, the photon counting signal (532 channel only) would tend to follow a Poisson distribution. Thus, the degree to which the histogram deviates from a Poisson distribution would tell us something about how much signal is contained in the return. For instance, if the system were totally out of boresite, then the lidar would receive only background, which should closely follow a Poisson distribution. If the system were in boresite, the histogram should deviate from the Poisson distribution, depending on how much cloud or aerosol signal were contained therein. One problem with this approach is that if the atmosphere is totally clean (devoid of cloud or aerosol), then the only signal contained in the return would be from the molecular return and the ground signal. The histogram in this case may not deviate much from the Poisson distribution.

Other ideas for quality flags are discussed in section 4.1.4.

3.2 Attenuated Backscatter Cross Section (GLA07)

3.2.1 Theoretical Description

The attenuated backscatter cross section falls easily from the normalized lidar signal developed in section 3.1. Essentially, the only computation required to obtain the attenuated backscatter is the calculation of the lidar calibration constant (C). The calibration constant can be obtained from first principles (equations 2.2 and 2.3), but in practice it is much easier and in the long run more accurate, to obtain C from the data itself, provided sufficient signal is available. This approach is beneficial because it overcomes the problems associated with instrument drift and is self-regulating. Our simulations indicate that the 532 photon counting channel will have adequate signal for the computation of C from the data itself, but it is unlikely that we may do so with the 1064 channel. We have therefore decided to use the laboratory calculation of C for the 1064 channel, but will calculate C from the lidar data itself for the 532 channel. Even so, GLA07 will be structured to compute the 1064 calibration constant from the data, but it will most likely not be used in the computation of calibrated attenuated backscatter unless we can verify its integrity in post processing.

The main functions of the GLA07 algorithm are to compute the calibration constant for both the 532 and 1064 channels, compute the calibrated attenuated backscatter (β') for both channels at 5 Hz and 40 Hz, and correct the 532 channel β' for times when it became saturated. Another important function that GLA07 will perform is the vertical alignment of the data so that each bin is referenced to height above mean sea level. The data acquired by GLAS (as well as the data output from GLA02) range in height from 40 to –1 km for the 532 channel and 20 to –1 km for the 1064 channel. This height is with respect to the height above ground at the point of the laser footprint (where the laser strikes the surface). This is based on a DEM onboard the spacecraft which can have different values for each second of lidar data. This means that the same lidar bin number can correspond to different heights above mean sea level from second to second. The data will thus have to be shifted in the vertical to account for this. See section 4.2.3 for further discussion of this point.

The proper vertical alignment of the lidar bins is very important for the calculation of the calibration constant, where it is required to average over a long horizontal distance at a particular reference height. The reference height, heretofore referred to as the calibration height, must be in a region of the atmosphere that is horizontally homogeneous and devoid of aerosol and cloud (non molecular) scatterers. These characteristics are generally found in the upper troposphere or the mid stratosphere. For both channels, we will search for the signal minimum in the upper troposphere between the altitudes of about 8 to 15 km. The calibration constant will be calculated at the height of the signal minimum. For the 532 channel, the calibration constant will also be computed at 35 km. The minimum signal between 8 and 15 km will be found by constructing the average backscatter profile through the calibration latitude band and then searching between 8 and 15 km for the height of the minimum signal. During the construction of the average profile, the data will be searched between 8 and 15 km for the occurrence of high signal values caused by aerosol or clouds. If the signal exceeds a predetermined threshold value, it will not be included in the average. If the number of such profiles exceeds 30 percent of the total number of profiles within the calibration latitude band, the calibration calculation is aborted and the calibration values are set to

–999 and of course are not used in the computation of calibrated backscatter for the subsequent half-orbit.

Since the signal return which is used in the computation of C is from purely molecular scattering, and the atmospheric density at these altitudes is very low, the return signal is very weak. Therefore, one must first integrate the return signal through a layer 2 kilometers thick centered on the calibration height and then average over a sufficient time span to insure adequate signal to noise for the computation of C. Based on simulations and theoretical considerations, we believe that averaging the data for 1/8 to ¼ of an orbit should provide ample signal to compute C (at least for the 532 channel). What we do not know is how often it will be required to re-compute C. In theory, if all components of the lidar system are stable, then the value of C should not change. Of course in the real world, electrical and optical components that comprise this complex instrument do change their characteristics with time (theoretically, the 1064 calibration should be more stable than for the 532 channel). How fast these changes occur will ultimately determine how often the calibration constant will have to be calculated. This is something that we may not know until after launch. Our approach used here is to calculate C twice per orbit and build in the capability of either using the newest calculated value of C (to compute the attenuated backscatter cross section) or continue using a value of C that can be hours or days old. By calculating C twice per orbit, with each calculation centered about the equator, we are usually insured both a nighttime and daytime calculation (at least most of the time). There is reason to believe that the nighttime calculation would be more accurate and stable (because of the lack of background signal), however we will not know this for sure until we can analyze a time series of C values. Thus, in addition to calculating and storing C as part of GLA07, it is desirable to flag each C value as being calculated during night, day or indeterminate. This can easily be done by looking at the background during the time that C is being calculated. The average background for the calibration segment can be calculated from 3.1.3. If that average value is greater than about 10 photons per microsecond, then it can be safely assumed that it is daytime. A background less than 2 photons per microsecond would indicate nighttime conditions and in between would be labeled indeterminate. Suggested values for the flag are –1 = night, 0 = indeterminate, and 1 = day.

As noted above, there may be considerable error in the calculation of C (from the atmosphere) for the 1064 channel. If this occurs and it is found that the laboratory calculation of C is not accurate, then we do have a backup plan for the computation of C for the 1064 channel. However, because of its complexity, it can not be implemented in the GLA07 processing. It would have to be done as special offline processing by the science team. In this event, the data would have to be re-processed (GLA07 re-run) with the new, correct value of the 1064 calibration constant. Without specifying details, the procedure involves using calibrated 532 channel cloud returns to calibrate the 1064 channel. In theory, there is a range of backscatter cross section where the 532 channel is not in saturation, but the 1064 channel will produce a substantial signal above the 1064 noise floor. If the 532 cross section is known, then the 1064 cross section can be computed (or at least estimated) if the type of cloud producing the scattering is known. We anticipate using cirrus clouds for this, identifying them by their height and scattering characteristics.

A requirement for the calculation of C is a knowledge of the average molecular backscatter cross section through the calibration layer. The molecular backscatter cross section will be needed in other GLAS processing modules in the form of profiles with the same vertical resolution as the lidar data (76.8 m). Thus, they will be computed in GLA07 as complete profiles from 40 km altitude to

the surface with a 76.8 vertical resolution. This requires knowing the atmospheric density at a vertical resolution of 76.8 meters (the lidar bin size). The pressure, temperature and relative humidity along the flight track will be calculated from the ancillary MET data which will be available to the GLAS ground processing system or from standard atmosphere tables (in the case of the 35 km calibration height). The MET data are reported at standard pressure levels which include temperature, relative humidity and the geopotential height. The geopotential height must first be converted to the equivalent geometric height and then the pressure (P(z)), temperature (T(z)) and relative humidity (R(z)) calculated for the bins (heights) between the standard pressure levels. This is accomplished with the hypsometric formula. From the calculated temperature and pressure, the atmospheric density ($\rho(z)$) is calculated from the ideal gas law as:

(3.2.1) $$\rho(z) = P(z)/(RT(z))$$

where $\rho(z)$ is in units of grams per cubic meter (gm^{-3}), assuming negligible water vapor, and R is the ideal gas constant for dry air. The value of R in 3.5 can be taken as 0.0028769 $m^2\ s^{-2}\ °K^{-1}$. The relative humidity can be included in the computation of atmospheric density, but it has a negligible effect for all but the lowest few km of the atmosphere. From the atmospheric density profile, the molecular backscatter cross section ($\beta_m(z,\lambda)$) in units of $km^{-1}sr^{-1}$ is then:

(3.2.2) $$\beta_m(z,\lambda) = 1.0411501x10^5\,\rho(z)/\lambda^4$$

where λ is the wavelength in nanometers (532 or 1064 nm in our case). The computation of the calibration constant then is:

(3.2.3) $$C_\lambda = \overline{P'_\lambda(z_c)}/(\overline{\beta_m(z_c,\lambda)}T^2(\lambda))$$

where $\overline{P'_\lambda(z_c)}$

and $\overline{\beta(z_c,\lambda)}$

are the horizontal average (through the calibration latitude band) of the vertically integrated lidar signal and molecular backscatter through the 2 km thick calibration layer, respectively. The length of the horizontal average will most likely be between 1/8 and ¼ of an orbit. In equation 3.2.3, $T^2(\lambda)$ represents the two-way path transmission from the top of the atmosphere to the calibration height. $T^2(\lambda)$ is calculated by first computing the molecular extinction profile from the molecular backscatter as in equation 3.2.4.

(3.2.4) $$\sigma(z,\lambda) = 8\pi\beta(z,\lambda)/3$$

The molecular transmission from the top of the profile (ztop) to height z is equal to one minus the integral of the extinction profile from the top of the profile to the height z as shown in equation 3.2.5.

(3.2.5) $$T(z,\lambda) = 1.0 - \int_{ztop}^{z} \sigma(z,\lambda)dz$$

In a purely molecular atmosphere, $T^2(\lambda)$ is very close to one for altitudes above 15 km, especially at 1064 nm (see figure 3.2.1). At 9 km, the two-way molecular transmission is about 0.95 at 532 nm and 0.99 at 1064 nm. Thus, we can assume that the two-way transmission is unity for the 1064 channel at the calibration height, but we must use the value of 0.95 for the 532 channel at the lower calibration height. Deviations from a purely molecular atmosphere (from aerosol above the calibration height) will lead to error in the assumed value of the two-way path transmission and thus to error in the calculated calibration constant (see section 3.2.2).

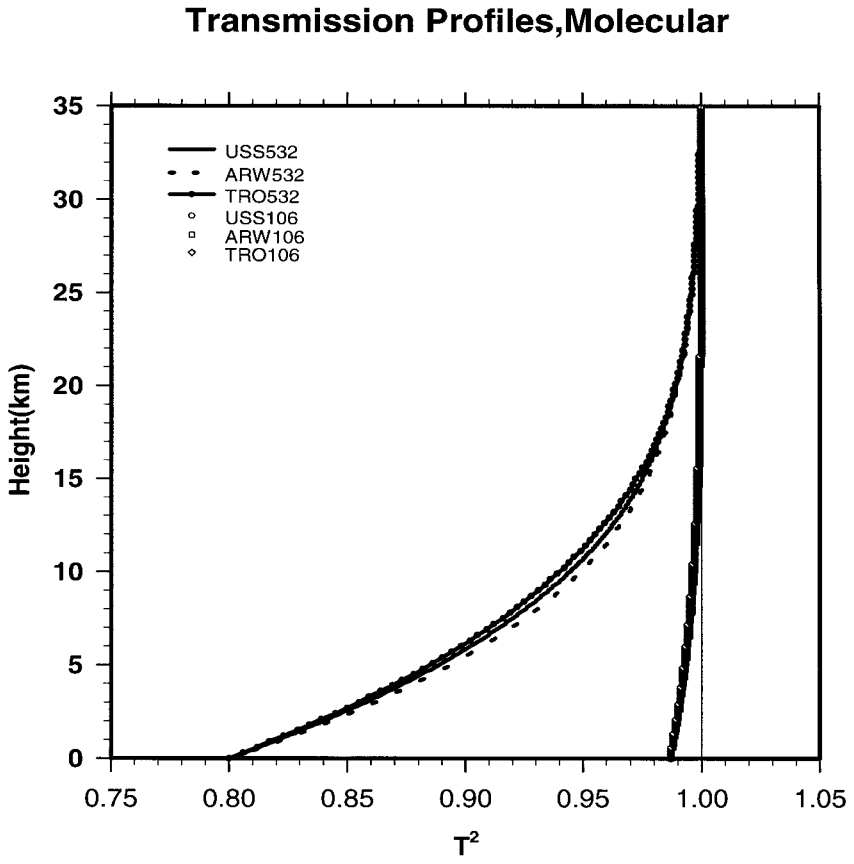

Figure 3.2.1. The two-way molecular transmission at 532 nm (left set of curves) and 1064 nm for various standard atmospheres.

In the actual implementation of the GLAS data processing system, profiles of attenuated molecular backscatter (the denominator in equation 3.2.3) will be generated on a continuous basis based on either interpolated MET data or standard atmosphere tables which correspond to the spacecraft location (i.e. tropics, mid-latitude, arctic, etc). As an example, figure 3.2.2 shows the attenuated molecular backscatter profiles for US Standard, Arctic-winter and Tropical atmospheres.

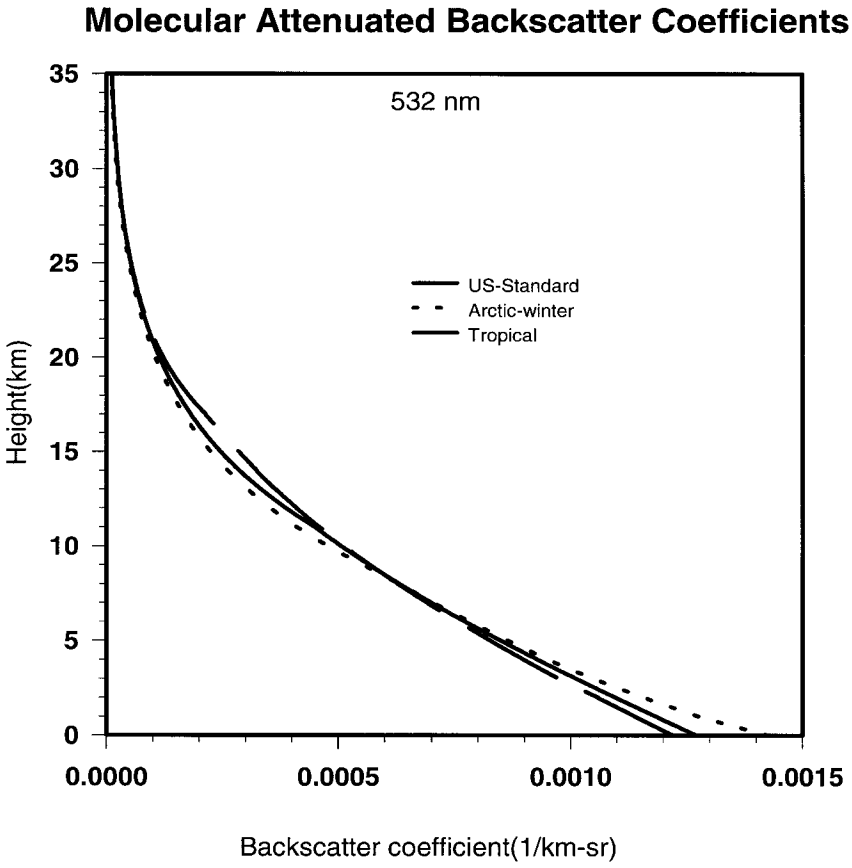

Figure 3.2.2. Profiles of the attenuated molecular backscatter cross section (coefficient) for three standard atmospheres. Note that the tropical atmosphere curve is denoted by the long dashed curve.

Since standard atmosphere tables will be used in the computation of C (in addition to MET data), and the standard atmosphere is defined for 3 latitude zones (tropical, mid-latitude and arctic), it might make the best sense to compute C in latitude bands about 45 degrees wide. For instance it could be done twice per orbit when the satellite was between 22.5 degrees south and 22.5 north using the tropical standard atmosphere. Once a C value is computed, there are two options as to how it could be applied to the data. It could be applied to all data from that point on until a new value of C is calculated, or the data segment used to calculate C can be buffered into memory and the C value just calculated could be applied to that data and all the data from there to the starting point for the next C calculation. In practice, the former is the easier approach to implement and is preferred here. We know that we want to compute C on a continuous or at least regular basis (at least once per orbit). What we do not know is how much C will change from calculation to calculation and how often we will need to apply the new C values.

Once the calibration constant is calculated, it must be applied to the data to obtain the calibrated, attenuated backscatter cross section ($\beta'_{532}(z)$ and $\beta'_{1064}(z)$) for the two channels as:

(3.2.6) $$B'_{532}(z) = P'_{532}(z) / C_{532} \qquad FOR \qquad SF(z) = 0$$

(3.2.7) $$\beta'_{1064}(z) = P'_{1064}(z) / C_{1064}$$

Note that equation 3.2.6 is used only if the saturation flag (SF(z)) is zero, meaning that the 532 photon counting channel was not saturated (as determined in GLA02). If the data were saturated, then we estimate the 532 backscatter from the calibrated 1064 backscatter. While this procedure can give us a useable estimate of the 532 backscatter, it is not entirely accurate because the magnitude of the scaling depends on the scattering phase function of the scattering medium which is not known. However, a reasonably good approximation for the 532 cross section is to simply use the 1064 backscatter cross section as in 3.2.8. This approximation can be considered accurate to within 10 percent for both ice and water clouds. Note that the 532 channel will be saturated most frequently from water clouds which tend to have larger scattering cross sections than ice (cirrus) clouds. Theoretical simulations indicate that the 532 channel will not saturate from most naturally occurring aerosol plumes, but may saturate from dense smoke from large scale (biomass burning) fires.

(3.2.8) $$B'_{532}(z) = B'_{1064}(z) \qquad FOR \quad SF(z) > 0$$

The implicit assumption here is that we have correctly calibrated 1064 data and that multiple scattering (in the 1064 signal) is relatively small. The 1064 channel, with its much wider field of view, is much more prone to multiple scattering than the 532 channel. It is mainly the multiple scattering that limits the accuracy of 3.2.8.

The intended output product for GLA07 consists of 5 Hz full profiles of $\beta'_{532}(z)$ from –1 to 40 km and 40 Hz profiles from –1 to 10 km. The former requires averaging 8 shots from the lowest layer and the duplication of 8 profiles from the upper layer to form one continuous profile from 40 to –1 km. For the 1064 channel, the output will consist of 5 Hz profiles of $\beta'_{1064}(z)$ from –1 to 20 km and 40 Hz profiles from –1 to 10 km, again requiring the averaging of 8 profiles from the lowest layer to form the entire 21 km profile.

Output from GLA07 will include the saturation flag profiles (SF(z)) for the 532 channel output as 5 Hz full profiles from –1 to 40 km and 40 Hz profiles from –1 to 10 km. Since the former requires averaging of the lowest layer, SF(z) should be set to 1 (indicating saturation) if any of the 8 shots that make up the average was saturated. A detailed list of additional data output by GLA07 is listed in section 4.2.3.

3.2.2 Error Quantification

Here we try to identify the major sources of error in the calculation of calibrated attenuated backscatter. This essentially boils down to identifying the major source and magnitude of error in the calculation of C. For the 532 channel, C is computed from the atmospheric scattering at specific heights (Equation 3.2.3). The error in 3.2.3 comes from two major sources. The first is the assumption of a purely molecular atmosphere in calculating the two-way transmission from the top of the atmosphere to the calibration height ($T^2(z_c)$). At the 35 km height this is ok, but the lower one

goes, the higher the probability that some aerosol will be present. Normally, this is small since most of the aerosol is confined below 10 km. However, during episodic volcanic eruptions, a significant amount of aerosol can be injected into the lower stratosphere. Thus, the magnitude of this error will vary in space and time and is difficult to quantify. However, in most situations, this error will be negligible at the 35 km calibration height, and less than 5 percent for a 9 km calibration height. Further, at the lower calibration height, it will be necessary to identify and eliminate the occurrence of clouds in the data segment that is used to calculate C. While it is easy to find and eliminate dense clouds, it will be difficult to locate very thin cirrus or aerosol layers.

Another problem that can occur in the calculation of C is the error involved in computing the molecular backscatter cross section ($\beta_m(z_c,\lambda)$) at the calibration height. For instance, if the temperature and pressure used to compute $\beta_m(z_c,\lambda)$ were in error by 2 and 10 percent respectively (4.5 °K and 1.1 mb), then the molecular backscatter cross section would be in error by 10 percent. Thus, this error is likely to be of greater magnitude than the transmission error discussed above. A good way to quantify this is to plot β_m for various standard atmosphere models. Figure 3.2.3 shows a plot of the 532 nm molecular backscatter profile for the arctic winter atmosphere (solid line) and the tropical atmosphere, normalized by the molecular profile for the U.S. standard atmosphere. This shows that at about 16 km, β_m calculated from the standard atmosphere can differ as much as 18 percent from the β_m calculated from the tropical atmosphere model. Essentially, this is illustrating the effect that differences in temperature and pressure have on the magnitude of β_m. For most cases, we think that the accuracy of the MET data used to compute β_m will limit this error to within about 5 percent.

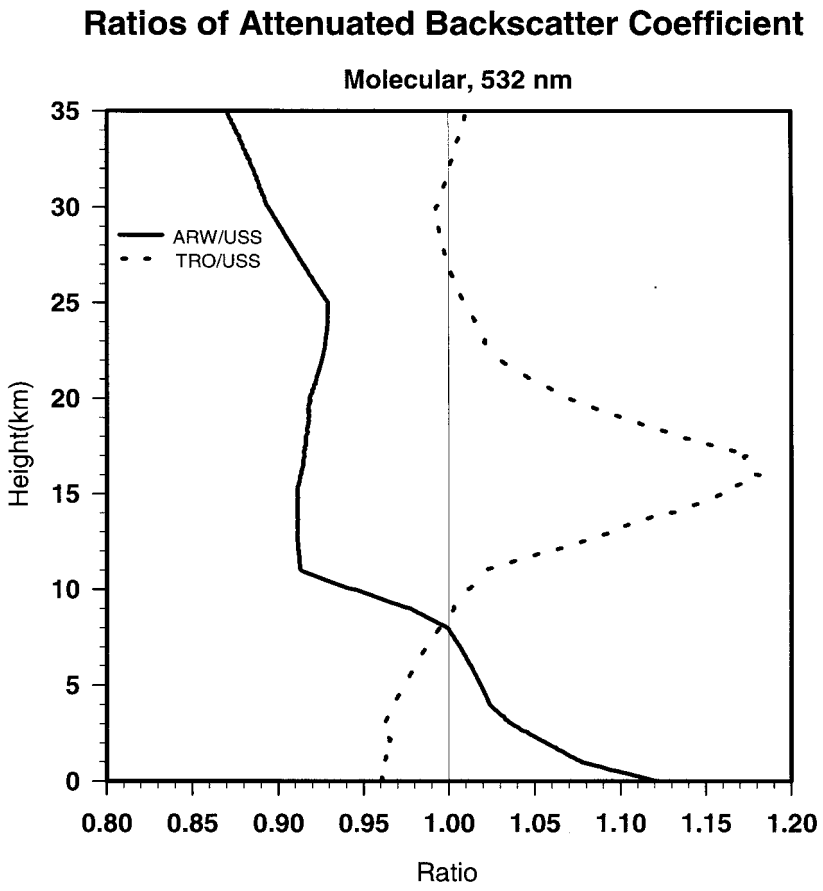

Figure 3.2.3. Ratio of the molecular backscatter profile computed from Arctic winter (solid) and tropical (dashed) atmosphere to the molecular profile computed from the U.S. standard atmosphere.

3.2.3 Confidence Flags

Confidence flags for GLA07 will include a measure of the variability of the calibration constant (for both channels) as a function of time as well as an objective measure of the quality of the attenuated backscatter profile. See section 4.2.4 for a full discussion.

3.3 Cloud Layer Height and Earth's Surface Height (GLA09)

3.3.1 Theoretical Description

3.3.1.1 Cloud Layer Height

The GLAS atmospheric channel signal will be used to locate the vertical positions of horizontal surfaces of both cloud layers and aerosol layers. The techniques to find these will be similar but not

identical in that the characteristic signatures of the two types are different. Therefore, detection of cloud and aerosol will be separated in the data processing code and separate output products will be produced. This section will present a description of the algorithms and techniques that will be used to find the locations of constituents considered to be clouds. A description of the algorithm to find the location of the earth's surface from the lidar return (ground signal) will also be given.

Cloud particles are those atmospheric constituents that are composed primarily of H_2O and that are formed by condensation of atmospheric water vapor around condensation nuclei. Cloud particles can be either liquid or ice and both phases can exist together. Liquid water can exist in a supercooled state. Clouds are aggregations of these particles. The aggregations typically have a layered structure, as in stratus, or a towering structure, as with cumulus. The two types can exist together and often a cloud has characteristics of both structures. A given location may be cloud free, clear, or be occupied by one or more types of clouds. Often, the combination of cloud types is quite complicated. Liquid water droplets are approximately spherical in shape. The shapes of ice particles are controlled by the effects of temperature, humidity, and local dynamics upon the crystalline structure. Cloud particle sizes usually extend over a particle size spectrum.

For our purposes, we consider the cloud structure to consist of a specific number of layers at any location. Each of these layers is a region of cloud particles defined by a top boundary and a lower boundary. The lower boundary of a fog layer is the surface of the earth. A boundary exists where the density of cloud particles exceeds an arbitrary threshold which serves to distinguish clear air from cloudy air. A region between top and bottom boundaries of a layer contains cloud particles that could have either homogeneous or inhomogeneous characteristics.

Because of the additive nature of scattering, cloudy atmospheric regions have greater volumetric backscatter coefficients than clear regions. In clear regions, radiative scattering stems entirely from air molecules; it is referred to as Rayleigh scattering. When particles are present, scattering is increased above Rayleigh scattering values. It is this enhancement in the scattering of photons in the lidar pulse that provides a signal that can be used to delineate cloud layers in a lidar profile. Since absorption by water at the GLAS lidar wavelengths is negligible, the backscatter coefficient in cloudy regions always exceeds the Rayleigh backscatter coefficient. Because of this, a vertical profile of Rayleigh backscatter coefficient could be established as a baseline threshold to distinguish cloudy regions in a profile. This would be convenient since the profile can be readily computed when the air density is known. However, attenuation of the lidar pulse by intervening layers reduces the lidar backscatter signal from any given volume. Therefore, the Rayleigh backscatter coefficient profile can serve as only an upper limit for a cloud threshold.

Figure 3.3.1 provides a conceptual view of a representative lidar profile of attenuated backscatter coefficient together with a profile of Rayleigh backscatter. The profile was fabricated by applying the basic lidar equation to an arbitrarily specified atmosphere and using the GLAS lidar system specifications to characterize the measured signal. Cloud boundaries are clearly evident from a visual inspection of the lidar profile. One's perception of the profile is such that the signals above and below a layer provide a threshold against which the protrusion of the cloud signal is compared. Even where the cloud density increases gradually, such as in the cirrus layer at about 8-km, the boundary can be discerned to within one or two sample elements. A profile characteristic that masks a weak cloud boundary is the random noise superimposed upon the basic signal. The signal from the second layer (from the top of the profile) of cirrus is diminished because of the attenuation

of the first. The signal from the stratus layer at 1 km is very much lessened by attenuation. Also, notice how the (lidar) molecular signal is diminished by attenuation in the region between 8.0 and 10.5 km and below 6.0 km. Despite reduction of the signal due to noise and attenuation, the locations of cloud layers are evident. The task of an objective algorithm is to mimic what is perceived by eye.

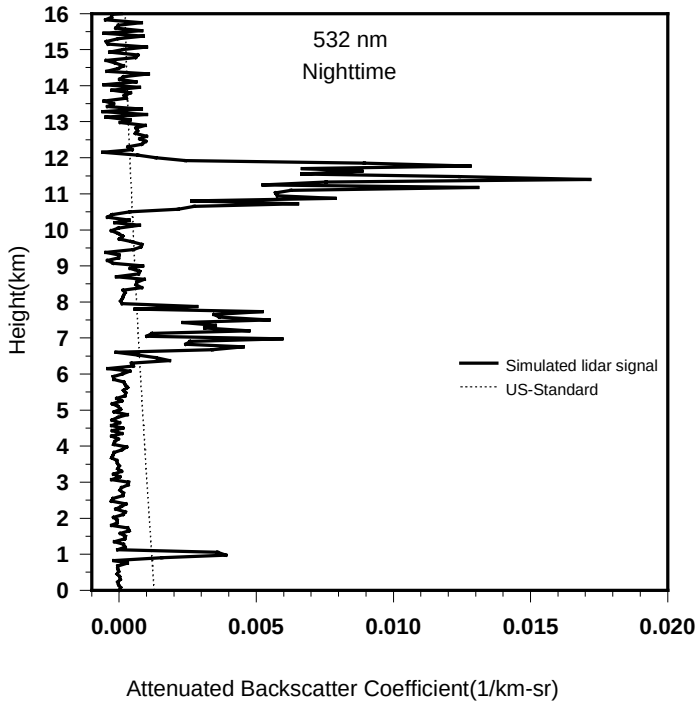

Figure 3.3.1. Simulated GLAS profile in a cloudy atmosphere. Two cirrus layers and one stratus are present. The optical depths are from top to bottom 0.5, 1.0, and 1.5.

An examination of cloud signatures in lidar profiles summarized above leads us to the assertion that an algorithm to find cloud boundaries in lidar profiles should use localized segments of small signal as a baseline in testing for cloud signals. By using the profile itself, rather than a threshold based upon some a priori determination, we can bypass the complications that arise from the many different atmospheric and background conditions that will be encountered by GLAS. Also, the threshold can be made to be a function of altitude, which permits using values that are more attuned to the different types of clouds at various heights. Such an algorithm can be designed to be an approximation of the results that would be attained from a visual inspection of a profile.

A positive attribute of an algorithm whose threshold is derived from the profile is that it can be implemented with very efficient computer code. The techniques required to find localized minimums are elementary. Only a small amount of coding is required and the solutions can be computed quite quickly. This will permit cloud boundaries to be found operationally at the highest resolution produced by the lidar. The following presents a detailed description of the algorithm

Cloud boundaries will be found at four time resolutions. These are, from coarsest to finest, 0.25 Hz, 1 Hz, 5 Hz, and 40 Hz. To do this, the GLAS time series will be divided into a sequence of

independent 4-second segments. These segments will be subdivided into four 1 second segments. Each of these will be divided into 5 segments and these will be divided into 8 segments, which will occur at the basic GLAS 40 Hz. frequency. Profiles of attenuated backscatter coefficients will be produced at 40 Hz and 5 Hz by GLA07 and serve as input into the cloud boundary algorithm. The 1 Hz and 0.25 Hz profiles will be produced by averaging the higher frequency data.

Boundary search operations will be applied to 0.25 Hz profiles first. Results at finer resolutions will be made only in vertical regions where clouds were detected at a coarser resolution first. The reason for this procedure is that the smaller signal to noise characteristic at higher resolutions will tend to obscure any clouds not detected at lower resolutions. This technique will fail to detect some cloud layers that are composed of horizontally sparse and rarefied patches. But such cloud layers are presumed to be insignificant for climatological studies.

The basic cloud boundary search technique will be the same for each of the four resolutions. Since the 0.25 Hz resolution profiles will be those first searched for the presence of cloud layers, we will focus first on those in our description of the search algorithm. The finer resolutions will use the results of coarse resolution searches to eliminate portions found to be cloud free.

Four one second attenuated backscatter coefficient profiles will be averaged together to produce a four-second averaged profile. A discussion of the potential difficulty caused by varying ground height among the four one second profiles will be given in a later section. The profile will be divided into a small number of segments. The optimum number will be found by applying the technique to simulated and proxy data sets to determine the means to obtain the best results. The number will likely be in the range of five to ten. The objective is that each segment has some samples that are in cloud free portions of the profiles. A characteristic signal from cloud free segments can reasonably serve as a cloud signal threshold. In general, it will not be known, a priori, whether a segment has cloud free samples. The difficulty is that rarefied clouds are not easily discerned in a noisy profile. Each of the segments will be searched for its minimum value. Also, in order to characterize better each segment, the mean and variance of the sample values will be computed for each. In the cases where a segment has cloud free regions, the minimum values will represent the attenuated signal from atmospheric molecules with negative random noise excursions superimposed. These will thus represent the absolute minimum that any cloud-distinguishing threshold could be in each of the segments. A reasonable maximum threshold would be the computed molecular backscatter coefficient. Together, these values represent a range of values that could serve as cloud signal threshold.

To find an optimum threshold value within the threshold envelope, it is necessary to find a measure of random noise because the lower limit boundary of threshold values is strongly influenced by the magnitude of random noise. This magnitude can be represented by the standard deviation of the lidar signal in a cloud-free profile segment. Based upon our experience, we can assert that the atmosphere is, in general, free from non-molecular, strong-scattering species in the 18-19 km layer. Therefore, the noise of the lidar signal there stems mostly from the molecular scattering signal and the background energy. Below that layer, it will not be known if any individual profile segment is cloud free. In situations with a strong background signal, it is reasonable to obtain the variance from the portion of the signal where there is no signal from the atmosphere. The last 5-20 samples of each signal profile will be recorded after the laser pulse has encountered the surface of the earth and thus will represent only background signal, with random noise superimposed This is

typically referred to as the background portion of the profile. Reflected sunlight is the overwhelming component of daylight background signal. Noise caused by the energy of sunlight dominates that from molecular scattering so the variance in the background region can be used as a measure of random noise in all of the cloud free regions, during daylight observations. For nighttime observations, the variance from the high layer will be used.

Once a typical molecular signal variance has been computed, cloud signal thresholds can be computed for each of the profile segments. In each segment, the threshold will be the sum of the minimum and a constant fraction of the square root of the variance. In the occasional cases where a profile segment is fully within a cloud, the sum would exceed the computed molecular signal. In these cases the value from an adjacent segment would be assigned to the threshold The value of the fraction will be determined from GLAS signal modeling studies but it will likely have a value in the range of 0.25-0.5. A profile of cloud signal threshold will be then constructed by piecemeal, linear interpolation of the segment values. The interpolation would be done at GLAS vertical resolution. The interpolated profile will serve as a cloud signal baseline upon which the presence of cloud signals will be tested.

The threshold profile described above will have the following positive attributes: 1) threshold values will be computed from the profile itself and will automatically adjust to the current situation; 2) the threshold computed at given level will be influenced by the attenuation of the lidar signal by higher clouds; 3) the technique will be valid for any time resolution. A negative attribute is that the statistical nature of the computation of variance introduces some uncertainty into any particular result.

Once the profile of cloud signal thresholds is established for a lidar signal, the cloud boundaries are sought in the following manner. Starting at the top of the profile, the lidar profile is tested on a sample by sample basis. If a value is found to exceed the threshold, it is deemed a potential cloud sample. If a specified number of potential consecutive cloud samples are found, the segment is designated a cloudy region. The top of the cloud is located at the height where the highest of the consecutive samples was found. The high-to-low testing continues under the stipulation that the profile is in a cloudy segment. The cloud designation continues until several consecutive samples are found to be less than the cloud threshold. In that situation, the profile is considered to be in a cloud free region. The bottom of the cloud layer is the point where the first of the consecutive cloud-free values was found. The testing continues downward for the top of another cloud layer. The profile will be so analyzed for cloud layers to the DEM based location of the earth's surface.

The cloud boundary analysis for a 0.25 Hz profile will be used as the basis for the equivalent analysis of the four 1 Hz profiles that it encompasses. The layers at which 1 Hz cloud boundaries will be produced will be limited to those vertical intervals where clouds are detected at 0.25 Hz. The reason for this design is that averaging to produce 0.25Hz profiles will result in samples with a large signal to noise characteristic, which will make it least likely to result in the fewest cases of incorrectly identifying cloudy layers. The 1 Hz data will have a smaller signal to noise ratio value. Limiting the results of the 1 Hz search to the layers as 0.25 Hz will minimize false cloudy results at 1 Hz. For practical reasons, the search for clouds at 1 Hz will use entire 0-20 km profiles, but the cloudy regions found will be limited to those found at 0.25 Hz. The implication of these limitations is that any cloud layers which are not substantial enough to produce a detectable signal at 0.25Hz are not considered to be significant at finer resolutions.

The results of the search for cloud layers from 5 Hz. profiles will be limited by the results from the 1 Hz profiles in a manner equivalent to the limitations imposed upon 1 Hz by 0.25 Hz. The same search algorithm will be applied from 0-20 km but the resulting detected layers will have to be among the layers detected at 1 Hz. or they will be discarded in the output. The situation for 40 H. will be slightly different to accommodate to relatively small signal to noise at that frequency. Cloud detection at 40 Hz will be limited to regions where one or more cloud layers were detected in the 5 Hz profiles. If one or more layers are found in a 40 Hz profile, only the lowest one will be recorded. This procedure will allow detection of low cloud layers that typically have strong lidar signals and that have horizontal distributions that vary at relatively high frequencies.

There are difficulties that arise from the variable ground height that may exist along the distance interval over which the average profiles will be produced. GLAS will produce vertical profiles that will use the local DEM value as the reference and lower boundary. The DEM values will be updated every 1 second and so four DEM values will be used in the construction of the 20, 5 Hz profiles which will be used to produce a 0.25 Hz profile. For purposes of cloud boundary detection, the value of the highest DEM boundary used within the 4-second interval will be considered the lowest altitude at which to search the profile for clouds. Also, since the one-second period of the DEM updates will probably not be synchronized with the 1 Hz lidar profiles, the higher of the two DEM values spanned by the duration of the profile will be used as the lower boundary for the search. Individual 5Hz and 40 Hz profiles will be contained within a single DEM interval, so this overlap problem will not exist.

A very important characteristic of downward looking lidar must be noted. As the laser pulse travels through the atmosphere, the scattering processes diminish its energy. In the case of a relatively small cumulative optical depth, the reflection of the pulse from the earth's surface has enough energy to be detected. If the cumulative optical thickness of the scatterers is large enough, the lidar signal will be reduced to the background level regardless of the magnitude of backscatter coefficients and no ground signal will be detected. No bottom boundary can be detected. Thus, when no return signal is detected from the earth's surface, the height of the bottom of the lowest layer is, in general, an invalid value with no relationship to the actual location. If a ground signal is detected, the uncertainty in the location of the bottom of the lowest layer increases as the ground signal's strength decreases.

3.3.1.2 Remedy for Day/Night Bias

Reflected solar energy is the source of two major components of total lidar signals from sunlit regions. These are constant offset signals, which are usually referred to as background, and random noise fluctuations, which are measured by the square root of the variance (root mean square, RMS) of random noise superposed upon the profile. Both components increase as the strength of reflected energy increases. The background component of a GLAS signal profile will be determined by averaging the signal in the portion of the profile where no laser signal is present (the background region of a profile). The background signal will be subtracted from the total to leave only the laser signal and random noise to comprise the total signal.

Our methodology to determine cloud boundaries is based upon constructing a cloud signal threshold profile where the value of the threshold is strongly dependent on the RMS value of signal

random noise. A larger RMS value will lead to larger threshold values. As indicated above, the magnitude of the RMS noise will be larger, in general, during daylight observations than those in taken in darkness. The resultant threshold values become larger. This results in the cloud detection technique being less sensitive to a given, small cloud signal during daylight observations than during night observations. Clouds with a certain level of weak signal will be detected in night observations but not in day observations. A day-night cloud detection bias is the result of this procedure. Such a bias would hamper certain types of cloud studies.

A solution to the day-night bias is to determine a threshold profile that is diurnally invariant and use this profile for all cloud detection operations. A constant threshold profile would eliminate the differences caused by changing RMS magnitude of random noise. But, in order to eliminate false cloud detection during daylight observations, such a threshold profile would have values that are greater than necessary for dark observations. For nighttime application, the method would be less sensitive than what is possible. Significant cloud layers that could be resolved would go undetected.

In order to give both complete and unbiased cloud boundary results, the GLAS algorithm will be applied twice. One application will use a threshold profile based upon the observed RMS noise of the backscatter profile (as discussed in section 3.3.1.1). The second application of the algorithm will use a threshold profile based upon a diurnally invariant threshold profile. The procedure is as follows. The boundary algorithm will be applied exactly as described in prior sections. This algorithm employs a threshold profile that uses the RMS magnitude of the profile noise as one of its components. Detection of clouds in this manner will be the most sensitive for a given situation. Cloud locations will be found and recorded at each of the temporal resolutions (0.25Hz to 40 Hz). After this operation is completed, the algorithm will be reapplied, this time using a threshold profile that incorporates an invariant noise component. The lidar signal will be compared to the threshold only in portions of the profile where clouds were detected using the variable threshold profile. If the presence of a cloud is indicated during this testing, it will be recorded in a true/false variable but its top and bottom boundaries will not be re-computed. This application will proceed through each of the resolutions. The result of the dual application of the cloud boundary algorithm will be: a) a set of cloud boundaries at each of the temporal resolutions, determined with the variable threshold profile; b) a set of corresponding true/false flags indicating whether each of the layers was detected using the diurnally invariant threshold profile.

Determination of the invariant RMS noise component will require appropriate GLAS simulation studies. A threshold profile must yield results where few significant cloud layers are missed and where few false positive results occur. A trade-off between these two competing requirements always exists in finding a threshold. Modeling studies will permit the final determination of the threshold to be based upon the expected performance of the GLAS lidar and will permit an estimate to be made of the sensitivity and tolerance of the algorithm.

3.3.1.3 Polar Stratospheric Clouds (PSCs)

Polar stratospheric clouds are layers of particles that occur in Polar regions during winter seasons at the respective poles. These layers reside in the stratosphere from 15 to 30 km in altitude. The layers are composed of particles of various chemical compositions. Because these layers are more properly classified as aerosol layers than as H2O cloud layers, and because they can reside above

the cloud boundary algorithm upper limit (20km), detection of these will be done as part of the aerosol detection algorithm (see section 3.4.1.2) and not as part of cloud detection algorithm.

3.3.1.4 Bottom of Lowest Layer

A short discussion concerning the ambiguity in the altitude of the bottom of the lowest detected cloud layer is given in the final paragraph in section 3.3.1.1. Two additional assertions can be made concerning this. First, if the ground signal is not detected, the bottom of the lowest detected layer is not determinable and additional layers may exist below the last layer. Second, the uncertainty in the location of the tops and bottoms of each detected layer increases as the cumulative optical thickness from the spacecraft increases. These uncertainties will be evaluated and quantified with the appropriate modeling and empirical studies of the expected GLAS signal.

3.3.1.5 Earth's Surface Height

The detection of the earth's surface (GLAS ground signal) presents a problem very similar to that of detection of cloud boundaries. In fact, the algorithm is simplified because only one surface is to be found. Also, because the timing of the GLAS laser is synchronized with a 1 degree DEM of the earth's surface, the algorithm will have an approximate location available and the search can be limited to a small interval surrounding that height.

The characteristics of the ground signal in a GLAS profile are affected by the time resolution of the profile. Since the profile samples are much larger than the length of the laser pulse, the ground signal will be contained in only one or two samples at 40Hz resolution. However, the effective ground signal can broaden when more than one laser pulse is used to generate a profile. This broadening is caused by the variability of ground location over the horizontal extent that is used to generate the profile. If the terrain is rugged, the broadening would extend over 10 or more pixels for a 0.25 Hz profile, which would lead to a significant ambiguity in the meaning of ground location. Thus, a modified definition of ground signal is required of low resolution profiles.

Random noise can mask the ground signal. This is especially true for higher frequency profiles where signal attenuation reduces the pulse strength. This effect is generally less important when multiple shots are used to produce a profile.

The competition between higher precision results from high frequency profiles and higher reliability from lower frequency profiles leads to compromise algorithm design where the 5 Hz profiles will be used as the primary ground-location analysis frequency. The 5 Hz results will be averaged to produce ground locations at 1 Hz and 0.25 Hz. In addition, the location of the 40 Hz ground signal will be limited to an elevation interval close to that found for the encompassing 5 Hz profile.

The search for ground signal in a 5 Hz profile will proceed as follows. Since the GLAS laser is timed so that the final 13 samples of a profile occur after the level of the DEM elevation, the initial guess for the height of the earth's surface is at the 13th sample from the end of the profile. In such a case, the signal in the final 12-13 samples would be purely background with random noise superimposed. This permits a ground signal threshold to be computed from the signal in this segment. To do this, the mean, median, maximum, minimum, and variance of the final 20 samples will be computed. A threshold will be computed by adding the median and the square root of the

variance multiplied by a factor that is a function of the current conditions. The value of the factor will be determined from simulation and proxy-data studies, which will reveal the optimum value to use in different circumstances. The values of the samples, beginning with the latest and proceeding to the earliest (bottom to top), will then be compared to the threshold. If a single value or several non-consecutive values exceed the threshold by a relatively large amount (perhaps three standard deviations for instance) then the earliest (lowest height) of these will be considered the ground signal. Otherwise, if there are one or more occurrences of one or two-only consecutive samples that exceed the threshold, then the lowest of these will be considered the ground signal. The higher sample of any ground signal pair will be selected as the ground signal. If no such results are found, then the ground signal will be considered undetectable for the profile. Once all of the 5 Hz ground signals within a 1 Hz or 0.25 Hz averaging segment are found, the detected ground signal heights of the 5Hz results will be averaged to produce the ground height for each of the lower frequencies.

Finally, this same ground signal detection algorithm will be applied to each of the 40 Hz profiles. The parameters that are derived from modeling studies will have different values than those for 5 Hz. The low signal to noise will result in a higher rate of falsely detecting ground signal.

3.3.2 Error Quantification

Multiple scattering is a potential source of large error in determining the boundaries of clouds and the earth's surface from a space-borne lidar. The multiple-scattering process causes secondary photons to take deviated paths back to the lidar receiver where they are combined with the single-scattered signal of later samples. This causes the later sample to appear to have a larger signal than that based upon the density of the scatterers A possible result of this is that a cloud's lower boundary is analyzed to be at a lower altitude than it actually is. Fortunately, the vertical resolution of the boundary analysis is, at best, 76 .8 m. Our experience with spaceborne lidar indicates that the multiple scattering effect is significant, at this resolution, only in dense low clouds. Since these clouds usually fully extinguish the laser pulse, no ground signal would be detected and the lower boundaries of these clouds would be unknown. Because of this, it is not expected that multiple scattering will have a significant effect on the quality of the results of the boundary algorithm for most clouds.

The quality of the results of a cloud layer boundary algorithm can be divided into two components: a) true or false determination of the existence of cloud layers; b) precisely locating the top and bottom of layers. Errors in component a), designated false positive or false negative, lead to inaccurate qualitative description of the atmospheric situation. Errors in the second component lead to imprecise computations of the optical and radiative parameters affected by clouds.

Errors in the determination of cloud layer boundaries from lidar profiles are largely controlled by the signal to noise ratios of small signals. The crucial objective of the boundary algorithm is to find a threshold small enough to detect signals from rarefied clouds but large enough to reject random noise as clouds. A large percentage of cloud layers could be detected simply by using a single constant backscatter coefficient, based upon the computed molecular backscatter coefficient, as a threshold. If such a threshold were greater than the molecular value, the boundaries would be known to acceptable accuracy for many purposes. No false clouds would result if the threshold were high enough. However, many significant rarefied, optically thin clouds would be overlooked. If

a threshold were too low, random noise would be often interpreted as cloud signals. In both of these situations, the boundaries of identified cloud layers would be uncertain. The occurrences of false negative results and false positive results are the competing detrimental effects in the selection of a proper threshold value.

The uncertainties associated with determination of cloud boundary locations will be measured in terms of probabilities that boundary results are within specified confidence intervals. The magnitudes of these probabilities will be determined through studies of simulated profiles and proxy GLAS data. These studies will consist of application of the boundary algorithm to situations where the desired results are known. Comparison studies of the results of the output of the algorithm with the known situation will be conducted. Probabilities of deviations of the algorithm output from the truth will be computed from these studies and tabulated. Tables 2 and 3 illustrate two important types of confidence relationships that will be generated.

Probability of layer detection failure

	β_{x1}	β_{x2}	β_{x3}
T_1	P_{11}	P_{21}	P_{31}
T_2	P_{12}	P_{22}	P_{32}
T_3	P_{13}	P_{23}	P_{33}

Table 2. Probability that the GLAS cloud boundary algorithm will fail to detect an actual layer. T_n represents threshold values, β_{xn} represents the maximum backscatter coefficient in a layer and P_{mn} represents probability of failure.

Probability of cloud boundary height error

	Δh_1	Δh_2	Δh_3
T_1	P_{11}	P_{21}	P_{31}
T_2	P_{12}	P_{22}	P_{32}
T_3	P_{13}	P_{23}	P_{33}

Table 3. Probability that an analyzed boundary height will deviate from the actual boundary height. T_n represents threshold values, Δh_m represents a magnitude of height deviation and P_{mn} represents probability of failure

Many types of relationships could be developed but those relating the cloud/no cloud result and the location of cloud edges to selected threshold value are those that are most appropriate for the GLAS product output.

3.3.3 Confidence Flags

Based upon the studies referred to above, the following confidence parameters will be given for the cloud layer boundary results of each profile.

a) for each layer detected: a flag to indicate a high, medium, or low confidence
b) for the top and bottom of each layer, a single number indicating a number of sample bins within which the boundary exists at a specified probability
c) for each profile, a single number representing the probability that an undetected layer exists
d) for a positive ground signal, a flag to indicate a high, medium, or low confidence
e) for a positive ground signal, the number of sample bins within which the actual ground height exists at a specified probability
f) for negative ground signal detection, a probability that a detectable ground signal actually exists but the algorithm fails to do this.

3.4 Planetary Boundary Layer and Elevated Aerosol Layer Height (GLA08)

The Planetary Boundary Layer (PBL) height constitutes one of the most important and useful parameters to be retrieved from the GLAS atmospheric lidar data. PBL height is related to the fluxes of heat and moisture at the surface and can be used to estimate the bulk water vapor content of the PBL (Palm et al, 1998). Because of the large aerosol gradient normally encountered at the top of the PBL, it is relatively easy to find the height of the PBL from high signal to noise (S/N) lidar data. The higher aerosol and moisture content of the PBL results in a much larger backscatter cross section, resulting in increased return signal. A strong inversion normally present at the PBL top traps the aerosol and moisture, thereby maintaining the large gradient of moisture and aerosol at the PBL top. The ability to measure the height of the PBL with both ground based and airborne lidar is well documented. Algorithms used with both types of data basically search the lidar signal for the large gradient of aerosol scattering within certain pre-defined levels of the atmosphere. Comparison of the lidar derived PBL heights with coincident radiosonde or dropsonde data has verified the accuracy of these methods. (Boers et al, 1984, 1986; Melfi et al, 1986; Palm et al, 1998).

Airborne lidars have frequently been used to gather high resolution measurements of tropospheric clouds and PBL structure over large areas (Melfi et al, 1986; Boers et al, 1991). Most airborne lidar systems consist of relatively large and powerful lasers which fly in the lower or mid troposphere. Consequently, the signal to noise ratio is high which makes the task of retrieving PBL and aerosol layer height from the lidar data fairly easy. The Cloud and Aerosol Lidar System (CALS), developed at NASA Goddard Space Flight Center, is an exception since it flies in the lower stratosphere and utilizes a relatively low power laser. Through the analysis of data from CALS and more recently, simulated GLAS data, we have developed schemes to retrieve PBL height from data with very low S/N (Palm and Spinhirne, 1987; 1998). This technique is described in section 3.4.1.1.

Elevated aerosol layers (EAL) are not as ubiquitous as the planetary boundary layer, occurring only sporadically at various altitudes throughout the troposphere and lower stratosphere. Lidar is one of, if not the only remote sensing technique which can accurately resolve the height distribution of EALs. They are important because of their effect on the radiation balance and their contamination effect on many passive remote sensing measurements. The detection of EAL from lidar data is similar to that for the PBL height, but requires a somewhat different approach. Because of this, it will be addressed separately in section 3.4.1.2.

3.4.1 Theoretical Description

3.4.1.1 Planetary Boundary Layer

Retrieving PBL height from the GLAS data can be difficult especially if the PBL is relatively dry and aerosol free. Even under the best of conditions (optically dense PBL and after sunset) it is unlikely that the PBL top could be retrieved from GLAS data on a shot to shot basis. Averaging of lidar shots to increase S/N will undoubtedly be necessary. The degree of averaging will depend on the optical depth of the PBL and lighting conditions (background noise). Under typical conditions, we believe that the PBL top can be recovered after averaging between 5 and 10 lidar returns. GLA08 will be designed to detect the PBL height at two horizontal resolutions – high resolution (5 Hz or 8 shot average) which corresponds to 1.4 km, and low resolution (1/4 Hz or 160 shot average) which is about 30 km. There will undoubtedly be times when very little aerosol exists within the PBL, making the height determination very difficult or impossible at the high resolution. We believe that at the lower horizontal resolution, we should be able to detect the PBL top well over 90 percent of the time.

GLA08 will use the 5 Hz, 532 nm attenuated backscatter profiles which are output from GLA07 for the calculation of PBL height. The algorithm must be designed to remove bad lidar shots and spurious noise spikes within shots. Failing to do so could result in noise spikes that are mistaken for PBL top. The filtering process can be done most efficiently by examining the quality flags that are output from GLA07.

The PBL height algorithm processes the data in roughly 150 km chunks, which corresponds to 20 seconds of data. The overall procedure is to first average 20 seconds of data to form one profile. That profile is searched below 7 km for the presence of the PBL and a ground return. If the PBL top is not found from this average profile, then it is assumed that the PBL top is not detectable for this segment of data and all the PBL heights for that time segment are set to zero. This would mean that the 100, 5 Hz (high resolution) and the 5, ¼ Hz (low resolution) PBL heights would all be set to zero. This is only expected to happen in cases where overlying clouds have attenuated the lidar beam, or in rare cases where the PBL is exceptionally devoid of aerosol. Now, there are certain criteria placed on the data within the 20 second data segment. First, if a cloud was detected for that shot (shot here means a single 5 Hz profile) via GLA09 above 5 km and the ground return was not detected, then that shot cannot be used in the 100 shot average. Further, if more than 50 percent of the shots fall into this category, then all the PBL heights for that segment are set to –1. If a time gap of greater than 5 seconds occurs, while forming the 20 second average, the 20 second average will have to be re-computed beginning after the time gap and all the PBL heights up to the time gap set to –2.

Assuming that a 20 second average is successfully formed and that an average PBL height is detected, the next step is to go back through the 20 seconds of data and form five, 4 second (20 shot) averages and search each for the PBL top, using the 20 second average PBL top as a guide to where to search for the low resolution top. Similarly, when a PBL top is found from the 4 second average, the 20 shots that make up that segment will be examined individually for the high resolution PBL top, using as a guide the location of the 4 second PBL top. The output from this step represents the high resolution, 5 Hz PBL height. Thus, the general idea of the algorithm is to locate the PBL top at low horizontal resolution and gradually increase the resolution in a three step process. The exact technique used to locate the PBL top at any given resolution is discussed below.

We need to identify the average ground bin (G_b) for the data segment under consideration. The position of the ground bin should not change within a high resolution segment (5 Hz), but may change for a low resolution segment (4 seconds). For the 20 second average segment, the position of the ground bin could change substantially over mountainous terrain. The ground bin together with the last 20 second average PBL height in meters (H_{20}) gives us a reference from which to calculate various signal levels required by the algorithm. GLA09 will locate the ground bin from the 532 nm return signal. When available, this will be used by GLA08 for the ground bin. However, there will be times when clouds attenuate the signal and no ground return is found. In this case, a calculated value of the ground bin will be used. Next, we need to compute the average signal level within the boundary layer and above the PBL (within the troposphere). Let us call these average signals β_{pbl} and β_{trop}, respectively. We also need to find the maximum signal within the PBL. Let us denote this as β_{max}. The above filtering and averaging procedure should have eliminated all shots with no ground return and a cloud above 5 km. The reason that we do not want to eliminate all data with no ground return is that to do so would be to eliminate all cloud-capped boundary layer data. Instead, we want to eliminate all data with no ground return that was due to attenuation of the laser beam from mid and upper layer clouds, not from clouds that are associated with the PBL top.

We begin by applying a 3 point binomial filter to the attenuated backscatter data below 7 km to form a smoothed profile (β_s):

(3.4.1) $$\beta_S(i) = \sum_{j=1}^{3} S(j)\beta(i) \quad \text{for } G_b - 91 < I < G_b$$

where I represents the lidar bin number, $G_b - 91$ represents the lidar bin corresponding to 7 km above the ground and S(j) is the binomial filter function with values: S(1) = 0.25, S(2) = 0.50, S(3) = 0.25.

To obtain the average signal within the PBL (β_{pbl}), compute the bin number that corresponds to half the average PBL height as $k = H_{20}/(2.0*76.8)$. Then define the average PBL signal as:

(3.4.2) $$\beta_{pbl} = (\beta_s(k-1) + \beta_s(k) + \beta_s(k+1)) / 3.0$$

Similarly, to define the average signal above the PBL in the free troposphere (β_{trop}), we compute the bin number that corresponds to 500 meters above the average PBL height as $l = (H_{20}+500)/76.8$. Where l is constrained to be greater than $G_b - 91$. The average signal above the PBL is then:

(3.4.3) $$\beta_{trop} = (\beta_s(l-1) + \beta_s(l) + \beta_s(l+1)) / 3.0$$

Next, define a signal level (β_t):

(3.4.4) $$\beta_t = \beta_{trop} + F_{pbl}(\beta_{pbl} - \beta_{trop})$$

where F_{pbl} is a threshold factor between 0.0 and 1.0. In practice, the value of F_{pbl} may vary from about 0.4 to 0.7. A discussion of how to estimate the magnitude of F_{pbl} is given in section 4.3.1. Finally, we find the maximum signal between bins k and l. Call this β_{max}, occurring at bin m. The algorithm then searches from that point (bin m) upward until 2 consecutive bins have signal values less than β_t. The lidar bin corresponding to the top of the PBL is considered to be the first bin that is less than β_t. If we call this bin n, then the height in meters above ground of the PBL is:

(3.4.5) $$H_{pbl} = (G_b - n)76.8$$

An example of a typical GLAS return for a clear marine boundary layer is shown in figure 3.4.1. The increase in signal due to the trapped moisture and aerosol within the boundary layer occurs at about 900 m in this case. The various signal levels discussed above are labeled on the figure.

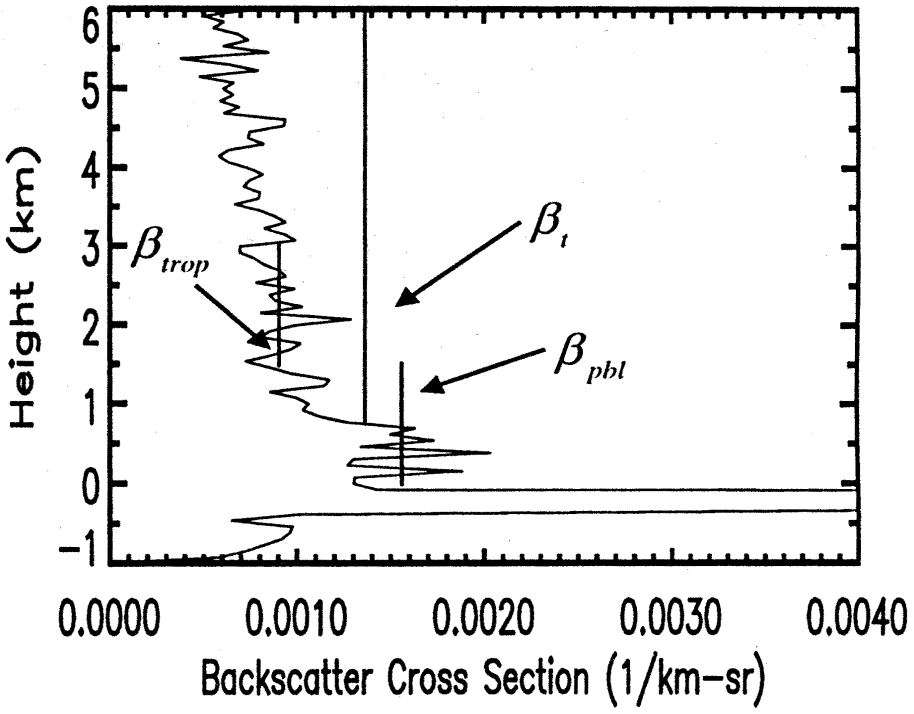

Figure 3.4.1. A nighttime simulated GLAS lidar return at 5 HZ showing the increase in signal associated with the marine boundary layer (below 1 km) and the various signal levels that would be computed by the algorithm from equations 3.4.2, 3.4.3 and 3.4.4 . The threshold value β_t was computed with F_{pbl} = 0.5.

Note that H_{20} is the average PBL height defined by the processing of the last 20 seconds of data. This means that when we begin processing or resume processing after a large data gap, the initial value of H_{20} must be assumed. While this is somewhat of a problem, it can be overcome by using the height of the maximum signal from the initial 20 second averaged profile as an estimate of H_{20}. The maximum signal would be computed based on the data form 7 km altitude to 2 bins above the ground bin.

After we have computed H_{20} from the 20 second average using the above procedure, we go back into that segment and form five, 4 second averages (20 shots). Each of these five profiles is searched for the PBL top in exactly the same way as described above, except for the following: the limits within which to search for the PBL top are more narrow. Now we use n – 5 and n + 5, which is a 750 m wide window centered on the 20 second average PBL height (H_{20}). After each of these segments have been processed to obtain the low resolution PBL height (H_4), the 20 shots which comprise them are individually searched for the PBL top in a similar manner, except we use a 600 m wide window centered on the low resolution height for that segment (H_4).

3.4.1.2 Elevated Aerosol Layer Height

The identification of elevated aerosol layers is a procedure similar to the detection of PBL height, but in this case, we do not know apiori where in the profile to look as we do for the PBL. Elevated aerosol layers can occur anywhere above the PBL and thus require searching nearly the entire profile. They are usually very tenuous and like the PBL will require a certain amount of profile averaging to detect. We have decided to search for aerosol layers below 20 km at a 4 second resolution (30 km) and at 20 second resolution (150 km) above 20 km using the 532 nm attenuated backscatter profiles output from GLA07 at 5 Hz.

Like the PBL height algorithm, the Elevated Aerosol Layer (EAL) algorithm will first average 20 seconds of data to form one profile. That profile is searched for the presence of aerosol layers. If an aerosol layer (or layers) are found at that resolution and they are below 20 km, then that 20 second segment is broken into five, 4 second averages and the aerosol layer height is determined at the higher resolution using the 20 second average height(s) as a guide. The bottom search limit for a given 20 second segment will be defined by the cloud height information generated by GLA09. The highest optically thick cloud height of the 100 shots defines the bottom search limit for the EAL algorithm. The term 'optically thick' means that the lidar signal has been totally extinguished by the cloud and there is no meaningful signal below the cloud. This information will be recorded in the GLA09 output. In the case of optically thin cirrus at 12 km above a thick stratus deck at 3 km, the search limit for the EAL algorithm would be 300 meters (4 bins) above the highest reported height of the stratus deck for that 20 second segment. In this case, when the EAL algorithm searches for aerosol layers, it must avoid the cirrus cloud. This can be done by defining a 'zone of exclusion' 300 meters above the highest cirrus cloud top height and extending down to 300 meters below the lowest cirrus cloud bottom (both cloud top and bottom are defined by GLA09). This approach will enable us to detect aerosol layers beneath optically thin cloud layers. If there were no clouds detected within the 100 shots, then the lower limit for the aerosol search is 1 km above the highest PBL top for that segment. If a time gap of greater than 10 seconds occurs, while forming the 20 second average, the 20 second average will have to be re-computed beginning after the time gap and all the high resolution aerosol layer heights up to the time gap set to 0. Unlike the PBL height algorithm, the EAL algorithm will need to find both the top and bottom of each aerosol layer. Above 20 km, the algorithm will search for a maximum of 3 layers at a horizontal resolution of 20 seconds (150 km). Below 20 km, a maximum of 5 layers are possible at a horizontal resolution of 4 seconds (30 km).

At this point, we want to take a moment to discuss Polar Stratospheric Clouds (PSC's). PSC's are extremely tenuous (optically thin) clouds that form at altitudes between 15-25 km in the polar regions during winter. Very few observations of PSC's exist, especially for the antarctic region. Because of their critical role in polar ozone depletion, they are of intense interest (McCormick et al, 1982, 1985).

GLAS, with its polar orbit and extremely good spatial coverage of the polar regions, will provide a unique opportunity to measure the height, extent and coverage of PSC's for the first time. The magnitude of the return signal that GLAS is expected to receive from a typical PSC is very small. We expect the return signal will look more like that from an aerosol layer than from a normal cloud layer. This, together with the fact that GLA09 will search for clouds only below 20 km, makes it more appropriate to search for PSC's in the EAL algorithm (GLA08) than in the cloud detection algorithm (GLA09).

McCormick et al (1985) present observations of PSCs by satellite and aircraft lidar data which indicate that they occur mainly poleward of 65 degrees and only in very cold atmospheric temperatures less than about –75 °C and that they usually occur between 14 and 30 km. Further, when temperatures are lower than –85 °C, PSCs occur virtually 100 percent of the time. When the EAL algorithm detects a layer that is above 14 km and the latitude is above 65 degrees in the winter hemisphere, a flag will be set that indicates that this layer is likely a PSC. Additionally, the temperature at the level of the layer can be estimated from the MET data to help identify a PSC. If the temperature at the height of the detected cloud later is below –80 °C, and the latitude is above 65 degrees, then the flag will be set to another value indicating that there is a very high likelihood that the layer is a PSC.

We now move on to the details of the elevated aerosol layer algorithm. If $\beta_{20}(z)$ is the 20 second average attenuated backscatter profile, we first apply a 3 point binomial filter (S(j)) to form a smooth profile as:

(3.4.6) $$\beta_s(z) = \sum_{j=1}^{3} S(j)\beta_{20}(z) \quad \text{For } H_b < z < 40 \text{ km}$$

where H_b is the bottom search height as described above. We begin searching $\beta_s(z)$ at the 37 km level and work downward. The general scheme is to define a threshold level based on the local value of the signal and look for a signal consistently above that level. The threshold value is re-computed every 2 km to account for the increasing molecular signal as we move downward. To commence, compute the average signal at 38km altitude as:

(3.4.7) $$\beta_s(38) = \sum_{j=13}^{39} \beta_s(j) / 27.0$$

which represents an average over a 2 km thick layer centered at 38 km. Next we form the initial threshold level (L_t) for the aerosol layer top as:

(3.4.8) $$L_t = \beta_s(38) + F\sigma$$

where σ is the standard deviation of the signal between 39 and 37 km, and F is a scaling factor most likely between 3 and 5. The exact value of F will be determined by running prototype code on simulated data in the near future. We begin the search at 37 km (bin 39) and search downward for the occurrence of 3 consecutive bins which have signal levels above L_t. Let b1 represent the first bin of the three above the level L_t. The height (above mean sea level) of the top of the first aerosol layer is then:

(3.4.9) $$H1 = 40.0 - (0.0768)b1$$

If we have searched downward in the profile for 2 km without detecting an aerosol layer, we must redefine our top threshold level (L_t), because of the increasing molecular signal as we go to lower altitudes. If k is the the bin that is 2 km below the height of the last definition of L_t, and is the current bin of the search, then:

(3.4.10) $$L_t = F\sigma + \sum_{j=k}^{k-6} \beta_s(j) / 7.0$$

Where F is the same factor as in Equation 3.2.8 and σ is the standard deviation of the data in the 2 km layer of data just searched (ie bins k through k-26). The search then continues downward from bin k, checking as before for the occurrence of 3 consecutive bins with signal magnitudes greater than L_t.

Once the top of a layer is found, the bottom threshold (L_b) is formed based on L_t and the change in molecular scattering from H1 to the current height ($\Delta\beta_m$):

(3.4.11) $$L_b = L_t + \Delta\beta_m$$

Initially, of course, $L_b = L_t$, but as you progress downward, L_b becomes greater than L_t . For thick aerosol layers, L_b can be considerably greater than L_t (see figure 3.4.2). The bottom threshold level will be computed for each bin below bin b1 and compared with the signal level at that bin. The bottom of the aerosol layer is defined as that height (H2) where the first of 3 consecutive bins (b2) are less than L_b.

(3.4.12) $$H2 = 40.0 - (0.0768)b2$$

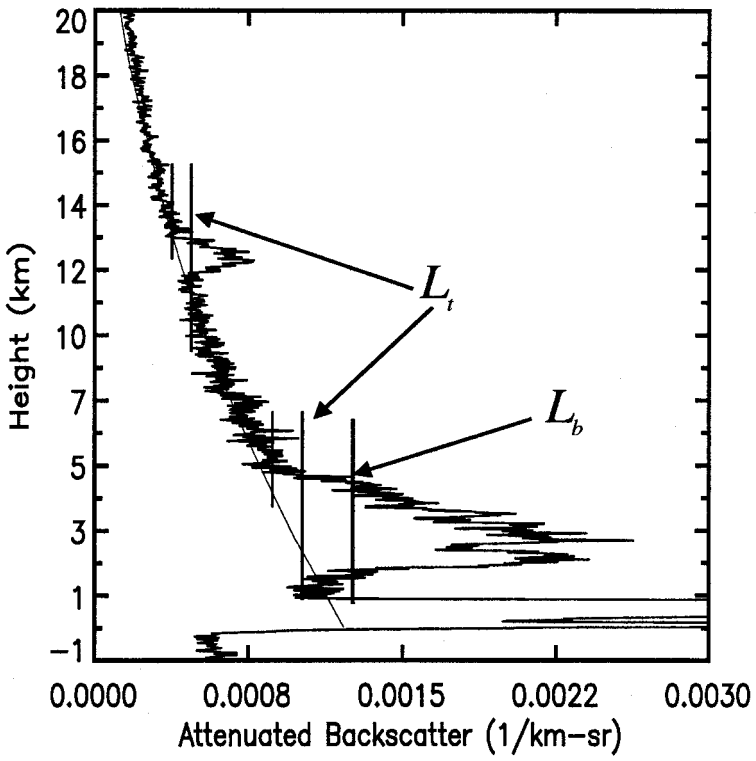

Figure 3.4.2 An example of the signal from a space-borne lidar system (LITE) showing two aerosol layers (13 and 5 km) and a strong ground return at 1 km. The threshold levels for detection of layer top (L_t) and bottom (L_b) are shown. Note how much larger L_b is than L_t for the lower aerosol layer because of the large increase in molecular signal from the top to the bottom of the layer. The molecular backscatter is plotted as a solid, thin line.

The search then continues downward in the profile looking for the next aerosol layer in the same manner as the first, except a new threshold level (L_t) is defined based on the average signal level just below the bottom of the last aerosol layer:

(3.4.13) $$L_t = F\sigma + \sum_{j=b2+1}^{b2+6} \beta_s(j)/6.0$$

where, as before, F is a scaling factor most likely between 3.0 and 5.0, and σ is the standard deviation computed from the 2 km of data just above the aerosol layer just detected. The search is resumed starting from bin b2+6. The 40 to 20 km region is searched for a maximum of 3 aerosol layers, though a large portion of the data will be devoid of aerosol layers in this region. The search continues below 20 km until it reaches the bottom height defined by the highest optically thick cloud within that 20 second segment. If there were no clouds in the segment, then the highest PBL height for that segment is used instead. If layers were found below 20 km, then five, 4 second averages are formed and the 5 profiles are searched for the aerosol layer height using the 20 second average layer height as a guide. If a layer top is found above 20 km, but the layer bottom is located below 20 km, it is considered to be a layer above 20 km.

If b1 and b2 represent the bin numbers corresponding to the top and bottom of an aerosol layer below 20 km, respectively, then to search for the high resolution top and bottom of the layer we first form the vertically smoothed 4 second average profile ($\beta_s(z)$) as:

(3.4.14) $$\beta_s(z) = \sum_{j=1}^{3} S(j)\beta_4(z) \qquad \text{For } z < 20 \text{ km}$$

where β_4 is the 4 second average attenuated backscatter profile and S is the 3 point binomial filter defined in section 3.4.1.1. The search then proceeds much in the same way as for the PBL height. Average signal levels are computed just above b1 and from b1 to b2 which represent the scattering levels above and within the aerosol layer, respectively as:

(3.4.15) $$\beta_{abv} = \sum_{j=b1-6}^{b1-4} \beta_s(j)/3.0$$

(3.4.16) $$\beta_{aer} = \sum_{j=b1}^{b2} \beta_s(j)/(b2 - b1 + 1)$$

where the subscript 'abv' refers to the signal level in the free atmosphere above the aerosol layer. Next, a threshold level (β_a) is defined based on β_{abv} and β_{aer} as:

(3.4.17) $$\beta_a = \beta_{abv} + F2(\beta_{aer} - \beta_{abv})$$

where, as with the PBL, F2 is a scaling factor with a magnitude of about 0.5. With this threshold level thus defined, the 4 second average profile is searched downward in a narrow window from b1-4 to b1+4 for 2 consecutive bins with signal values greater than the threshold level β_a. The first of the two consecutive bins above this level is the bin number corresponding to the top of the layer. The bottom of the layer is found in exactly the same way, except we search backwards, up the profile in a narrow window 9 bins wide. The signal threshold is defined using an average signal below the layer (β_{bel}) and the average signal within the layer (β_{aer}).

(3.4.18) $$\beta_{bel} = \sum_{j=b2+6}^{b2-4} \beta_s(j)/3.0$$

(3.4.19) $$\beta_a = \beta_{bel} + F2(\beta_{aer} - \beta_{bel})$$

where F2 has the same value as in Equation 3.4.17. The search begins at bin b2+4 and continues to bin b2-4, again looking for 2 consecutive bins with a signal value greater than β_a. The first of the two bins above the threshold level (β_a) defines the bottom of the layer. The above process is repeated for each of the five, 4 second average profiles yielding the high resolution elevated aerosol layer heights for the 20 second data segment.

3.4.2 Error Quantification

The accuracy of PBL or elevated aerosol layer height retrieval is governed by a number of factors. These are:

1.) Signal to noise ratio of the data.
2.) Accuracy of satellite altitude and time of laser fire in the absence of a detectable ground return.
3.) Sampling frequency (bandwidth, which determines the vertical resolution of the data).
4.) Number of lidar shots averaged together (horizontal resolution)
5.) Optical depth of the PBL

Factor one encompasses numbers 4 and 5 as the signal to noise ratio increases with the square root of the number of shots averaged and the optical depth of the layer. Thus, the ability and overall accuracy with which we can detect the PBL top at low resolution (30 km, or 160 shot average) is going to be much better than high resolution (1.4 km, or 8 shot average). Since the sampling frequency is every 76.8 meters in the vertical, under the best of conditions, with high signal to noise levels, the PBL or aerosol layer can be resolved to a vertical accuracy of +/- 76.8 meters. As signal to noise values decrease (corresponding to either higher horizontal resolution or smaller aerosol backscatter) the retrieval accuracy will diminish. The magnitude of this effect must be determined by applying the algorithm to simulated GLAS data. For the horizontal resolution we hope to obtain with the GLAS measurements (1.4 km), 76.8 meter vertical accuracy is too optimistic. We estimate that for the high horizontal resolution, the PBL top can be retrieved to within 150 meters. However, under typical conditions we estimate that we can obtain average PBL and aerosol layer height to within 76.8 meters at low resolution (30 km).

PBL height is normally defined thermodynamically based on a rapid increase of potential temperature with height (temperature inversion) and a simultaneous decrease in relative humidity. A number of studies have shown that a rapid decrease in backscatter cross section also occurs at the inversion height, allowing lidar to provide a consistent and accurate measure of PBL height. Thus, we expect that the technique described here will usually yield the thermodynamic height of the PBL, but there are times when this might not be true. For example, elevated aerosol layers can lay directly on top of the boundary layer or there are cases where the boundary layer is growing into a residual boundary layer from the previous day. In these instances, the gradient of scattering at the PBL top might be relatively small and difficult to detect. Instead of yielding the PBL height, the algorithm might pick up the height of the elevated aerosol layer or residual boundary layer. Unfortunately, these types of errors are unavoidable when processing lidar data autonomously, without human interaction.

GLA08 calculates the height of the PBL or elevated aerosol layer with respect to the ground return bin. If the ground return has not been detected from the data (from GLA07 or GLA09 processing), then clouds are assumed to be present. In this case, the algorithm will rely on either the last ground return bin found or a calculated ground return bin based on the onboard DEM value used for that shot. The onboard DEM is accurate to about 200 meters. Thus, when there are clouds obscuring the ground return, there could be a 200 meter error in the determination of aerosol or PBL layer top.

It should be noted that the vertical resolution of the data combined with the technique used to find the PBL height place an upper and lower bound on the height of the PBL which can be detected by the PBL algorithm. It is estimated that the algorithm will have trouble detecting boundary layers which are

less than about 150 m thick. Boundary layers this thin are relatively infrequent but do occur at times near the center of subtropical high pressure ridges over the oceans (and possibly elsewhere). Similarly, the algorithm as coded will not detect boundary layers that are higher than 7 km. As far as we know, the highest boundary layers occur over the Sahara desert and normally range from 4 to 6 km in height.

3.4.3 Confidence Flags

Confidence flags for both the PBL height and elevated aerosol layer height can be constructed out of the difference between the average signal levels outside of the layer and inside the layer (ΔSI). These levels are computed by the respective algorithms as detailed in sections 3.4.1.1 and 3.4.1.2. Basically, the confidence in our height determination increases as ΔSI increases. If β_{aer} and β_{abv} represent the average signal levels inside and above an aerosol layer (or boundary layer) respectively, then we can form the ratio:

(3.4.20) $$\alpha = (\beta_{aer} - \beta_{abv}) / \beta_{abv} = \Delta SI / \beta_{abv}$$

If the value of α is less than or equal to zero, then there is no confidence in the resulting height. As α increases, so does the confidence in the corresponding height measurement. It should suffice to compute and store α for the confidence levels of both the PBL height and elevated aerosol layer height.

Another measure of confidence that could be used is the standard deviation of the heights for a given segment. Normally, for segments less than a few hundred kilometers, the PBL heights should have a standard deviation on the order of 200 to 400 meters. Any significant deviation outside of this range may indicate trouble with the algorithm. This approach could also be used for the elevated aerosols, except that the standard deviation is expected to be somewhat less, perhaps 50 to 200 meters.

3.5 Optical Properties of Cloud and Aerosol Layers

Before we examine the equations that will be used to retrieve optical properties of clouds and aerosols from the GLAS atmospheric data, we will present a short description of the physical processes which govern the light-particle interactions and the notable difficulties in using these.

First, we note that the primary atmospheric observation channel of the GLAS will be at 532 nm. Gas absorption processes are negligible compared to scattering processes at that wavelength and so they will be omitted in the derivation of the particulate optical depths given herein. Ozone absorption, although small, will be factored into the optical properties algorithm by calculating ozone transmission profiles from standard atmosphere databases then dividing the lidar signal profile (attenuated backscatter) by the ozone transmission before regular optical processing begins (See section 3.5.1.1).

The observed or effective optical depth of a horizontal layer of particles between the orbiting lidar and a given altitude is the logarithm of the ratio of a laser's initial normalized pulse energy to its energy at that altitude. Thus, the basic physical effect which permits finding the cloud and aerosol

layers' optical depths is the diminution of the lidar pulse energy as it is scattered or absorbed by the atmospheric constituents. As the laser pulse travels from the instrument, its photons interact with and are scattered (redirected) by the molecular and aerosol particles of the atmosphere. The lidar detector measures those photons which are redirected into a small solid angle centered at 180 degrees (backscattered) into its receiver. The number of laser pulse photons received in a short time interval from a given atmospheric volume are recorded. This quantity is the lidar signal strength. It is proportional to the densities of particles in that volume and the combined scattering characteristics of the particles. These scattering characteristics are strongly affected by the shape of the scattering particles and the size of the particles relative to the wavelength of the laser light. A given scattering volume may contain zero (in a vacuum) to several scattering species each of which has its own density, size distribution, and scattering characteristics.

A major challenge in optical analysis of lidar signals from cirrus clouds is that these clouds are composed of particles whose shapes and size distributions are not readily discernible by any remote sensing techniques. This forces us to incorporate some crucial assumptions in order to obtain quantified results. The validity of these strongly rely upon former experience with cirrus lidar observations (Spinhirne et al., 1990,1996).

In particular, when attempting to obtain cloud optical depth from a spacecraft lidar, two assumptions are required regarding the scattering characteristics of the cloud. One of these assumptions is that the multiple scattering effect can be reliably quantified. The multiple scattering effect is the modification from the true optical depth caused by the increase in detected signal strength due to the portion of the detected signal which has experienced more than one scattering interaction. It is primarily the result of photons that are deflected only slightly during the scattering process. This is referred to as forward scattering and it serves to decrease the perceived optical depth. Ice particles typically have a very pronounced forward scattering component which will cause the multiple scattering effect to be quite significant. Multiple scatter is also a factor for aerosols, though much smaller. From calculations (Spinhirne, 1982), it is estimated that aerosol multiple scattered signals will have less than an 8 percent effect for even the most hazy conditions. Details of the procedure to handle multiple scattering are discussed in section 3.6. The other assumption is that the value of the extinction to backscatter ratio is known. The extinction to backscatter ratio is the total scattered energy divided by the amount of backscattered energy. For a given scattering layer, it is assumed to be constant. Sometimes, under favorable circumstances, this ratio can be estimated from remotely sensed data, but computations based upon satellite observations often will require externally computed values. These are discussed in sections 3.5.1.1 and 4.5.1. The values of both of these parameters are determined by the details of the volumetric scattering phase function that quantifies the scattering effect as a function of scattering angle.

3.5.1 Theoretical Descriptions

3.5.1.1 Transmittance Solution to the Lidar Equation and Calculation of Backscatter Cross Sections (GLA10)

The goal of the optical properties analysis of the GLAS lidar signal is to obtain particulate extinction cross section profiles (σ_p) and particulate layer optical depths (τ_p), involving clouds, aerosols, and

polar stratospheric clouds (PSC's). The discussion given below essentially restates a derivation given many times in the literature. For example, see Spinhirne(1980,1996), Elouragini(1995), and Marenco(1997). The derivation of the multiple scattering factor (η) will be handled in its own section (3.6). At this point one needs to note that transmittance, extinction, and optical depths obtained directly from the solution of the lidar equation are actually the apparent or effective values (Platt, 1979) without multiple scattering effects factored out and are denoted with the superscript prime.

First, as discussed above, ozone absorption must be factored out of the lidar signal. A straight-forward method is to develop ozone transmission squared (T_o^2) profiles derived from standard atmospheric conditions in databases such as LOWTRAN for various climatological regions, based on season and latitude. Next, apply the small ozone attenuation correction factor to the lidar signal, where z is the vertical distance from some arbitrary horizontal plane:

(3.5.1) $P_n(z) = \beta'(z) / T_o^2(z)$.

$\beta'(z)$ is the observed attenuated backscatter cross section discussed in section 3.2 and can be defined as: $(\beta_m(z) + \beta_p(z))\exp[-2(\tau_o(z) + \tau_m(z) + \tau'_p(z))]$. The subscripts *o, m,* and *p* designate ozone, molecular, and particulate contributions, respectively. Furthermore, the influence of the multiple scattering effect (η) on the particulate optical depth is described by:

(3.5.2) $\tau'_p(z) = \int \eta(z)\sigma_p(z)dz \cong \overline{\eta}\int \sigma_p(z)dz$.

The working lidar equation for a spaceborne and nadir pointing lidar has been stated previously and can be rewritten in the following form:

(3.5.3) $P_n(z) = \beta(z)T'^2(z)$,

The left side of the equation is the calibrated normalized lidar signal or attenuated backscatter coefficient corrected for ozone attenuation. The total (particulate and molecular) volumetric backscatter coefficient at z is denoted by $\beta(z)$ and the two-way particulate and molecular transmission factor from z to the spacecraft altitude is given by $T'^2(z)$.

Since the molecular contribution to the total backscatter and transmission can be computed from theory, it is advantageous to separate the scattering terms into components which represent the molecular and particulate contributions independently.
With $\beta = \beta_p + \beta_m$ and $T'^2 = T'^2_p T^2_m$
the equation becomes:

(3.5.4) $P_n = \beta_p T'^2_p T^2_m + \beta_m T'^2_p T^2_m$.

The following relationships must now be defined:

(3.5.5) $T_p'^2 = e^{-2\int \sigma_p' dz}$ and $S_p' = \dfrac{\sigma_p'}{\beta_p}$ (initially assigned a constant for each layer), and

(3.5.6) $T_m^2 = e^{-2\int \sigma_m dz}$ and $S_m = \dfrac{\sigma_m}{\beta_m}$,

where S_p' and S_m are the effective particulate and molecular extinction to backscatter ratios, respectively. T_m^2 (z) can be calculated accurately given the vertical temperature and pressure structure of the atmosphere from MET data or appropriate standard atmosphere data and the fact that S_m is known to be $8\pi/3$ throughout the vertical profile. The purpose of this derivation is to solve the equation for the vertical profiles of β_p. The true particulate optical depth and extinction profiles can be then be computed from the values of S_p, β_p, and η.

From these relationships, we see that:

(3.5.7) $$\frac{d(T_p'^2)}{dz} = T_p'^2\left(-2S_p'\right)\beta_p$$

We can use this relationship to substitute for β_p in (3.5.4) to arrive at:

(3.5.8) $$P_n = -\left(\frac{1}{2S_p'}\right)T_m^2\frac{d\left(T_p'^2\right)}{dz} + \beta_m T_m^2 T_p'^2 \quad \text{or}$$

$$\frac{d\left(T_p'^2\right)}{dz} - 2S_p'\beta_m T_p'^2 = -\frac{2S_p' P_n}{T_m^2}$$

By specifying z as the independent variable and $T_p'^2$ as the dependent variable, this is a first order linear ordinary differential equation; it is a special form of the Bernoulli equation. The solution can be found by using the common integrating factor method where the integrating factor is $F = e^{-2X\int \sigma_m dz}$, and $X \equiv \dfrac{S_p'}{S_m}$. The general solution is:

(3.5.9) $$T_m^{2X} T_p'^2 = -2S_p'\int T_m^{2(X-1)} P_n dz + K$$

where the integrand is defined only where particulates are present and K is a constant of integration.

For convenience, we define the vertical coordinate z as the distance from the spacecraft, increasing downward. If we visualize the situation where the lidar pulse encounters one layer of particulates after traveling through the molecular atmosphere from the spacecraft, we can define the boundary condition (total transmission value) at the top of the layer as:

(3.5.10) $T_p'^2 \equiv T_p'^2(z_t) \equiv 1$ and $T^2(z_t) \equiv T_m^2(z_t)$.

The calculation of $T^2(z_t)$ for multiple layers is covered in Section 4.5.2.

So in general, the two-way particulate transmission within the particulate layer, whether cloud or aerosol, is

$$(3.5.11) \qquad T_p'^2(z) = \frac{T^2(z_t) - 2S_p' \int_{z_t}^{z} T_m^{2(X-1)} P_n dz'}{T_m^{2X}(z)}.$$

Processing continues throughout each particulate layer until $T'_p(z) < T_L$ or the signal from the earth's surface is detected. T_L is a limit defined through error consideration (see section 3.5.2). Extensive automated use of this algorithm has been incorporated into the Global Backscatter Experiment (GLOBE) with aircraft lidar and into the Atmospheric Radiation Measurement (ARM) program with the ground-based Micro pulse lidar (MPL) with good results (Hlavka, 1998).

An important ingredient of this transmission solution is the factor S'_p, which will be assigned as a constant for each layer based on pre-defined look up tables of S_p and η, distinguishing between different cloud and aerosol regimes. Initial decision matrices for S_p look up tables are presented in section 4.5.1. S'_p will be determined as:

(3.5.12) $S'_p = \eta S_p$,

where η, the multilple scattering factor, is separately estimated from appropriate look up selection distingushing between apparent cloud or aerosol type and particle size (see section 3.6). Initial determination of S_p for clouds will be driven by cloud temperature, cloud thickness, and geographic location, with temperature the most important factor. The underlying surface signal attenuation is an additional factor to improve retrievals. When the backscatter profile being analyzed is determined to meet the appropriate criteria for underlying signal analysis, an algorithm to calculate an estimate of S'_p will be called. If S'_p is found to be within tolerances, it will be used instead of the value derived from the look up table. Appropriate criteria would be 1) cloud is optically thin with either a lower cloud or earth's surface sensed and 2) enough clear air (no aerosols) exits both below and above the cloud to determine signal loss through the cloud. Ice clouds above 5 km are the most likely candidates. Under these conditions, the two-way effective cloud particulate transmittance ($T_c'^2$) can be estimated by $T_c'^2 = \frac{e^{-2\tau_c'}}{T_{mc}^2}$, where $2\tau_c'$ represents the loss of signal at cloud bottom compared to cloud top on a natural logarithm scale and is found by least squares analysis of the signal just above and below the cloud. T_{mc} is the total molecular transmission in the cloud. S'_p can then be calculated through an iterative solution from the following equation:

(3.5.13) $$S'_p = \frac{T^2(z_t) - T'^2_c T^{2X}_m(z_b)}{2\int_{z_t}^{z_b} P_n(z) T^{2(X-1)}_m(z)\,dz},$$

where z_t and z_b denote the range at the cloud top and bottom, respectively. A version of this routine has worked well during automated MPL processing of aerosols using the calibrated signal to resolve the layer optical depth similar to the loss of signal in the cloud (Spinhirne, 1999). This routine should also function for PSCs and enhanced upper tropospheric aerosol layers.

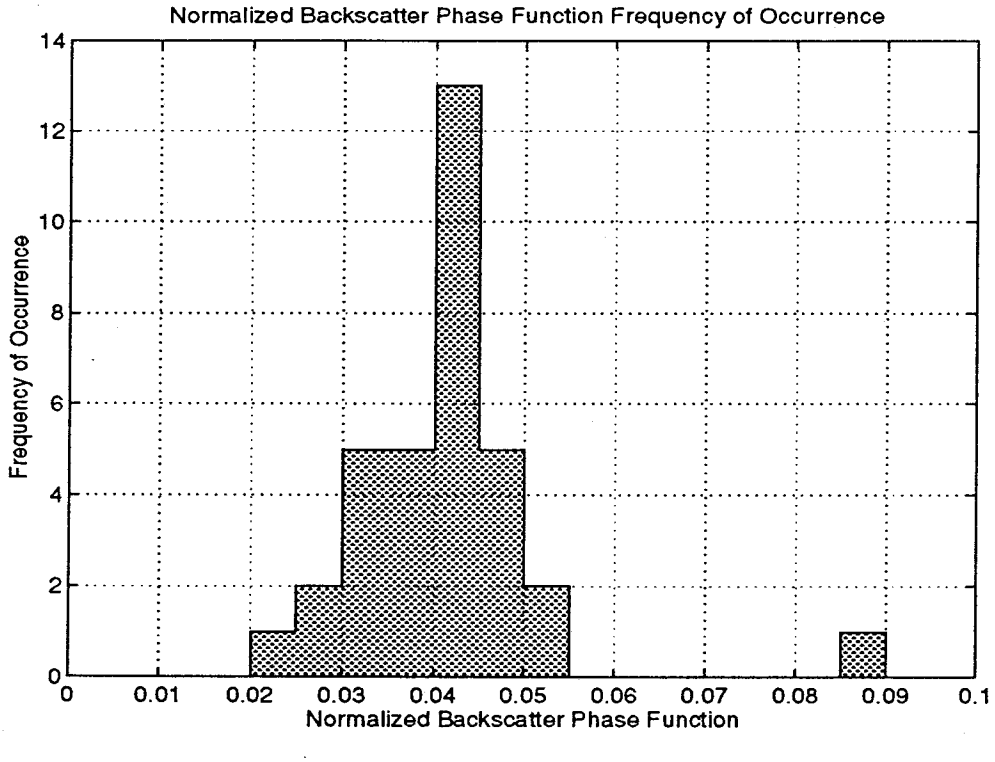

Figure 3.5.1 Phase function ($1/S_p$) for Midlatitude Cirrus Observations

A lidar study of mid-latitude cirrus (Eloranta, 1999) indicates that although S_p can vary by 30 or more, by far the highest frequency of occurrence is near 24 sr (refer to figure 3.5.1). Water clouds have a much lower variation. Determination of S_p for polar stratospheric clouds will be handled as a special subset of the aerosol look up table because they have more of an aerosol origin than a water origin and will be processed at the aerosol time resolution. Determination of S_p for regular aerosol will be driven by geographic location, relative humidity, layer height, layer scattering, surface signal attenuation analysis and possibly wavelength ratios of solar reflectance at 532 and 1064 nm, with geographic location the most important factor. Geographic location can be channeled into three main aerosol regimes: continental, desert, and maritime (Ackermann, 1998) with functions relating the influence of relative humidity. Analysis of the GLOBE data set of 1990 suggests that, on average, aerosol S_p equals 28±5 sr for all height levels, even though there were distinct boundary layer and upper tropospheric layers with different sources. An example is shown in figure 3.5.2.

Note that if $T_m^2(z) \equiv 1$, which means that molecular scattering is negligible at all processing levels, the transmission equation reduces to:

(3.5.14) $$T_p'^2(z) = 1 - 2S_p' \int_{z_t}^{z} P_n dz',$$

which many times is sufficient for cirrus cloud analysis.

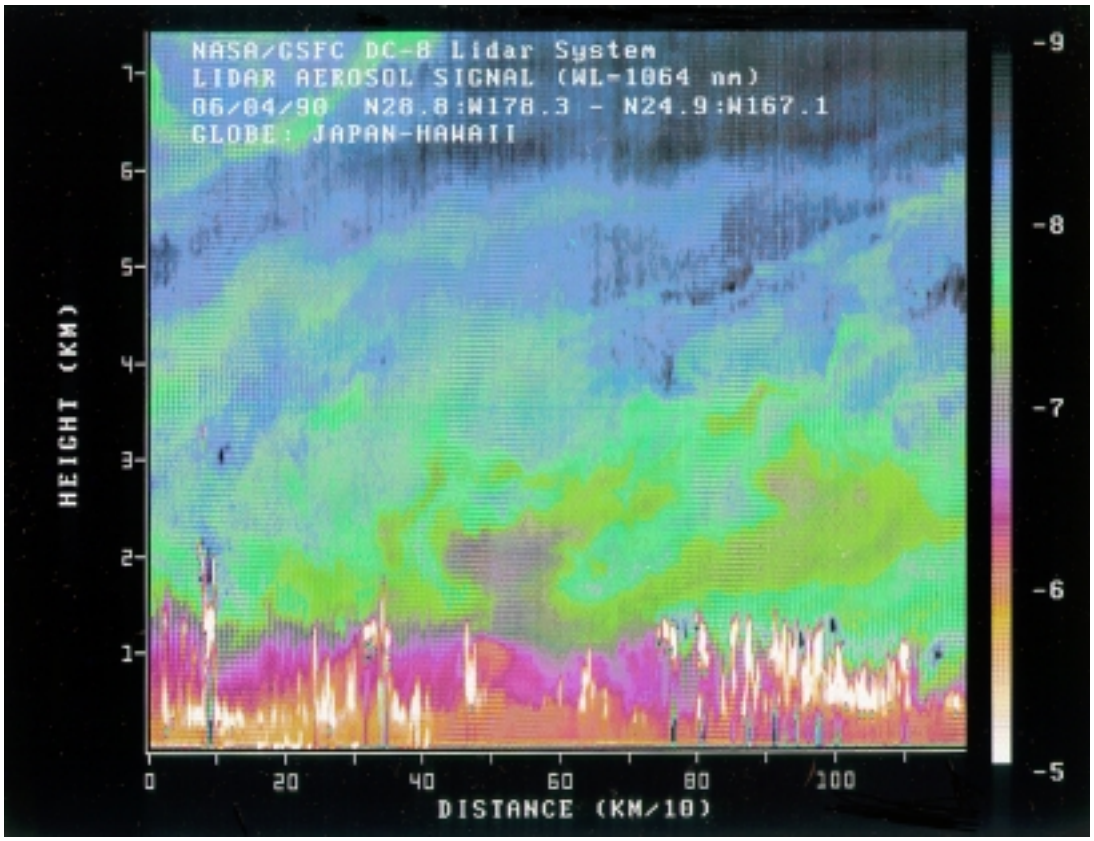

Figure 3.5.2 Despite complicated vertical structure, the GLOBE project showed that S_p did not vary appreciably in the vertical.

Finally, in order to obtain the relative density for aerosol and cloud scattering, it is useful to solve the lidar return signal for the actual particulate backscatter cross section without attenuation. To solve for this backscatter cross section profile, use results from (3.5.11) as input to (3.5.4) by rearranging:

(3.5.15) $$\beta_p(z) = \frac{P_n(z)}{T_m^2(z) T_p'^2(z)} - \beta_m(z).$$

3.5.1.2 Aerosol Extinction Cross Section

Once the particulate effective transmission and backscatter profiles for each aerosol layer sensed have been calculated, it is a straightforward procedure to determine the aerosol extinction cross section profiles. Extinction cross section for particulates (σ_p) is defined as the total scattered energy at height z or the change in optical depth with height:

(3.5.16) $\sigma_p(z) = \frac{d\tau_p(z)}{dz}$, where

τ_p is the particulate optical depth at distance *z* and is defined in Section 3.5.1.4. However, since the backscatter cross section profile has, at this point, already been calculated, the aerosol extinction to backscatter ratio (S_p), earlier obtained through table look up or its relationship with S'_p, could also be easily used to obtain the extinction profile for visible wavelengths:

(3.5.17) $\sigma_p(z) = S_p \beta_p(z)$

Note that multiple scattering has already been accounted for in the calculation of β_p and S_p.

3.5.1.3 Cloud Extinction Cross Section

As discussed in section 3.5.1.1, the calculation of the extinction cross section of clouds from backscatter lidar data requires knowledge of the 180 degree scattering phase function, or extinction to backscatter cross section, (S_p) and a correction, in the case of space born lidar especially, for multiple scattering (η). In all cases an extinction solution, or correction, for cloud lidar can only be applied for a limited range of optical thickness. Our experience with ER-2 remote sensing indicates an upper limit of approximately 1.5 effective optical depth. Signal to noise issues and others will be a factor for other systems, and modeling and testing with simulated GLAS data will determine the applicable limit. In order to determine the effective attenuation, neglecting first multiple scattering, most generally previous work has made the assumption of a constant phase function within cloud layers. With this assumption it is well know that integration of the observed attenuated backscatter cross section for optically thick clouds is equal to half the backscatter to extinction cross section

(3.5.18) $\int B'(z)dz \Rightarrow k/2\eta$ as $\tau \Rightarrow \infty$

By identifying the limiting integral value, a solution for the effective backscatter to extinction value is known. For cirrus, Platt (1979) and others have used infrared emittance to determine asymptotic values. For nadir observations, Spinhirne and Hart (1990) have shown that the disappearance of the surface signal below the cloud can be used to identify the asymptotic value. For real time processing however there are limitations. The assumption must be made that near by thin clouds are in character with dense clouds. Also signal noise and the complexity of real cloud formations can be expected to introduce significant error, based on ER-2 experience. The noise effects and appropriate application routines can be examined from modeling. A more basic limitation is that

the multiple scattering correction to the derived effective extinction is already a large uncertainty term, and complex algorithm development for the effective attenuation may not be warranted.

Another approach to obtaining the extinction cross sections, which is the one we prefer for automated processing, is to start with assumed 180 degree scattering phase functions. For water cloud this is accepted as a good assumption where 17.8 (sr) is widely applicable (Spinhirne et al., 1989; Pinnick et al., 1983). For cirrus, modeling has not shown such an universal value, give the complexity and variation of cirrus shape and size. However experimental measurements have shown, likely because most cirrus are complexes of many different crystal types, that cirrus phase functions values tend to peak statistically toward characteristic values (E. Eloranta, personal communication; Spinhirne et al.,1996). With further work it will be possible to tailor values to geographic location and cloud temperature or height. When the profile is determined to be appropriate for direct S'_p analysis, an algorithm to calculate an estimate of S'_p will be called and the calculated value will be compared to the table. Similarly, modeling for the multiple scattering correction, discussed in a later section, will lead to look up tables for the correction based on the cloud location and temperature.

Given a 180 degree phase function value, we use equation (3.5.17) to get the vertical profile of visible extinction cross section, σ_p of a cirrus cloud from top to the upper limit of the effectiveness of an attenuation correction. Please note that multiple scattering has already been accounted for in the calculation of β_p and S_p.

Any conversion of the visible extinction coefficients in clouds to thermal infrared absorption coefficients will rely on the assumption that the ratio of these two parameters is constant through the vertical extent of a cloud layer. A profile of lidar derived backscatter coefficients can be converted to absorption coefficients by a direct multiplication. The value of this constant absorption ratio, q, can be approximated from the results of theoretical studies. The investigation into cloud infrared absorption conversion will be investigated as a level 3 product.

*3.5.1.4 Cloud and Aerosol Layer Optical Depth (GLA11**)***

A fundamental use of the spaceborne lidar is to detect and quantify the layers of optically dilute clouds that often reside in the mid to high troposphere where the temperatures are cold . These temperatures result in low water vapor density. Because the total amount of water must be conserved, when clouds form, the particle density will likewise be low. Clouds which form at lower altitudes are generally denser because of the greater availability of water. In such clouds, the useful geometrical penetration of the lidar signal is limited because of laser pulse attenuation.

The clouds of interest are generally classified as cirrus clouds. They are usually composed primarily of ice crystals with some coexistent supercooled water droplets. Analysis of PSC's are also of strong interest. Both these clouds often have a sufficiently small optical depth that a meaningful lidar signal can be detected at the bottom of the cloud layer. In these cases, a total layer optical depth can be derived by the lidar. Sometimes, two or more layers exist and the optical depth of each layer can be determined.

The lidar signal can also be used to determine the optical depth of the layer of non-cloud aerosols which reside in the planetary boundary layer. These aerosols can be composed of a variety of

substances that are trapped by the temperature inversion which tends to exist at the top of the boundary layer. In some cases elevated haze layers of significant density are also found higher in the troposphere or stratosphere which have appreciable optical thickness. Examples include volcanic dust layers, smoke layers, and dust layers caused by periodic continental dust storms. The boundaries of any of these layers that are significant would be located by using the backscatter discontinuity algorithm of Section 3.4.

The solution to the lidar equation to obtain particulate effective optical depths (τ'_p) at any range *z* from a nadir pointing spaceborne lidar is by definition a straightforward relationship with the particulate effective transmission calculated in (3.5.11):

(3.5.19) $$\tau'_{\mathrm{p}}(z) = -\left(\frac{1}{2}\right)\ln\left[T'^2_p(z)\right] \quad \text{or} \quad T'^2_p = e^{-2\tau'_p}.$$

This solution will achieve best results in terms of the magnitude of error when applied to situations where the optical depth is relatively small. To evaluate and quantify this declaration we examine the relationships from which τ'_{p} is computed from cirrus data:
We neglect molecular scattering within the cloud such that

(3.5.20) $$T'^2_p(z) = 1 - S'_p 2\gamma(z) \qquad \text{where } \gamma(z) = \int_{z_t}^{z} P_n dz'$$

We see that $T'^2_p(z)$ approaches zero as 2γ approaches $1/S'_p$. Random noise excursions superimposed upon the detected signal can cause the computed value of $T'^2_p(z)$ to become less than 0 as the integral to evaluate gamma is numerically computed from the lidar signal. In this situation, τ'_{p} becomes undefined. Also, differentiation of (3.5.19) and (3.5.20) shows

(3.5.21) $$d\tau'_p = \frac{S'_p d\gamma}{T'^2_p}$$

This means that a given excursion $d\gamma$ causes an error in τ'_p in inverse proportion to the value of T'^2_p; that is, the magnitude of the error becomes larger as the effective transmittance become small and the effective optical thickness becomes relatively large. Based upon experience gained from aircraft lidar studies (Spinhirne, 1990), computational errors in cloud optical depth for GLAS due to random noise remain tolerable until the value of T'^2_p reaches 0.12-0.20 or τ'_p =1.1-0.8. Where the clouds are more optically thick, the lidar cannot give meaningful results. We will discuss the details of computational uncertainty more fully in section 3.5.2.

The specific method we will be using to calculate the particulate layer optical depth stems from the same transmission solution to the lidar equation, put uses the relationship of the extinction cross section profile in the layer (described in sections 3.5.1.2 and 3.5.1.3) to optical depth. The final optical depth products from these calculations will be the optical depth (τ_l) for each of the particulate layers meeting the analysis criteria:

(3.5.22) $$\tau_l = \int_{z_t}^{z_b} \sigma_p(z)dz\,,$$

where z_b and z_t are the bottom and top locations of the particulate layer, respectively and multiple scattering has already been factored out.

The vertical coordinate limits on the integration in the transmittance equation in (3.5.11) will be determined by the cloud boundary algorithm described in Section 3.3. In practice, the integration will be carried out starting at the first particulate layer top. Although the whole molecular transmission vertical profile starting at the top of the atmosphere and ending at the bottom of the lowest particulate layer sensed will have to be calculated, the particulate transmission vertical profile will be calculated only inside cloud and aerosol layers. The total transmission initial condition (3.5.10) at the top of any secondary layer will be the product of the particulate transmission squared at the bottom of the layer above and the molecular transmission squared at the top of the current secondary layer.

The attenuation of the pulse energy due to molecular scattering in the intervening clear air layers is small in the mid to high troposphere where the optically thin clouds reside. The magnitude of the molecular scattering is a significant fraction of the aerosol scattering since the gaseous atmosphere is relatively dense at the low altitudes of the boundary layer and the optical density of the aerosol particles are typically much lower than that found in even cirrus clouds.

Optical parameters would be obtained either empirically or from prior studies for aerosol layers. In practice, three necessary conditions for determination of the boundary layer or elevated haze optical depth will be that: 1) the top of the layer is detected, 2) there is no intervening cloud layer present, and 3) the earth's surface level or a lower particulate layer has been found by the lidar. Evidently, the most prominent source of uncertainty will be how closely the actual aerosols which are being observed match the characteristics of the assumed aerosol type. Re-processing from level 3 extinction-to-backscatter investigations will help reduce these uncertainties.

3.5.2 Error Quantification

The most important optical measurements derived from the lidar measured backscatter profiles are the total effective optical thickness and transmission of particulate layers which are fully penetrated by the laser pulse. We will inspect here the effect that various uncertainties have on the uncertainty of the derived values of these physical quantities.

To begin, we will use the relationships

(3.5.23) $T_p'^2(z_b) = 1 - 2S_p'\gamma(z_b)$ (ignoring the molecular component),

(3.5.24) $\tau_p'(z_b) = -\frac{1}{2}\ln\left[T_p'^2(z_b)\right]$, and define the parameter

(3.5.25) $\alpha = S'_p \gamma(z_b)$, where $0 < \alpha < 0.5$ and $\gamma = \int P_n dz$

The subscript *p* denotes particulate and α will represent actual value of the product which the measurements are attempting to attain. Because practical computations become unstable for relatively optically thick clouds, the useful limits of lidar measurements are exceeded as the value of α goes above 0.475.

Differentiation gives us,

(3.5.26) $$dT'^2_p = -2\gamma dS'_p - 2S'_p d\gamma = -2\left(\alpha \frac{dS'_p}{S'_p} + d\alpha\right) \text{ and } d\tau'_p = -\frac{1}{2T'^2_p} dT'^2_p$$

If we let dS'_p and $d\alpha$ represent deviations from the correct values of the respective parameters, then we can assess the effects that such deviations will have on the derived values of these parameters. To simplify this assessment, we will estimate the effects of each deviation independently.

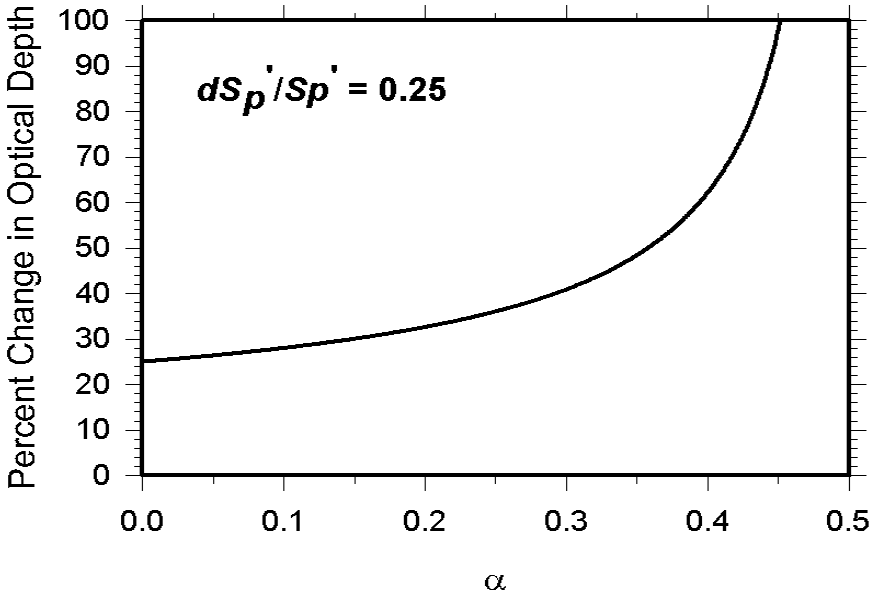

Figure 3.5.3 Computed sensitivity in optical depth from error in S_p'

Figure 3.5.3 shows an example of expected error if $d\alpha \equiv 0$. The plot in the figure summarizes the percent change produced in the computed values of τ'_p by an error of 25 percent in the estimate of

S'_p. The importance of such errors is determined by what the purpose of the computed values are.

The plot in figure 3.5.4 illustrates expected magnitude of deviation in the computed optical depth as a function of α when $dS'_p \equiv 0$ and there is a typical 5 percent error in the magnitude of the integrated backscatter. We see that the magnitude of the error in the optical thickness becomes very large as the limit in meaningful measurements is approached at $\alpha \approx 0.475$. For larger errors in the evaluated magnitude of α, the uncertainty in τ'_p is even larger. A fact that reduces the detrimental effect revealed by these relationships is that, for a given evaluation of optical depth from a lidar profile, the random fluctuation contribution to $d\gamma$ will become smaller as more samples are used to compute the result. This means that for layers of a given optical depth, the error in the optical thickness will be less for layers of greater geometrical depth. These are typically the types of layers of cirrus and aerosols which are the greatest interest to climatological studies.

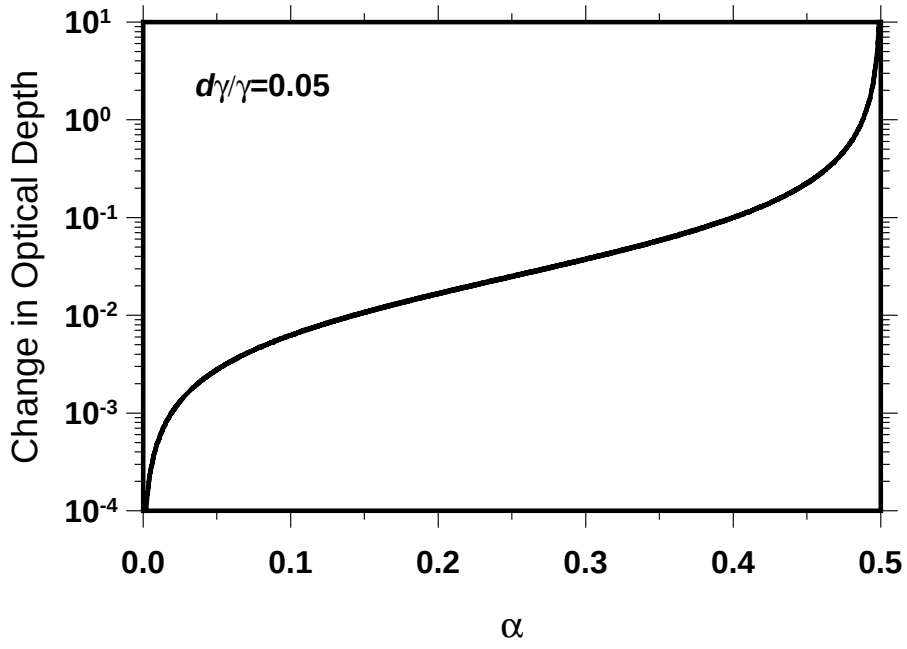

Figure 3.5.4 Sensitvity in optical depth from errors in integrated backscatter

The accuracy of the retrieved backscatter lidar signals relies heavily on the signal to noise ratio of the data. The signal to noise ratio rises and falls with the following:

1) inverse of the strength of the background signal,
2) strength of cloud or aerosol return, and
3) horizontal smoothing of lidar shots.

Errors in the transmittance solution due to lidar signal degradation and atmospheric molecular misrepresentation are discussed further in Section 3.2.2.

The above graphs represent an initial analysis into quantifying errors in optical products from the GLAS atmosphere channel. Error analysis is on-going and will result in more detailed projections during protocode development using simulated lidar returns. Because the particulate transmission is restricted to a value of T_L and above ($.35 < T_L < .45$) to keep the integration stable, effective accumulative particulate optical depth is restricted to ≈ 0.9 or below, and true optical depth is restricted to roughly 3.0, depending on the value of η. With cloud profiles averaged to 1 Hz or 7.5 km and aerosol profiles averaged to .25 Hz or 30 km, we believe optical depths can be calculated to within an error of 50% in the troposphere.

3.5.3 Confidence Flags

Confidence flags for GLA10 and GLA11 will include a measure of quality for the following parameters: aerosol backscatter cross section, cloud backscatter cross section, aerosol extinction cross section, cloud extinction cross section, cloud optical depth, elevated aerosol optical depth, and boundary layer optical depth. Polar stratospheric clouds are incorporated into the aerosol analysis. See Section 4.5.4 for a discussion on quality control.

3.6 Multiple Scattering Correction

The multiple scatter factor is a complex function of particle scattering phase function and the vertical distribution of the scattering plus the field of view and the height of the lidar receiver. A procedure for the correction of the GLAS lidar signal for multiple scattering from cirrus and other optically thin clouds is presented in this section. Two methods have been developed for calculations of GLAS multiple scattering using cloud and aerosol models. One is a precise Monte Carlo radiative transfer model, and the second is a computational fast analytic approximation. However a precise radiative transfer calculation to account for the effects of the multiple scattered contribution is not practical for real time analysis, and approximation by semi-empirical methods is necessary. For initial level 2 processing, the value of the multiple scattering factor may be decision matrixed into a look up table based on parameterized calculations. The best method to ultimately correct for multiple scattering is a subject in development but a preliminary acceptable procedure can be described.

3.6.1 Theoretical description

As was indicated in the optical properties introduction, some of the scattered energy in an atmospheric layer (particularly clouds) will undergo additional scattering and reenter the lidar detector's field of view. This multi-scattered energy is indistinguishable from once scattered energy. The multiple scattering produces an ambiguity in the interpretation of the lidar signal. The laser pulse at any level z appears to be more energetic than would be calculated from the simple optical thickness attenuation.

The component of the lidar signal from multiple scattering arises chiefly due to the strong forward scatter component, or diffraction peak, where the forward scattered photons stay within the receiver FOV. The width of the forward scattering is strongly dependent on particle size and may be approximated by

$$\theta^2_s \approx \lambda^2/\pi^2\mathbf{r^2}$$

where θ_s is the width of the forward diffraction peak containing one-half of the scattered photons and r represents the particle radius. If none of the forward scattered photons were lost from the FOV of the receiver, higher order scattering is neglected, the transmission term in the lidar equation can be written as $e^{-2(\tau-1/2\tau)}$. This is equivalent to $e^{-2\eta\tau}$ where η=0.5. In actuality neither assumptions just mentioned will necessarily hold. Only for the cases where the ratio of the diameter of the receiver FOV foot print at the top of a scattering layer is sufficiently large, and width of the forward peak sufficiently narrow will the approximation be close. However for space borne lidar the FOV footprint is large compared to terrestrial systems, approximately 100 m diameter, and for cloud scattering, especially cirrus, the narrow forward peak is expected. Under these situations prior work with ground based and airborne lidar indicate that the constant η value near 0.5 is an acceptable approximation. A constant value of η can be assumed and variation in the value from 0.5 determined for a first order correction of higher order scattering and loss of photons from the receiver FOV. For aerosol, or extended ranges due to multiple cloud layers, a constant η factor or values near 0.5 will not hold. In any case, values of η as a function of layer heights and propagation depth, and parameterized cloud and aerosol particle models, can be calculated as a basis for look up tables for real time processing.

Given the GLAS 532 nm channel specifications, Monte Carlo calculation show that the multiple scattering effect is expected to be significant (on the order of η=0.5) in cloud situations, but is less than 20 percent (with η=.83) in the worst aerosol situations.

To account for the multiple scattering effect, we assert then the transmittance and optical depths obtained from the solution to the lidar equation are apparent or effective values. For lidar cirrus studies Platt (1981) proposed an extension of the single-scattering lidar equation to account for multiple scattering by introducing the parameter η introduced before:

(3.6.1) $$\tau'_p(z) = \int_{z_t}^{z} \sigma_p(z')\eta(z')dz' = \int_{z_t}^{z} S_p \beta_p(z')\eta(z')dz' \quad \text{and}$$

(3.6.2) $$T'_p = e^{-\tau'_p}$$

The parameter η is the multiple scattering correction factor where $0 < \eta \leq 1$. The superscript prime is used to denote the effective value. Modeling studies have indicated that usefully accurate results can be obtained if a constant value of η is used within the integrations for typical cirrus layers. We use this to obtain:

(3.6.3) $$\tau'_p(z) = S'_p \int_{z_t}^{z} \beta_p(z')dz'$$

where $S'_p = \overline{S_p \eta}$ is denoted the effective extinction to backscatter ratio.

The multiple scattering factor is accurately calculated by Monte Carlo methods or approximated by analytic methods (Duda et al., 1999). As mention above, the η coefficient as a constant value is inaccurate to apply in for aerosol or some cloud layers. However, for the case of cirrus clouds (or other clouds) where the cloud particle sizes are much larger than the wavelength of the lidar, η is shown to be a property of the forward diffraction phase function and can be computed analytically. The question to be answered by a parameterization is the appropriate η factor.

Starkov and Flesia (1998) have developed an analytic formula to compute the multiple scattering correction factor (η) for optically thin cirrus clouds. They assumed that the atmosphere was divided into N arbitrary layers (layers 1 through N) with at least one clear-sky layer (layer 0) above cloud top. Letting the clear-sky atmospheric phase function equal $p_0(\theta,R)$, the cloud phase function in layer i equal $p_i(\theta)$, and θ_i equal the width of the forward diffraction peak for particles in layer i, the multiple scattering correction factor for the nth layer at range R can be computed from:

(3.6.4) $$\eta(R)\tau(R) = \sum_{n=0}^{n-1} \eta_i \tau_i + \eta_n \tau_n(R),$$

(3.6.5) $$\tau(R) = \sum_{n=0}^{n-1} \tau_i + \tau_n(R),$$

where $\tau_i(R)$ is the optical thickness of layer i at range R inside layer L_i

(3.6.6) $$\tau_i(R) = \int_{R_i}^{R} (\sigma_m(x) + \sigma_a(x))dx + \int_{R_i}^{R} \sigma_c(x)dx,$$

($\sigma_m(R)$ and $\sigma_a(R)$ are the molecular and aerosol extinction coefficients in the atmosphere, and $\sigma_c(R)$ is the cloud extinction coefficient)

and

(3.6.7) $$\eta_0 = 1 - 2\pi \int_0^{\theta_n} p_0(\theta, R) \frac{p_n(\pi - \theta)}{p_n(\pi)} \sin\theta \, d\theta,$$

(3.6.8) $$\eta_i = 1 - 2\pi \int_0^{\theta_i} p_i(\theta) \frac{p_n(\pi - \theta)}{p_n(\pi)} \sin\theta \, d\theta.$$

Wiscombe (1977) notes that the backscattering amplitude $p_i(\pi)$ (and similarly the ratio

$p_i(\pi-\theta)/p_i(\pi)$) is one of the most difficult Mie quantities to calculate accurately, and can vary over orders of magnitude for small changes in particle size. If spherical particles are used to compute $p_i(\pi)$, the backscattering amplitude can be integrated over a broad size distribution to make it a smoother function of particle size. Mishchenko et al (1997) have calculated the scattering of light from polydispersions of thin disks and oblate spheroids. Like ice spheres, size averaging in the distribution will smooth out the scattering phase function. If the particles are horizontally oriented, the phase function will have a strong peak at the 180° direction. Macke (1993) has shown using ray-tracing calculations that the backscattering phase function is dependent on the shape of ice crystals as well, ranging from highly peaked functions for crystals having parallel or perpendicular planes (columns) to approaching zero for hollow bullets. Recent calculations and observations, however, suggest that for most cirrus clouds, the ratio $p_i(\pi-\theta)/p_i(\pi)$ from equations 3.6.7 and 3.6.8 may be less variable than might be expected from Mie scattering theory. Nicolas et al (1997) have shown that for clouds with optical depths of one or larger, it may be possible to compute an effective backscattering coefficient that is an average of the scattering properties around 180°. Also, analysis of extinction to backscatter ratios in cirrus from high spectral resolution lidar data (Eloranta, 1999, personal communication) shows that the observed scattering from backscattering angles does not vary as much as theoretical calculations of pure ice crystal shapes. The relative invariance of the observed backscattering coefficients is mostly likely due to averaging effects from the different particle shapes and sizes found in cirrus. Therefore, for clouds with optical depths greater than unity, equations 3.6.7 and 3.6.8 can be approximated as

(3.6.9) $$\eta_0 = 1 - 2\pi \int_0^{\theta_n} p_0(\theta, R)\, p_{eff}(\pi) \sin\theta \, d\theta,$$

(3.6.10) $$\eta_i = 1 - 2\pi \int_0^{\theta_i} p_i(\theta)\, p_{eff}(\pi) \sin\theta \, d\theta,$$

where $P_{eff}(\pi)$ is the effective backscattering coefficient. Note that in equations 3.6.9 and 3.6.10, if $P_{eff}(\pi)$ is equal to one, then $1-\eta$ equals the portion of energy scattered in the forward diffraction peak.

From diffraction theory, the width of the diffraction peak may be alternatively defined as $1.21\ \lambda/d$, where λ is the lidar wavelength and d is the particle diameter. Using this definition of the diffraction peak width, the portion of the energy scattered in the peak can be calculated for ice spheres from Mie theory. The results are presented for the 0.532 nm channel in Figure 3.6.1 as a function of particle radius. For monodisperse spheres, the scattering in the diffraction peak oscillates. The central line in Figure 3.6.1 represents the diffraction peak scattering for a broad size distribution of particles, in which the size averaging tends to smooth out the oscillations.

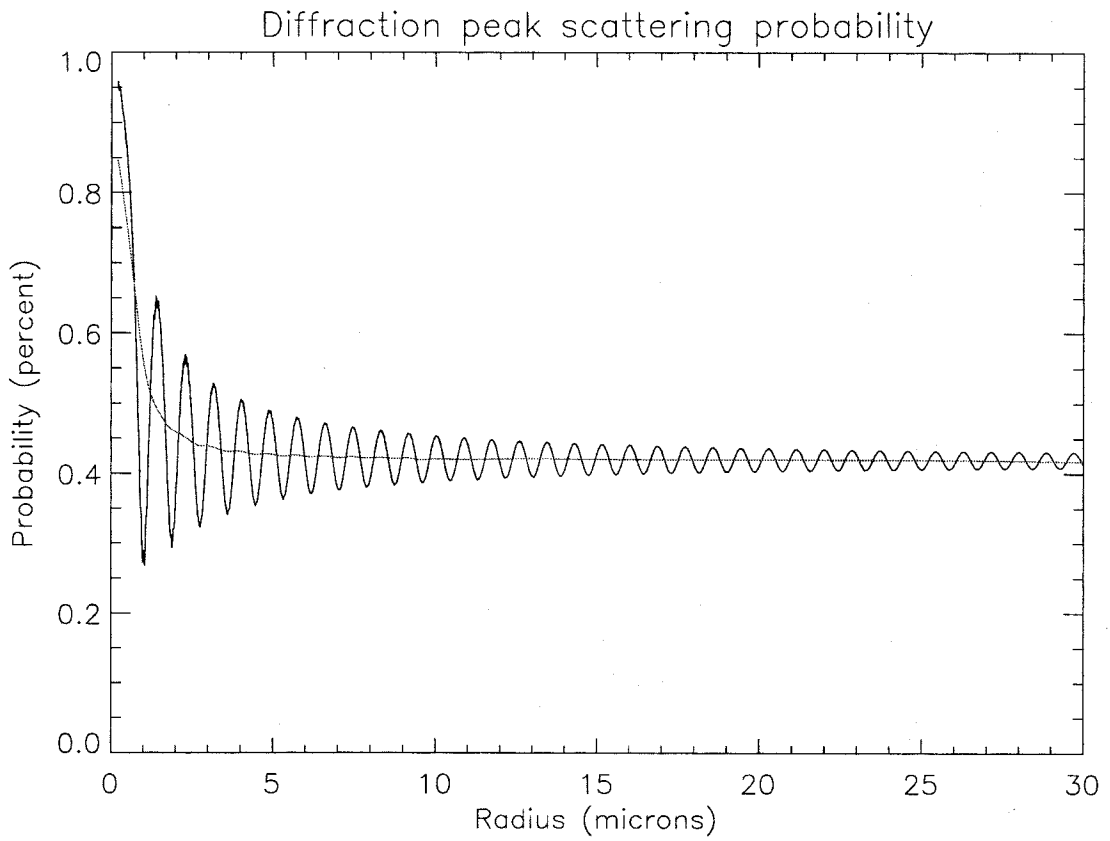

Figure 3.6.1 The portion of the energy scattered in the diffraction peak as a function of particle radius for ice spheres. For large particles, the portion approaches 0.42.

As the particle size increases, the fraction of the energy scattered into the diffraction peak approaches 0.42. Nicolas et al. introduce a similar model where the amount of energy scattered within the forward peak (1 - η) is given as

$$1-\eta = \frac{0.5}{\omega} + R, \tag{3.6.11}$$

where ω is the single-scattering albedo and R is a measure for nonspherical particles that describes the fraction of light refracted into the forward direction through opposite parallel faces.

From the methods and results as described above plus other available knowledge appropriate values to apply in calculations can be obtained. Also values of η for cirrus analysis can be parameterized based on the height of the cirrus layers and observed depth. As an example of the effectiveness of approximations, values of η beneath cirrus are shown as determined from accurate Monte Carlo calculations in figure 3.6.2. For a given depth below the cloud the η value is seen to be independent of optical depth as required. In addition the value immediately below the cloud has an η of approximately 0.4. The increase for depths below cloud base more than 2 km greater are not dramatic.

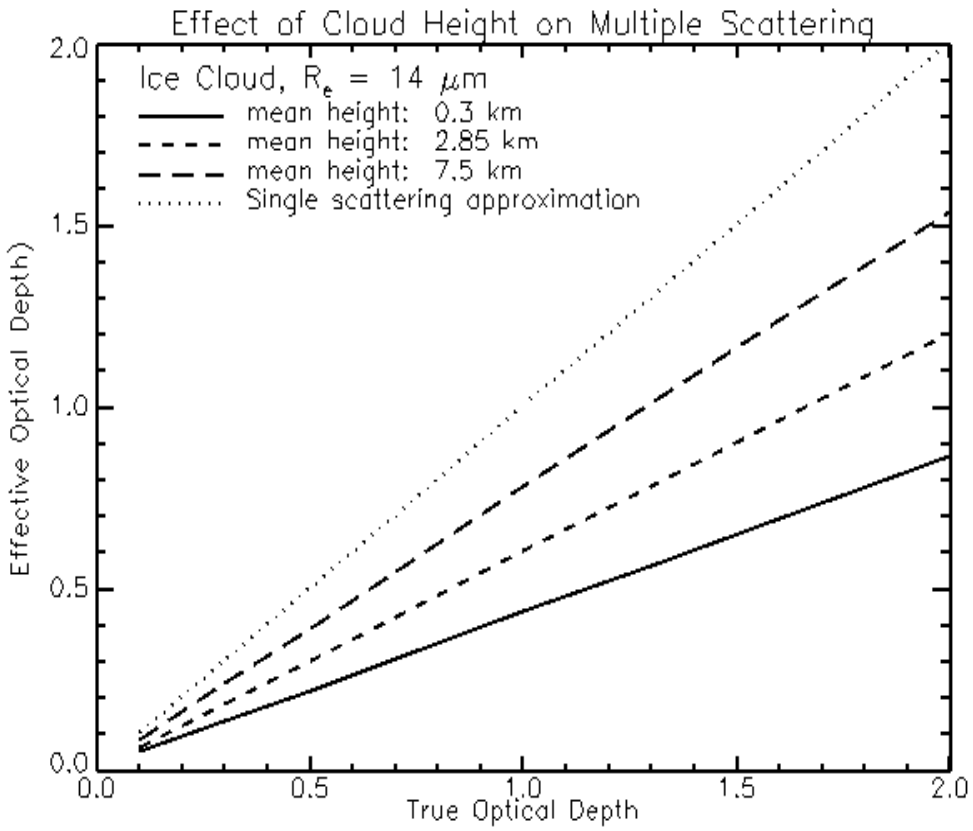

Figure 3.6.2 Cloud height plays an important role in determining multiple scattering from ice clouds. The results of Monte Carlo calculations of the apparent optical depth at the surface as a function of the true optical depth for differing cloud layers is shown. The lower the cloud, the lower the ratio of effective to true optical depth, or η.

A cloud classification based on cloud temperature, geographic location, cloud height, and integrated backscatter in the layer will be used to parameterize a systematic cloud multiple scattering factor look up table. The table will be generated by systematic Monte Carlo calculations supplemented by analytic models.

For aerosol, there is typically not the sharp forward scattering peak as there is for cloud and there larger particles. The approximation for a constant η with depth is not expected to hold as well for clouds. However the initial Monte Carlo calculations or GLAS parameters for the aerosol multiple scattering indicate that the multiple scattered component of the lidar signal is no more than 20%. Also most generally the more optically thick aerosol are concentrated in thin layers at the surface. The approximation of a constant η for aerosol will be tested. It is expected that the errors will not be a dominant uncertainty for optical depth retrievals. A scene classification based on geographic location, integrated backscatter in the layer, and aerosol height distribution plus a systematic aerosol multiple scattering calculation look up table will be used for an η factor. For a layer labeled as PSC, a special subset of the aerosol look up table will be used. Errors in η extracted from look

up tables based on modeled results have yet to be formulated due to the design work still in progress.

4 Practical Application

This section address the practical issues related to coding, implementing and running the algorithms. These topics include the type and source of input data required to run the algorithm, execution time, program flow considerations (execution order), and examples of output where appropriate. Each algorithm will be addressed separately, and in the same order they were presented in section 3.

4.1 Normalized Lidar Signal

4.1.1 Required Input Data

In addition to the raw lidar return signal for each channel, the normalized lidar signal (GLA02) algorithm will require the laser energy (reported at 40 Hz) and the two background measurements. Also required are the dead time correction table for the 532 photon counting channel, the Digital to Analog (DA) lookup table which is used to convert the 1064 digital counts to a voltage and the 1064 programmable gain amplifier setting. While not explicitly used in the algorithm, the 532 channel etalon filter settings should be supplied, as it will be needed in subsequent processing (GLA07). The first data bin of the 532 channel is supposed to be 40 km above local DEM. In order to compute the range (R) used in equations 3.1.1 and 3.1.2, either the height of the GLAS satellite or the time delta between laser fire and the start of data (the first 532 data bin) will be needed. While not required, it is assumed that Global Positioning System (GPS) time and position (latitude and longitude) will be provided in the input data stream.

4.1.2 Algorithm Implementation

This algorithm is relatively easy to implement and does not require a large amount of CPU time. A version of this routine has been coded in the C programming language and run with simulated GLAS data on a Silicon Graphics Indigo II workstation (R10000 processor). Results indicate that to process an orbit of data would take about 1 minute of CPU time. There will be 3 main loops for the processing of the 3 distinct data layers (2 layers for the 1064 channel). The data in the upper two layers for the 532 channel must be normalized by the number of shots summed in that layer before being used in equations 3.1.1 and 3.1.2 (as will the top layer of the 1064 channel). The bottom layer of both channels do not need normalization as they are single (un-summed) shots. Note that the laser energy must be computed at 5 Hz for the 1064 and 532 channels in order to compute P' from the 8 shot summed data (the 10 to 20 km layer). For the 532 channel, the laser energy at 1 Hz must also be computed in order to use equation 3.1.1 in the upper layer. Similarly, the background must be computed at 5 and 1 Hz in order to process the data in the 10 to 20 km layer and the 20 to 40 km layer (532 only), respectively. These calculations should take place as the 40 Hz data are being processed, using the 40 Hz laser energy and background values.

The saturation flag applies only to the 532 channel and will take the form of profiles, each bin of which will have a one-to-one correspondence with the data bins of the 532 channel. It will be a one byte value, where zero indicates that the 532 channel is not saturated and 1 denotes detector saturation. Whether a 532 bin is saturated will be determined from the magnitude of the 532 signal in that bin. The level at which saturation occurs will be determined during calibration procedures in the laboratory.

The predicted height of first cloud top will be calculated at 5 Hz using the raw 532 channel data, which means that an 8 shot average of the data from the lowest layer must be computed. This would be tacked on to the corresponding normalized 8 shot sum form the middle layer to form a profile from –1 to 20 km (at 5 Hz). A search would then begin as described in section 3.1 to find the first bin which exceeds a cloud threshold level, which will be about 10 photons per bin. The bin number that exceeded the threshold will be stored and the height will be calculated as described in section 3.1.1. The 5 Hz profile that is used to find the height of the first cloud top is not saved as output. It is discarded.

After the normalized signal for the 3 layers is computed using 3.1 and 3.2, it must be scaled to fit in a 4 byte signed integer. A signed integer is required because P' can be negative (due to the subtraction of the background value). The fairly large dynamic range of the computed signals warrants the use of a four byte integer. The scaling can be accomplished by applying a simple multiplicative scaling factor.

.

4.1.3 Interpreting the Output

The output from GLA02 consists of calculated parameters as well as passed-through quantities which are not calculated or used by the algorithm, but which will be used in the creation of level 2 data products. A list of all GLA02 output follows:

1. P at 532 nm for 3 layers: -1 to 10 km (40 Hz), 10 to 20 km (5 Hz), and 20 to 40 km (1 Hz)
2. P at 1064 nm for 2 layers: -1 to 10 km (40 Hz) and 10 to 20 km (5 Hz)
3. .532 nm saturation flag for the 3 layers: -1 to 10 km (40 Hz), 10 to 20 km (5 Hz), and 20 to 40 km (1 Hz)
4. Predicted height of first cloud top (5 Hz)
5. Ground return flag (bin number) and maximum ground signal
6. 532 background (40, 5 and 1 Hz) and 1064 background (40 and 5 Hz)
7. 532 laser energy (40, 5 and 1 Hz)
8. 1064 laser energy (40 and 5 Hz)
9. 532 laser energy quality flag (40 Hz)
10. 1064 laser energy quality flag (40 Hz)
11. 532 integrated return from 40 to 20 km (1 Hz)
12. 532 quality flag (1 Hz) – based on 11 above
13. 1064 nm programmable gain amplifier setting (1 Hz)
14. 532 nm etalon filter parameters (1 Hz)
15. GPS time (1 Hz)

Items 1 through 8 have been thoroughly discussed in section 3.1. The 532 and 1064 channel laser energy quality flags (9 and 10) are discussed in section 4.1.5 below, as is the 532 integrated return and associated quality flag (11 and 12). The 1064 programmable gain amplifier setting (13) is used to compute the normalized signal (Equation 3.1.2) and should be reported in the GLA02 input data stream. The 532 nm etalon filter parameters are as yet unspecified but should provide a measure of how well tuned the etalon was to the laser frequency. The etalon filter parameters are not used in GLA02, but may be needed in subsequent processing.

4.1.4 Quality Control

At this early stage of data processing quality control should be directed at assessing the health of the instrument and the fundamental soundness of the lidar return signal. The health of the laser can be assessed by monitoring the laser energy. For each channel, a quality flag should be set for every shot (40 Hz) which characterizes the laser as follows:

1 = full laser energy (within 90 percent of expected max value)
2= marginal laser energy (between 90 and 70 percent of expected max value)
3 = deficient laser energy (less than 70 percent of expected max energy)

Used in conjunction with the above flags, the boresite can be assessed by integrating the 532 return signal from 40 to 20 km altitude (I_s). This could be done using raw photon counts after the background (computed from equation 3.1.3) is subtracted out. A quality flag should be set much like for the laser energy flag above, depending on the magnitude of the integrated return. Based on simulations, the expected number of integrated photons (the summation of 268 bins) per second from this region of the atmosphere is about 1900. For the 532 channel a quality flag can be formulated as follows:

1= excellent signal strength ($I_s > 1800$)
2= good signal strength ($1400 < I_s < 1800$)
3= marginal signal strength ($1000 < I_s < 1400$)
4= poor signal strength ($500 < I_s < 1000$)
5= bad data ($I_s < 500$)

These limits are based on simulations and may be adjusted up or down after actual data are acquired.

4.2 Attenuated Backscatter Cross Section

4.2.1 Required Input Data

This algorithm requires the output from GLA02, the normalized lidar signal and associated output as described in section 4.1.3. In addition to this, the GLA07 algorithm requires MET data in order to compute the molecular backscatter cross section at the various calibration heights (see equations 3.2.1 and 3.2.2). Realizing that MET data will most likely not be available at all times, it is important to also provide the standard model atmosphere as a backup source to obtain the required temperature and pressure profiles. The standard atmosphere actually consists of 5 models defined

roughly by latitude and season as follows: Mid latitude and arctic for both summer and winter and tropical (5 standard atmosphere models in all). Additional required input includes the precision orbit determination (POD) data which includes latitude, longitude and spacecraft altitude. In order to transform the data height coordinate from above local DEM to above mean sea level, we need to know the DEM value used onboard the spacecraft for each second. This vertical shifting of the data is discussed more fully in section 4.2.2 below.

4.2.2 Algorithm Implementation

The main function of this algorithm is to compute and apply the lidar calibration constant to the data to form a continuous 5 Hz profile of attenuated backscatter cross section from 40 to –1 km for the 532 channel, and from 20 to –1 km for the 1064 channel (the altitude is with respect to mean sea level). In addition, 40 Hz profiles from 10 to –1 km will also be generated for both channels. The calibration constant (C) will be computed twice per orbit, in pre-defined latitude bands, 45 to 60 degrees wide at two altitudes for the 532 channel and at one height for the 1064 channel. While calculating C, an average background value will also be calculated so that each C value can be labeled day, night or undetermined as described in section 3.2.1. After the C values are calculated, one or an average of both (for the 532 channel) would be applied to all the data from that point until the end of the next C calculation (1/2 orbit later). However, the implementation of the algorithm will include a flag which will be used to tell the program how often to apply the newly calculated C value. This is something that we will not know until after we have a chance to analyze the stability of the C values. This scheme requires that initial values of C for both channels be specified. These will come from laboratory calibration measurements. The ability to compute accurate C values for the 1064 channel is in doubt. The algorithm will perform the calculations for the 1064 channel as described in section 3.2.1, but, at least initially, the laboratory calculated 1064 calibration constant will be used in equation 3.2.7. If subsequent analysis indicates that the 1064 C calculated from the flight data is good, then it may be used. Thus, for the 1064 channel, a flag should be built in which tells the software to use the laboratory C value or the C calculated from the atmospheric data.

The calculation of the lidar calibration constant requires the construction of accurate molecular backscatter profiles through the calibration layer(s). Since the entire (0 to 40 km altitude) molecular backscatter profiles will be required by other GLAS atmospheric data product modules, it makes sense to compute them here. When this is done from MET data or from standard atmosphere data, it will be required to interpolate between the standard pressure levels to a vertical resolution equivalent to the lidar profile (76.8 m) as discussed in section 3.2.1. Since the molecular scattering depends only on atmospheric density, it makes sense to first compute the density from the temperature, relative humidity and pressure at the geometric heights corresponding to the standard pressure levels and then use the hypsometric formula to compute the density between the standard heights. This will result in a smooth density profile with 76.8 meter vertical resolution.

It should be noted that while C is being calculated, the previous value of C is simultaneously being applied to the data via equations 3.2.6 and 3.2.7. Additionally, it must be recognized that each bin of the lidar data for a given second is not necessarily at the same altitude (above mean sea level) as the corresponding bin number of the profile acquired one second before or later. This is a result of the way the data are being acquired on board the spacecraft. For each second, the time (relative to laser fire) to gate on the 532 detector will be calculated from the GPS altitude of the spacecraft (above mean sea level) and the height of the topography at the nadir point of the spacecraft

determined from an onboard DEM. What this means is that the top bin of the 532 channel is always 40 km above the local topography, not above sea level and further that as topography changes, so will the height (above sea level) of a given lidar bin. Thus, the profiles have to be shifted by the appropriate value in order to put them in the proper reference frame (above mean sea level). To accomplish this, the DEM value used onboard the spacecraft for that shot (to compute the time to start data acquisition) must be known. It is our understanding that the time of the start of data acquisition will only change on second boundaries, and thus it can be assumed that all the data within a second do not have to be vertically shifted. The number of bins to shift is calculated by dividing the DEM value (in meters above mean sea level) by 76.8.

The output consists of 5 Hz full profiles (-1 to 40 km for 532 and –1 to 20 km for 1064) and 40 Hz profiles of only the lowest layer (-1 to 10km). In order to form the 532 full profile, 8 shots of the lowest layer are averaged and the corresponding 8 shot sum (after being normalized) of the middle layer (10 to 20 km) is placed above that, with the normalized 40 shot sum profile (20 to 40 km) above that. The same 20 to 40 km profile is used repeatedly for each of the 8 shots for a given second. The result is a 5 Hz full profile from –1 to 40 km with respect to mean sea level. For the 1064 channel, 8 shots of the lowest layer are averaged and combined with the normalized 8 shot sum of the middle layer to form one 5 Hz profile from –1 to 40 km. Note also that the 532 saturation flag full profile (5 Hz, -1 to 40 km) must also be formed. In this case, instead of averaging in the lowest layer, we sum up the saturation flag for the eight shots yielding a number between 0 and 8. This is then combined with the saturation flag from the middle layer and the saturation flag profile from the upper layer (which is repeated 8 times).

The algorithm is not computationally intensive. A version has been coded in the C programming language and run with simulated GLAS data on a Silicon Graphics Indigo II workstation (R10000 processor). Results indicate that to process an orbit of data would take about ½ minute of CPU time.

4.2.3 Interpreting the Output

The output of GLA07 consists of profiles of calibrated attenuated backscatter cross section and the calibration constants for both channels. The 532 channel will consist of 5 Hz, -1 to 40 km (534 bins) and 40 Hz, -1 to 10 km (144 bins) profiles which have had saturated bins replaced with estimated cross section provided by the 1064 channel. An example of one 5 Hz profile output from the algorithm is shown in figure 4.2.1. This calibrated, attenuated backscatter profile was created by running a prototype GLA07 algorithm on simulated GLAS data produced by the GLAS Atmospheric Lidar Simulator (GALS)..

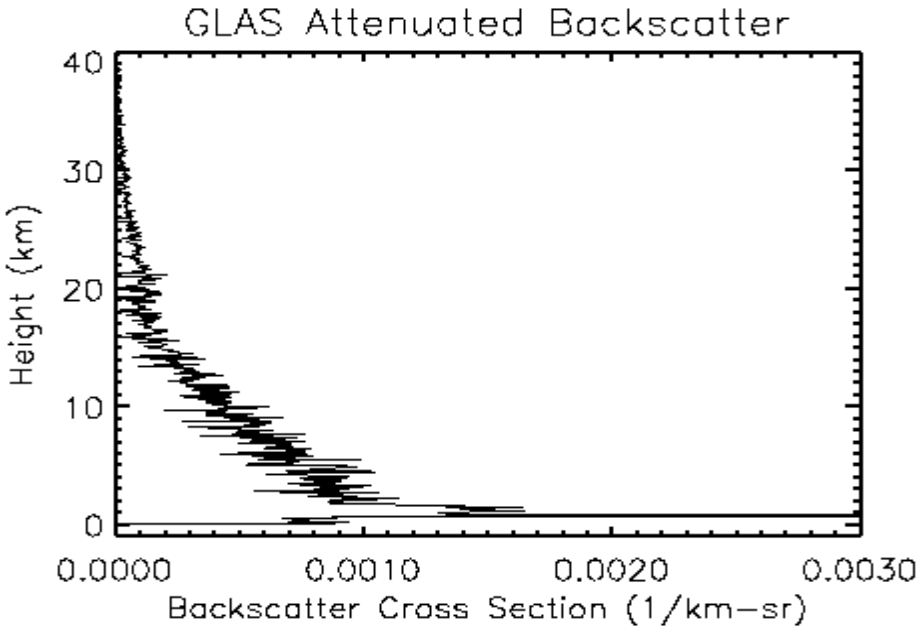

Figure 4.2.1. An example of a 5 Hz attenuated backscatter profile from 40 to –1 km which is output from the GLA07 algorithm. The profile was made by running a prototype version of the GLA07 algorithm on simulated nighttime GLAS data produced by the GLAS Amospheric Lidar Simulator (GALS).

Comparison of the above plot and figure 3.2.2 shows that the profile closely follows the molecular return until the top of the PBL is reached (at about 1.5 km height). Scattering within the PBL is much larger than the molecular scattering level due to the high concentration of aerosol there. Also seen in the figure is the large ground return signal which is truncated by the compressed scale. It is in reality several orders of magnitude larger than shown.

In figure 4.2.2, we have assembled many such profiles together and presented them in image form. This is probably the most informative way to display the data because it contains so much information. At a glance, one can see the various cloud layers, the boundary layer height and structure and any elevated aerosol layers that might be present.

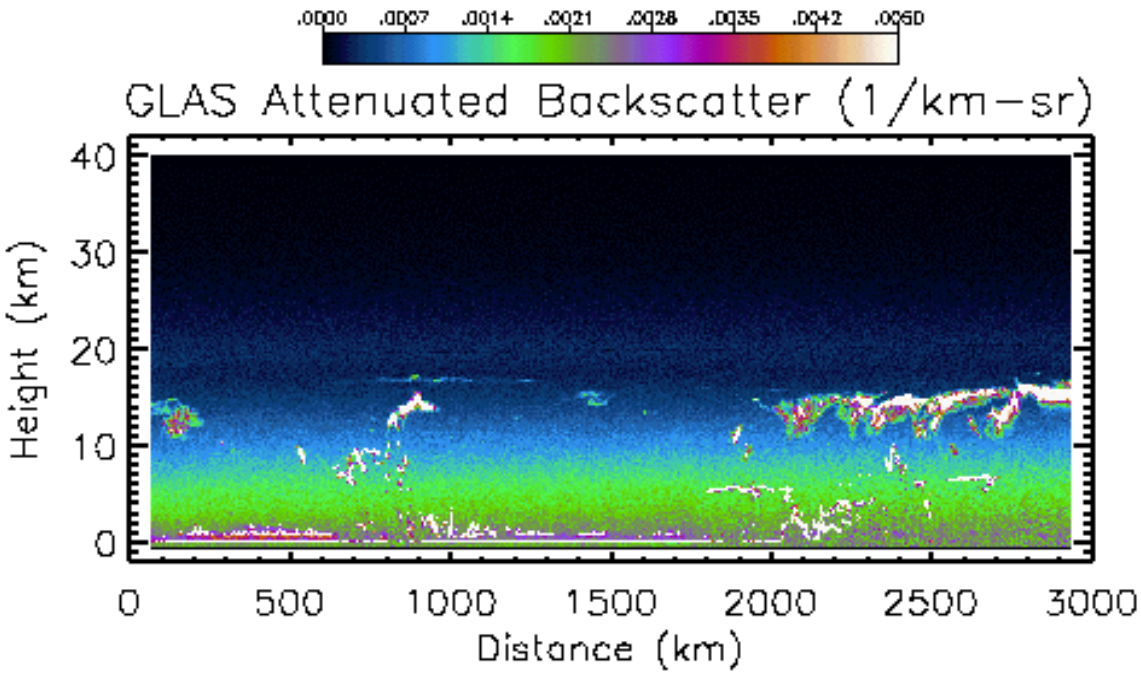

Figure 4.2.2. Attenuated backscatter cross section displayed in color image form. The image is comprised of 2000 separate 5 Hz profiles like the one shown in figure 4.2.1.

In addition to the backscatter profiles, the calculated calibration constants for both channels at the two heights are output as are the actual calibration values used in equations 3.2.4 and 3.2.5. Remember that the program is designed to use either the calculated value, a previously calculated C value or the laboratory calibration constant. With each calibration cycle (which occurs twice per orbit) a flag will be generated which characterizes the background condition (day, night or undetermined) which exisited during the calculation of that C value.The 532 saturation flag profiles will be output at 5 Hz for –1 to 40 km and 40Hz for –1 to 10 km as described in section 4.2.2.

The profiles of attenuated backscatter cross section, which are the main output from GLA07, will consist of 534 bins, each 76.8 meters wide and stretch from 40 km to –1 km above mean sea level. The process of shifting the bins to compensate for the varying topography will mean that some of the data will be cut off on top and some will be buffered with a missing data value at the end of the 548 bin profile. For example, if data are being acquired over a region which is 5 km above mean sea level (as determined from the onboard DEM), the resulting acquired 532 profile will actually cover the region 45 to 4 km above mean sea level. The profile which will be output from GLA07 will truncate the 5 km of data above 40 km, and fill the region of the profile below 4 km with a missing data value (-999 is suggested). The same is true of the 1064 channel, except it extends to only 20 km above mean sea level. Note that there will be a small percentage of time where the data are cut off at the bottom of the profile and padded at the top. This would occur when the DEM value is less than mean sea level. A complete list of the output for GLA07 follows:

1. 532 nm attenuated backscatter cross section, 40 to –1 km above mean sea level at 5 Hz
2. 532 nm attenuated backscatter cross section, 10 to –1 km above mean sea level at 40 Hz
3. 1064 nm attenuated backscatter cross section, 20 to –1 km above mean sea level at 5 Hz
4. 1064 nm attenuated backscatter cross section, 10 to –1 km above mean sea level at 40 Hz
5. 532 nm saturation flag profiles, 40 to –1 km above mean sea level at 5 Hz and 10 to –1 km at 40 Hz.
6. 532 nm calibration constants – C_{30}, C_9 , and the C value that was used in equation 3.2.4
7. 1064 nm calibration constants – C_{18}, C_9 , and the C value that was used in equation 3.2.5
8. Calibration constant day/night flag (see discussion, section 3.2.1)
9. Calibration constant quality flag (se discussion section 4.2.5, below)
10. Ground return bin as determined from POD and DEM
11. Predicted height of first cloud top, 5 Hz
12. Ground return flag (bin number) and maximum ground signal
13. 532 nm background at 40 and 5 Hz
14. 1064 nm background at 40 and 5 Hz
15. 532 laser energy at 40 and 5 Hz
16. 1064 laser energy at 40 and 5 Hz
17. 532 laser energy quality flag at 40 Hz
18. 1064 laser energy quality flag
19. 532 nm integrated return from 40 to 20 km at 1 Hz
20. 532 quality flag (1 Hz) based on 17 above
21. 1064 programmable gain amplifier setting (1 Hz)
22. 532 nm etalon filter parameters (1 Hz)
23. GPS time (1 Hz)
24. Precision Orbit Determination (POD) data (1 Hz)
25. Onboard Digital Elevation Model (DEM) value used (1 Hz)

Items 1 through 10 are calculated by GLA07. The remaining output is either from the output of GLA02 or another input source.

4.2.4 Quality Control

Quality control should be implemented during the calculation of the calibration constant by checking the data quality flags that were generated by GLA02. Specifically, the laser energy flag and the integrated (20 to 40 km) return flag should be used to eliminate bad shots. Based on these flags, a bad shot counter should be kept during the calculation of C. If the number of bad shots exceeds say 2 percent of the total number of shots expected to be processed for a given calibration cycle (there are about 27,000 shots per 1/8 orbit), then the C value calculated for this calibration cycle should be flagged as questionable. Also time continuity must be checked during the calculation of C to check for large time gaps in the data that might adversely affect the calculation of the calibration constant. If a time gap greater than 30 or 40 seconds is encountered (total time for 1/8 orbit is about 675 seconds), the calibration constant should similarly be flagged as questionable.

The quality of the calibration constant can be assessed by looking at its variability with time and the difference between the constants calculated at the two different heights. The 532 nm attenuated

backscatter cross section profiles can be checked by normalizing them by the attenuated molecular profile. This should produce a profile that ranges between 0.9 and about 10.0. This test could only be applied to data with a ground return as the values below thick clouds will approach zero.

A test that could be applied to all the data would be to integrate the attenuated backscatter (β') from 40 to 20 km and divide by the integrated attenuated molecular backscatter ($\beta_m T_m^2$) to form a ratio that should be very close to unity. A major deviation from one would indicate a problem.

4.3 Cloud Layer Height and Earth's Surface Height (GLA09)

The implementation of the algorithms to find vertical cloud boundaries and the height of the earth's surface (ground height) will require only modest resources in terms of coding and execution time. The processing will be done on a time series of 4-second segments. Each of these will be composed of matrices of values consisting of on the order of 10000 points. Only elementary arithmetic computational and logical functions and testing will be done on these to produce the output. The output will consist of tables of values, numbering in the range of 500-1000.

4.3.1 Required Input Data

The vertical boundaries of the horizontal surfaces of cloud layers and the earth's surface will be found by testing profiles of attenuated backscatter coefficients (backscatter cross-section) against thresholds developed from the profiles themselves. The profiles will be those developed in GLA07. Only the profiles from the 532nm channel will be needed. The following list summarizes the required input for each 4-second granule.
a) 160 40 Hz attenuated backscatter coefficient profiles, -1-10 km, from GLA07;
b) 20 5Hz attenuated backscatter coefficient profiles, -1-40km,
c) 4 sets of 1-second DEM values corresponding to the 4-second processing interval, with each set containing the mean, maximum and minimum values of the height of the earth's surface in the local 1-degree square grid
d) one current atmospheric profile, 0-20km, containing pressure, temperature and height.

4.3.2 Algorithm Implementation

Cloud boundary searches will be limited to the lowest 20 km above ground level.
For each 4-second interval, the computations proceed in the following manner.

The input profiles are acquired. These consist of 160 40Hz profiles and 20 5Hz profiles. Each of the 40Hz profiles extend from -1 to 10 km. The total number of samples therefore is
{[10-(-1)] km/ 0.0768 km}= 143 samples/profile;
143 samples/profile x 160 profiles=22880 samples.
Each 5 Hz profile extends from -1 to 40 km; thus, each has 533 samples. So, the total number of 5 Hz samples is

(533 samples/profile) x 20 profiles = 10660 samples. The total number of backscatter coefficient samples required for each 4-second interval is 22880+10660=33540. This value represents the most significant demand on computer memory storage for this algorithm.

The first task will be to detect and position the signal from the earth's surface (ground signal). As mentioned in Section 3.3.1.2, the ground height for the 1Hz and 0.25 Hz profiles will be the average of the ground height from the appropriate 5 Hz profiles. The details of the ground procedure are found in that section. Since the algorithm requires that cloud boundaries be found at the 4-second resolution first, a 4-second average profile will be found by averaging the 5 Hz profiles. The averaging will extend from -1 km to 20 km. One-second profiles will be analyzed after the processing of the 4-second profiles is complete.

The 4-second average profile will be divided into n_s segments. These will not necessarily be of uniform length. In each of these segments, a minimum value will be found. A measure of the random noise associated with the molecular signal will be computed. For observations taken in sunlight, the standard deviation of the background signal will be used. This value will be found by using values in the final 13 samples of the profile, which occur after the laser pulse is extinguished by the ground. The lack of a significant background signal in night observations requires that the variability be estimated from 18-19 km. portion of the profile. The atmosphere at that altitude will be free from strong non-molecular scattering constituents. Therefore, the variability of the signal found there will be representative of the variability found in the particulate free portions of the entire profile. A constant fraction of this variability will be added to each of the segment minimums. The optimum value for the fraction will be determined from modeling studies. A threshold profile, from 0-20km, will be formed by linear interpolation and extrapolation of the segment points.

Cloud boundaries can now be found from the 4-second profile. Starting at the first sample, which represents the highest point, each profile value will be compared to the threshold profile. The presence of cloud will be designated false. When a certain number of consecutive samples are found to be greater in value than the threshold, a top-of-cloud will be located where the first sample exceeded the threshold. The presence of cloud will be designated true. The comparison of profile values will continue downward. When certain number of consecutive values are found to be less than the threshold, a bottom-of-cloud will be located where the first of the consecutive samples was found and the presence of cloud will return to false. This process will continue to ground level. The location of the ground level will be average of the ground levels derived from the 5Hz profiles, as described in Section 3.3.1.2. If no ground signal was detected, the cloud search algorithm will continue to the minimum of the 4 DEM minimums associated with the 4-second segment. When this procedure is complete, the set of cloud boundaries and ground location of the 4-second profile will be known and stored.

Next, the procedure to find cloud boundaries for each of the 1 second profiles contained in a 4 second segment will be applied to the GLAS backscatter coefficient profiles. The algorithm will be the same as that described for the 4-second profile, with the following alteration. No boundaries outside of those defined by the results from the four-second profile(plus a small delta) will be accepted. If such a boundary or layer is found, it will be considered a false positive result caused by relatively larger random noise. Layers that are wholly outside of 4-second layers will be eliminated. Each 1 Hz result will be assigned a ground height computed from the average of the corresponding 5 Hz profiles.

In a like manner, the cloud boundary processing of the 5 Hz data will be same as the 0.25 Hz and 1 Hz. The 5 Hz layers will be required to exist in layers defined by the 1 Hz results.
Finally, the 40 Hz profiles will be processed. Two factors force the processing to be somewhat different than that at the other frequencies. First, the 40 Hz data extend only from –1km to 10 km. Second, the low signal to noise precludes reliable detection of rarefied, optically thin clouds. In general, it is expected that only dense clouds will be reliably detected at 40 Hz. But knowledge of the location of cloud layer boundaries of these types of clouds in the lowest part of the atmosphere is very important for certain types of studies. For these reasons, the processing of 40 Hz data will proceed as follows. A ground height search algorithm will be applied independently to each of the profiles. The random noise factor will be estimated from the background portion of each profile. A threshold profile will be developed for the region 0-4km. If any cloud layers are detected, only the lowest one of those, confined to layers detected at 5 Hz, will be designated as a layer.

4.3.3 Interpreting the Output

The output of GLA09 will consist of the following products, for each 4 second processing segment:

1) Results at 0.25 Hz frequency, 1 set
    a) Vertical locations of the top and bottom of up to ten cloud layers, 0-20 km ;
    b) probability that each detected layer is a false positive result;
    c) probability of one or more false negative results
    d) probability that each detected boundary is within 0.116 km of the algorithm result
    e) Ground height which will be the average of 20 5 Hz ground height results or indication of negative results if no ground was detected in the 4 second interval;
    f) probability that the ground height is within 0.116 km of the algorithm result
    g) time and location information
2) Results at 1.0 Hz frequency, 4 sets
    a) Vertical locations of the top and bottom of up to ten cloud layers, 0-20 km. confined to the layer boundaries detected at 0.25 Hz;
    b) probability that each detected layer is a false positive result;
    c) probability of one or more false negative results
    d) probability that each detected boundary is within 0.116 km of the algorithm result
    e) Ground height which will be the average of 5 Hz ground height results or indication of negative results if no ground was detected in the 1 second interval;
    f) probability that the ground height is within 0.116 km of the algorithm result
    g) time and location information
3) Results at 5 Hz frequency, 20 sets
    a) Vertical locations of the top and bottom of up to ten cloud layers, 0-20 km. confined to the layer boundaries detected at 1 Hz;
    b) probability that each detected layer is a false positive result;
    c) probability of one or more false negative results
    d) probability that each detected boundary is within 0.116 km of the algorithm result
    e) Ground height or negative results if no ground was detected;
    f) probability that the ground height is within 0.116 km of the algorithm result
    g) time and location information
4) Results at 40 Hz frequency, 160 sets

a) Vertical locations of the top and bottom of one cloud layer, in the range 0-4 km, the lowest of any detected and confined to layer boundaries detected at 0.25 Hz.
b) probability that the detected layer is a false positive result;
c) if no cloud is detected, the probability of a false negative results
d) probability the detected boundary is within 0.116 km of the algorithm result
e) Ground height or negative results if no ground was detected;
f) probability that the ground height is within 0.116 km of the algorithm result
g) time and location information

The tops and bottoms of the cloud layers are the heights h (in km above mean sea level) at which the cloud signal becomes distinguishable from the molecular signal. In general, within the meaning of cloud boundary at any of the time resolutions, the actual cloud boundary, h_a, will be within a range of $h-0.116km<h_a<h+0.116km$.

If a ground signal is detected, than all cloud boundaries are considered valid within the uncertainty limits. If no ground signal is detected, then the value of the bottom of the lowest layer has no meaning other than to indicate the height at which random noise first conceals the atmospheric signal. Any cloud of sufficient density and optical depth to cause multiple scattering to obliterate the location of the bottom of the layer will be assumed to fully attenuate the laser pulse. The bottom of the layer would not be meaningful in any such case.

4.3.4 Quality Control

The quality of the results of the GLA09 boundary procedure will be judged by how successful it is at finding all detectable cloud layers and locating their boundaries in the atmospheric profile. A significant advantage to the algorithm is that its application to a given time segment is independent of any GLAS observations outside of the segment. Quality of the results will be primarily controlled by the signal to noise ratio at any point in the profile. Modeling studies will be used to assign quality assessments based upon the signal to noise of any detected layer. The results for each layer will be flagged with quality flag based upon the noisiness of the signal.

The best way to judge the general quality of the results of the boundary algorithm is to plot the computed cloud boundaries on top of image segments constructed from lidar profiles. Such images reveal readily systematic and random faults in the results of the procedure. These inspections will be done on samplings of the results on a routine basis. If these reveal significant shortcomings in the method, the parameters used in the computation of thresholds will be adjusted to fix the discrepancies.

4.4 PBL and Elevated Aerosol Layer Height

4.4.1 Required Input Data

The algorithm requires the 5 Hz profiles of the 532 nm attenuated backscatter and selected other components of the GLA07 output. These include the ground bin and various data quality flags. In addition, GLA08 requires the 5 Hz (high resolution) cloud boundaries output from the cloud detection algorithm (GLA09). Also required from GLA09 is the 5 Hz ground detection flag. Profiles

of molecular backscatter cross section are also required since they are used to determine the bottom threshold as discussed in section 3.4.1.2.

4.4.2 Algorithm Implementation

The algorithm can be implemented on any standard workstation with sufficient memory and CPU resources. To be most efficient, the 150 km record (100, 5 Hz profiles) of lidar data used to find the average PBL height should be kept in memory. The total memory required is less than 1 Mb, and the CPU requirements fairly minimal. We estimate that processing all the data from one orbit (about 27,000 profiles at 5 Hz) would take less than 10 CPU minutes on a low-end workstation such as an HP-715 or SGI Indigo II.

Even though there are similarities between the PBL and EAL algorithms, we believe they should be implemented separately. For instance, the need for 20 second and 4 second averaged profiles is common for both the PBL and EAL portions of the algorithm. However, the criteria for the composition of the 20 second averages is not quite the same. For the elevated aerosol layer, all shots are used regardless of the presence of a ground return or clouds. The PBL height, on the other hand, eliminates all shots without a ground return that have clouds above 5 km. This means that the EAL algorithm will process nearly 100 percent of the data, while the PBL algorithm may discard 30 or 40 percent of the data (due to clouds). In addition, the EAL algorithm requires the PBL algorithm output to determine the lower bound for the aerosol layer search. Thus, the PBL height algorithm must be run prior to the EAL algorithm.

4.4.3 Interpreting the Output

The output from GLA08 will consist of planetary boundary layer height at high resolution (5 Hz or 1.5 km) and low resolution (0.25 Hz or 30 km). It will also contain the top and bottom height of a maximum of five elevated aerosol layers below 20 km at 0.25 Hz resolution, and a maximum of three aerosol layers above 20 km at a horizontal resolution of 0.05 Hz (150 km). When an aerosol layer is found above 14 km, and the temperature at the height of the layer is below –80 °C, and the latitude is poleward of 65 degrees, a Polar Stratospheric Cloud (PSC) flag is set to indicate a very high likelihood of the layer being a PSC. If the layer temperature is above –80 °C, but less than –70 °C, the flag is set to a different value to indicate a lesser likelihood of it being a PSC. The PSC flag will have the value of zero at all other times. All heights generated will be in kilometers above mean sea level. An elevated aerosol layer is defined as a region of increased lidar backscatter (above local ambient values) which has a minimum thickness of 153 meters (2 data bins). The data input to GLA08 will already have been processed by the cloud height detection algorithm (GLA09) and the EAL algorithm will search only those portions of the data that have been certified cloud free by GLA09. As discussed in section 3.3, differentiating between a very weak cloud signal (for instance from cirrus) and a strong EAL signal can sometimes be difficult if not impossible. However, an implicit assumption of this (GLA08) algorithm is that any layer detected by the algorithm (after screening the data based on output from GLA09) is an aerosol layer and not an optically thin cloud layer. It should be noted that there will likely be times when this is not correct. However, we anticipate that such occurrences will be very infrequent (less than 1 percent of the EAL heights).

In figure 4.4.1 we have included an example of the output from a prototype version of the PBL height algorithm form GLA08. The top panel shows the high resolution (5 Hz) PBL height obtained by analyzing the simulated nighttime GLAS attenuated backscatter data shown in the bottom panel. Visual inspection of the backscatter image reveals the presence of enhanced scattering below two kilometers, especially between 200 and 600 kilometers along the x axis. This is indicative of aerosol trapped within the PBL. Beyond 600 km, the aerosol scattering within the PBL is somewhat less, but still provides enough signal to detect the PBL top as seen in the upper panel.

At the present time, the elevated aerosol layer height algorithm has not yet been coded. Generation of additional simulated GLAS data sets are required for full testing of the EAL algorithm. We anticipate using LITE data sets which are now available from the NASA Langley Data Active Archive Center (DACC) for this purpose.

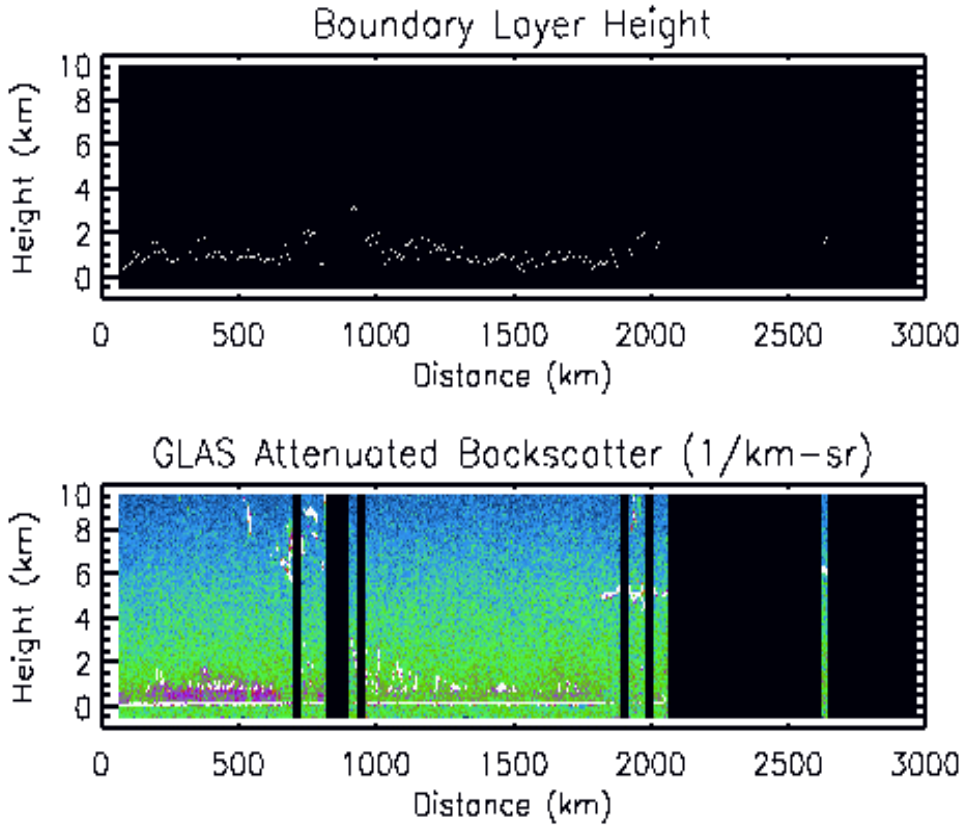

Figure 4.4.1. Top panel shows output of a prototype PBL height algorithm (GLA08) at a horizontal resolution of 5 Hz for the simulated GLAS attenuated backscattter data set shown in the bottom panel. The gaps in the image are sections of data where no ground return was found and the PBL height not calculated.

4.4.4 Quality Control

Validation of the algorithm output can best be accomplished by overlaying the PBL and aerosol layer heights on top of the images. We have found from experience that visual inspection can reliably distinguish aerosol boundaries when the data are presented in this form. The lidar retrieved PBL heights can then easily be compared with the visual estimation of PBL height. The same is true for the elevated aerosol layers. Other validation approaches include using nearby radiosonde data to determine PBL depth and checking it against the lidar measurement (provided it is within a certain distance to the radiosonde station). Over land, it may be possible to use the MET data which is ingested by the GLAS ground processing system.

4.5 Optical Properties of Cloud and Aerosol Layers

4.5.1 Required Input Data

The algorithm which produces the GLA10 and GLA11 level 2 standard products will have as its starting point the 1 second average and 4 second average 532 nm intermediate attenuated backscatter profiles [the β' term in (3.5.1)] which are created for the cloud boundary search algorithm. These profiles are averages of the GLA07 532 nm backscatter output and are discarded after GLA10 and GLA11 are calculated. In addition, this algorithm requires MET atmospheric profile data in order to compute the 532 nm molecular backscatter cross section throughout the vertical atmosphere (see sections 3.2.1 and 4.2.1). Appropriate standard atmosphere profiles will be substituted for the MET profiles when necessary. It is anticipated that the MET data will be refreshed every second and time matched to the two resolutions of the P_n profiles. Other important inputs include the GLA08 aerosol layer location products of PBL height, ground detection height, and top and bottom heights of elevated aerosols (including PSCs) below 20 km, all at low resolution (4 second). GLA08 will also provide top and bottom heights of elevated aerosol layers from 20-40 km (including PSCs) at very low (20 second) resolution. Similarly, cloud location products from GLA09 necessary for input into this algorithm are cloud top and bottom locations and ground detection height at medium resolution (1 second), and cloud top and bottom locations for low resolution (4 second). The cloud and aerosol layer locations will be time matched to the two resolutions of the P_n profiles. The multi-scattering factor, η, (relationships formulated from section 3.6) and the true particulate extinction-to-backscatter ratio, S_p, (see section 3.5.1.1) will all be calculated based in whole or in part on pre-defined look up tables distinguishing between cloud and aerosol regimes. Work done by Ackermann (1998) showed that reasonable estimates for aerosols can be matrixed using location information (continental, maritime, and desert) with a dependence on relative humidity. Similar estimates can be done for clouds involving cloud phase, temperature, and optical depth conditions. S'_p for PSCs will be gotten from a subset of the aerosol matrix coupled with an estimate of η. The following two sections describe the current decision matrices of the S_p look up tables in detail.

4.5.1.1 Aerosol Extinction to Backscatter Ratio (S_p) Assignments

Aerosol layers will be assigned a best initial value of S_p based on the matrix in figure 4.5.1.

GLAS Aerosol Extinction to Backscatter Ratio Matrix

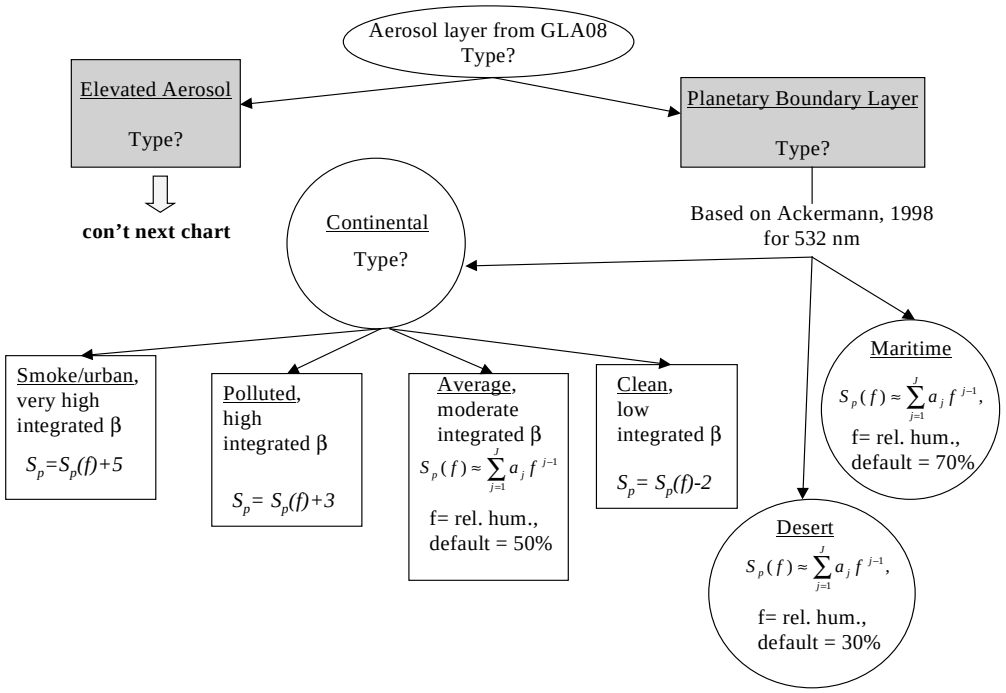

GLAS Aerosol Extinction to Backscatter Ratio Matrix (con't)

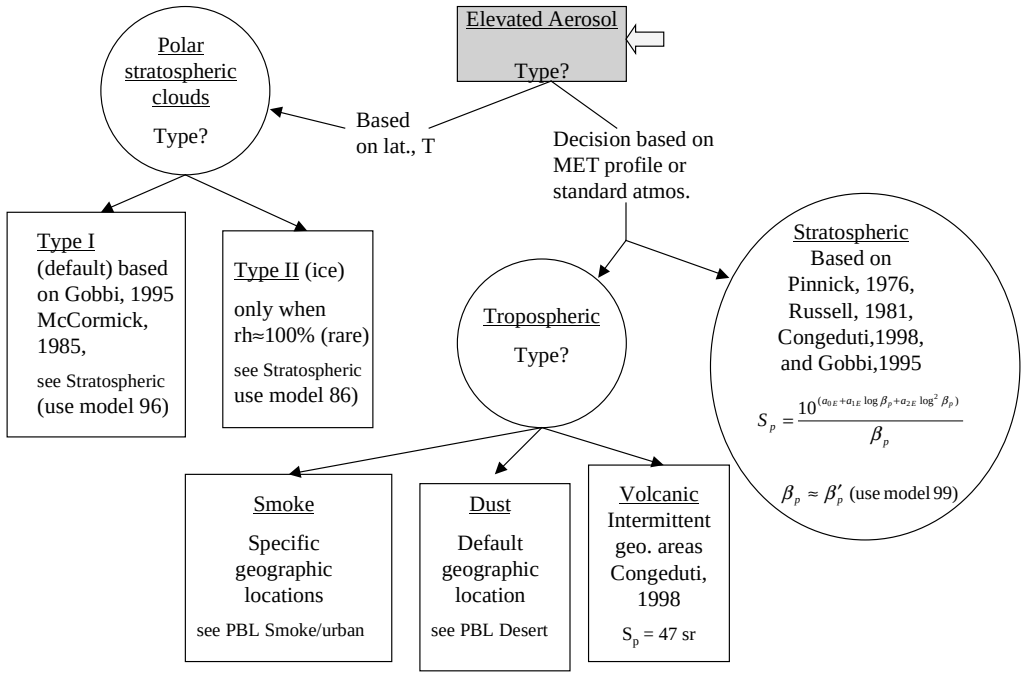

Figure 4.5.1 Flow diagram of aerosol S_p ratio assignments for use in optical property calculations.

4.5.1.2 Cloud Extinction to Backscatter Ratio (S_p) Assignments

Cloud layers will be assigned a best initial value of S_p based on the matrix in figure 4.5.2.

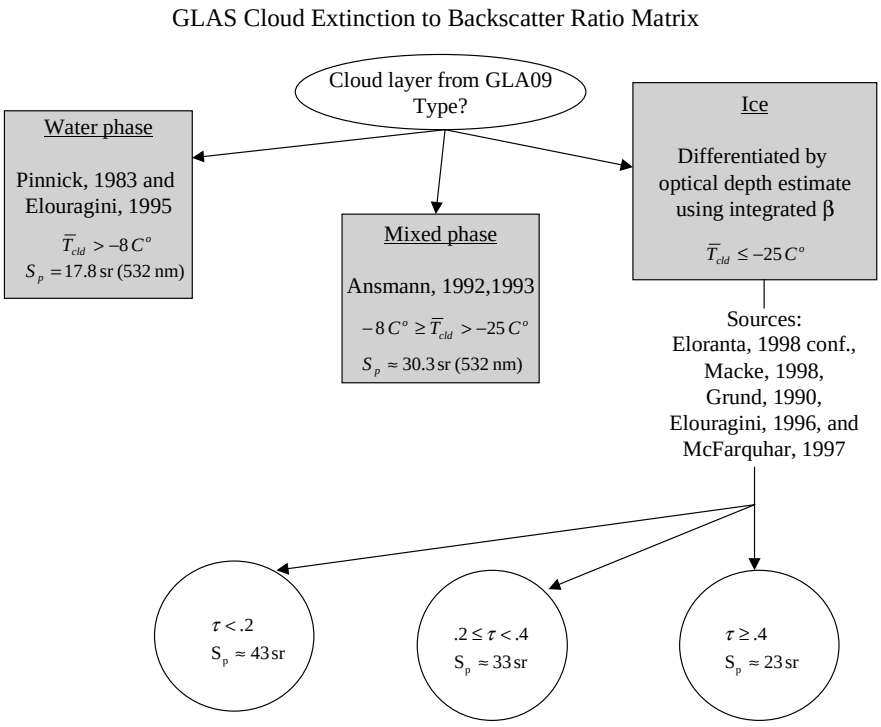

Figure 4.5.2 Flow diagram of cloud S_p ratio assignments for use in optical property calculations.

4.5.2 Algorithm Implementation

The underlying function of this algorithm is to compute molecular and particulate transmission squared for the full vertical profile of the atmosphere starting at 40 km and ending when the value of $T'_p \leq T_L$ or the lidar profile reaches the earth's surface, whichever occurs first. This will be done first at four second resolution, then at 1 second. The following rules will be adhered to:

1. Molecular attenuation is negligible between 40 and 30 km above sea level and T_m^2 will be calculated based on a standard atmosphere look up table in this height zone.
2. Ozone attenuation is small, mounting to an average optical depth of 0.014 at 532 nm, most of which occurs above 20 km. T_o^2 will be factored in to the attenuated backscatter signal (see section 3.5.1.1) and chosen based on standard atmosphere look-up tables based on climatic regimes derived form sources such as LOWTRAN.
3. $T_p'^2$ for aerosol layers will be processed at four second averages below 20 km height, but will use the 20 second average aerosol layer location and signal profile above 20 km to analyze

the optical parameters, and then transfer the results to the 4 second average aerosol layer locations by duplication of five 4 second segments.

4. $T_p'^2$ for areas between layers will be estimated at 1.0.
5. If an aerosol layer is found above any cloud layer, the 4 second average aerosol optical depth for that layer will be used to calculate a transmission factor (representing the aerosol) that will be multiplied to the last calculated $T_p'^2$ for each 1 second average transmission profile before proceeding to the next layer.
6. Any aerosol layer found underneath a cloud layer and which is the final (bottom) particulate layer located, will not be processed.
7. If no cloud layers have been located for a 1 second average transmission profile, then no optical calculations are performed for that profile. Similarly, if no aerosol layers have been located for a 4 second average transmission profile, then no optical calculations are performed for that profile
8. Both the one second and four second resolution particulate transmission profile algorithms will process the observed mix of cloud and aerosol layers in the order sensed by the lidar, using the medium resolution cloud location data set for the 1 second profile and the low resolution cloud location data set for the four second profile.

Once the transmission profiles are calculated (equations 3.5.6 and 3.5.11), all other optical calculations can be directly obtained (see equations 3.5.15, 3.5.17, and 3.5.22). Each parameter will either use the 1 second resolution transmission profile (for cloud calculations) or the 4 second resolution transmission profile (for aerosol and PSC calculations). The multiple scattering warning flag will be based on a surface ranging error ranking developed in the multiple scattering factor (η) look up table. A flow chart of the optical parameter calculations is found in figure 4.5.3.

The critical component of the algorithm is the evaluation of the integral to compute γ (see equation 3.5.20). The flow of the algorithm proceeds as follows. For each profile P_n (first the four second and then the one second resolutions), the levels where aerosol and cloud boundaries exist are obtained and differentiated. For any 4 second aerosol layer, checks of the 1 second cloud boundaries and the 1 second ground detection height are needed to verify that no clouds or ground contaminate the aerosol signal. The molecular transmission squared to the top of the highest layer is computed and used as $T^2(z_t)$ in equation 3.5.11. S'_p for the layer is computed (see section 3.5.1.1) based on whether it is cloud, PSC, or aerosol. When the backscatter profile for a given layer is found to be appropriate for independent S'_p analysis, the calculated S'_p will be used instead of the value derived from the look up table if found to be within tolerances. The integral is evaluated using a straight-forward rectangular summation. The terms of the summation are $T_{m_i}^{2(X-1)} P_{n_i} \Delta z$. The value of $T_p'^2$ is computed for each level z in the layer. Computation for any subsequent layer will use the same method except that the $T^2(z_t)$ value will be re-computed as :

(4.5.1) $T^2(z_t) = T_p'^2(z_a) T_m^2(z_t)$,

where $T_p'^2(z_a)$ is the particulate transmission squared a the bottom of the layer above and $T_m^2(z_t)$ is the molecular transmission squared calculated down to the level of z_t, the top location of

the current layer. This continues throughout each particulate layer as per the eight rules outlined above until $T_p'(z) \le T_L$ or the signal from the earth's surface is detected.

The algorithm is not computationally intensive. Results indicate that to process an orbit of data for the GLA10 and GLA11 products would take about 0.357 minutes of cpu time.

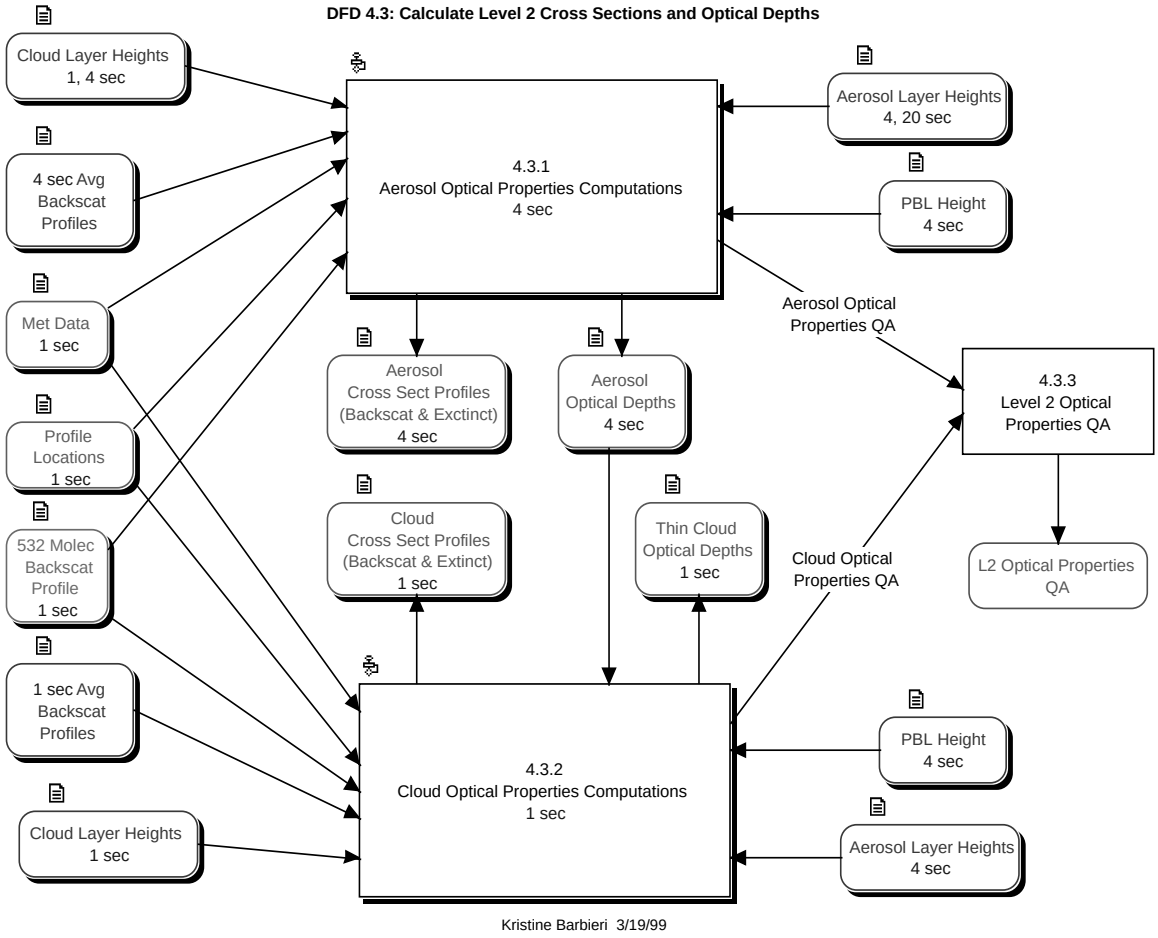

Figure 4.5.3 Flow diagram of level 2 optical parameter calculations.

4.5.3 Interpreting the Output

The output of this algorithm is separated into two standard product packages, GLA10 and GLA11. GLA10 focuses on the output of vertical profiles: cloud and aerosol backscatter cross section and cloud and aerosol extinction cross section. All layer locations are referenced from sea level. GLA11 focuses on particulate optical depths (cloud and aerosol). All extinction and optical depth values have been corrected for multiple scattering. Polar stratospheric clouds in both packages are part of the aerosol category. A complete list of the output for GLA10 follows:

1. 532 nm aerosol backscatter cross section, 40 to –1 km above mean sea level at 0.25 Hz, (-999.9 where not processed)
2. Aerosol backscatter layer use and quality flags at 0.25 Hz, 1 each per layer, 9 layers, (255 where not processed) [use flag will stipulate whether layer is regular or PSC aerosol]
3. 532 nm cloud backscatter cross section, 20 to –1 km above mean sea level at 1 Hz, (-999.9 where not processed)
4. Cloud backscatter layer use and quality flags at 1 Hz, 1 each per layer, 10 layers, (255 where not processed)
5. 532 nm aerosol extinction cross section, corrected for multiple scattering, 40 to –1 km above mean sea level at 0.25 Hz, (-999.9 where not processed)
6. Aerosol extinction layer use and quality flags at 0.25 Hz, 1 each per layer, 9 layers, (255 where not processed) [use flag will stipulate whether layer is regular or PSC aerosol]
7. Aerosol true extinction to backscatter ratios used at 0.25 Hz, 1 per layer, 9 layers, (-999 where not processed) [PSC ratio, if layer is PSC]
8. 532 nm cloud extinction cross section, corrected for multiple scattering, 20 to –1 km above mean sea level at 1 Hz, (-999.9 where not processed)
9. Cloud extinction layer use and quality flags at 1 Hz, 1 each per layer, 10 layers, (255 where not processed)
10. Cloud true extinction to backscatter ratios used at 1 Hz, 1 per layer, 10 layers, (-999 where not processed)
11. Medium resolution cloud top heights for layers which were selected for optical processing at 1 Hz, 1 per layer, 10 layers, (-999 where not detected or used)
12. Medium resolution cloud bottom heights for layers which were selected for optical processing at 1 Hz, 1 per layer, 10 layers, (-999 where not detected or used)
13. Medium resolution processed ground detection height at 1 Hz, 1 per profile, (-999 where not processed)
14. Low resolution aerosol layer top heights for layers which were selected for optical processing at 0.25 Hz, 1 per layer, 9 layers, including the planetary boundary layer and PSC (-999 where not detected or used)
15. Low resolution aerosol layer bottom heights for layers which were selected for optical processing at 0.25 Hz, 1 per layer, 9 layers, including the planetary boundary layer and PSC (-999 where not detected or used)
16. Low resolution processed ground detection height at 0.25 Hz, 1 per profile, (-999 where not processed)
17. Precision Orbit Determination (POD) data (1 Hz)
18. GPS time (1 Hz)
19. Orbit Number
20. HDF EOS Information per record at 1 Hz

Items 1 through 10 are calculated by the optical parameters algorithm. Items 11 through 16 are taken from GLA09 and GLA08 particulate boundaries output, but modified to suit the rules listed in section 4.5.2 so that only cloud and/or aerosol layers processed at least partially will show up in this data set's layer locations. The remaining output is passed along from GLA07 or from another input source.

A complete list of the output for GLA11 follows:

1. 532 nm cloud optical depth, corrected for multiple scattering, at 1 Hz, 1 per layer, 10 layers, (-999.9 where not processed)
2. Cloud optical depth use and quality flags at 1 Hz, 1 each per layer, 10 layers, (255 where not processed)
3. 532 nm elevated aerosol optical depth, corrected for multiple scattering, at 0.25 Hz, 1 per layer, 8 layers, (-999.9 where not processed)
4. Elevated aerosol optical depth use and quality flags at 0.25 Hz, 1 each per layer, 8 layers, (255 where not processed) [use flag will stipulate whether layer is regular or PSC aerosol]
5. 532 nm planetary boundary layer aerosol optical depth, corrected for multiple scattering, at 0.25 Hz, 1 per layer, 1 layer, (-999.9 where not processed)
6. Planetary boundary layer aerosol optical depth use and quality flags at 0.25 Hz, 1 each per layer, 1 layer, (255 where not processed)
7. Medium resolution cloud top heights for layers which were selected for optical processing at 1 Hz, 1 per layer, 10 layers, (-999 where not detected or used)
8. Medium resolution cloud bottom heights for layers which were selected for optical processing at 1 Hz, 1 per layer, 10 layers, (-999 where not detected or used)
9. Medium resolution processed ground detection height at 1 Hz, 1 per profile, (-999 where not processed)
10. Low resolution elevated aerosol layer (including PSC) top heights for layers which were selected for optical processing at 0.25 Hz, 1 per layer, 8 layers (-999 where not detected or used)
11. Low resolution elevated aerosol layer (including PSC) bottom heights for layers which were selected for optical processing at 0.25 Hz, 1 per layer, 8 layers (-999 where not detected or used)
12. Low resolution processed ground detection height at 0.25 Hz, 1 per profile, (-999 where not processed)
13. Low resolution planetary boundary layer height at 0.25 Hz, 1 per profile, (-999 where not processed)
14. Cloud multiple scattering coefficients used at 1 Hz, 1 per layer, 10 layers, (-999 where not processed)
15. Aerosol multiple scattering coefficients used at 0.25 Hz, 1 per layer, 9 layers, (-999 where not processed) [including PSC aerosol]
16. Multiple scattering effect warning flag at 1 Hz, 1 per profile (-999 where not processed)
17. Precision Orbit Determination (POD) data (1 Hz)
18. GPS time (1 Hz)
19. Orbit Number

Items 1 through 6 and 14 through 16 are calculated by the optical parameters algorithm. Items 7 through 13 are taken from GLA09 and GLA08 particulate boundaries output, but modified to suit the rules listed in section 4.5.2 so that only cloud and/or aerosol layers processed at least partially will show up in this data set's layer locations. The remaining output is passed along from GLA07.

4.5.4 Quality Control

Quality control will be implemented at all stages of the molecular and particulate transmission profile development. All input parameters and arrays will be evaluated for quality before being used:

1. Attenuated backscatter profiles
   - Bad shots will be detected by integration of the lidar signal in the 20 to 40 km height zone.
   - Lidar bins using 1064 nm backscatter in place of a saturated 532 nm condition will be tracked as far as which particulate layer they occur in.
   - Calibration constants which fall outside an expected range will be flagged.

2. Cloud and aerosol layer detection
   - The layers will be screened so they don't overlap or become embedded.
   - Visual screening with imagery will occur to make sure layers are labeled 'cloud' or 'aerosol' or 'polar stratospheric cloud' correctly.
3. Molecular backscatter
   - Monitor backscatter calculations from MET data to make sure they fall within expected boundaries based on atmospheric standards.
   - Default to atmospheric standards if MET data are missing or bad.
4. Extinction to backscatter ratios and multiple scattering factors
   - The accuracies of these input parameters are at times uncertain, especially for cirrus clouds, making this a limitation in the algorithm.
   - Calculations of these parameters in level 2 processing involve a decision matrix look up table, which will restrict these parameters to within theoretical and observed limits. If atmospheric conditions are favorable, S'_p will be calculated for thin clouds and PSCs, then compared to matrixed values. If more accurate calculations come out of level 3 processing, these will be used to re-process level 2 products.

As the transmission profiles are processed, the transmission calculations will be tested for out-of-bounds situations such as increasing transmission with range or large negative transmission. Confidence flags will be produced for each particulate layer or profile to help pinpoint how many and which input parameters are suspect, and whether the transmission profiles have passed their tests so far. This information will be transferred to each of the individual output parameter's confidence flags.

5 Mitigating Multiple Scattering Induced Ranging Errors

It has been calculated that the effects of multiple scattering from cloud and aerosol will introduce significant errors for precision surface altimetry. These results are presented in detail by Duda et al. (1999, a and b and available from the GLAS ftp site). The pulse spreading from multiple scattering will tend to introduce a positive bias to the range determination. The magnitude of the effect can be considerable under certain atmospheric conditions, ranging to larger than 1 meter for a single pulse depending on conditions. Since cloud cover varies seasonally and year to year, Duda et al. show that if uncorrected, the multiple scattering effect would introduce significant errors

for the GLAS surface altimetry yearly analyses. The atmospheric conditions most conducive to multiple scattering are optically transmissive cloud layers that are between 1 and 3 km above the ground. Over the ice pack, such low optically transmissive clouds appear to be the dominant type.

Application of the atmospheric channel of GLAS to perform an analytic correction to the multiple scattering induced ranging error is being developed. As the current baseline approach, the atmospheric channel can be used to identify those cases where multiple scattering is calculated to be an error term of significance. The determining factors are the cloud height range and optical thickness plus an assumption of cloud particle size. The factors are essentially the same as those to be used for the generation of the correction factors for the influence of multiple scattering on cloud and aerosol cross sections and optical thickness as described above. The ranking would be based on the height and optical depth of any cloud or aerosol layer that was detected for that shot (by GLA08 and GLA09). As described in Duda et al., an estimate of the magnitude of the pulse spreading error on the surface is computed based on a centroid analysis of a flat, normal surface. This information can then be used by the altimetry processing to eliminate shots that are likely to be severely affected by multiple scattering. A correction to increase the amount of usable altimetry measurement may also be considered. While we do not present a detailed plan for the implementation of such a scheme, it is certainly something that could be done by GLA11. A separate ATBD document to cover multiple scattering effects on surface ranging may be developed at a later date. The work presented in Duda et al. would be the basis of such a document.

6 Browse Products

Browse products are used to determine the health of the instrument as well as determining the performance of atmospheric algorithms. A list of possible browse products follows, but should in no way be considered complete. This list may be added to at a later date.

1. Laser energy as a function of time
2. Calibration constants as a function of time
3. Number of saturated 532 nm bins per 5 Hz profile as a function of time
4. Integrated 532 signal from 40 to 20 km as a function of time
5. 532 and 1064 nm background values as a function of time
6. 532 nm background at 70 km vs, 532 background at –5 km
7. Scattering ratio profiles
8. Percentage of time ground return was detected per orbit
9. Percentage of time clouds were detected per orbit
10. Color images of attenuated backscatter cross section with cloud layer, aerosol layer and PBL height superimposed on the image.
11. Cloud and aerosol optical depth as a function of time.

(1) It is important to monitor the laser performance since it is integral to data quality. Producing a plot of laser energy vs. time will be very helpful. (2) We have no idea how consistent the lidar calibration constant calculated from the data will be. We need to know how both the calculated 532 and 1064 calibration constants change with time and moreover, how their values are affected by

the varying background conditions. This can be accomplished by plotting the calibration constants as a function of time. Probably, it is best to plot the 532 calibration values separate from the 1064 values with each plot containing the calibration constant calculated at the two calibration heights, with the night calibration distinguishable form the day calibration. (3) There would interest in knowing how many 532 channel bins were flagged as saturated as a function of time. This could be done done by counting the bins in the 5 Hz saturation flag profile that is output from GLA07 and summing over one second. A plot of this value vs time would then be generated. (4) The integrated 532 signal (β') from 40 to 20 km would be of interest because it would tell much about system performance and optical alignment (boresite). This could be summed over one second using the 5 Hz profiles output from GLA07 and plotted as a function of time. (5) The 532 and 1064 background values should be computed at second intervals and plotted as a function of time. This would include all four background values – one before the atmosphere (about 70 km) and one after the ground (about –5 km) for each channel. (6) A scatter plot of the 532 background at 70 km vs the 532 background at –5 km could be constructed form the 1 second average backgrounds computed to produce (5). (7) The scattering ratio profile can be formed by taking the 5 Hz attenuated backscatter profiles ($\beta'(z)$) output from GLA07 and dividing by the attenuated molecular backscatter profile and averaging over a given time. Most likely these averages would be computed from 5 to 10 minute of data. (8) The percentage of time the ground return signal was detected (per orbit) is important for ascertaining cloud cover and optical depth statistics. This can be computed from the output of GLA09 which includes high resolution ground detection and would be plotted as one point per orbit. (9) The percentage of time that clouds were detected is computed from the output of GLA09 using the 4 second average cloud height. Item (10) represents one of the most useful browse products in terms of monitoring overall system performance and for validating the performance of the cloud, aerosol and PBL height algorithms. The image is made from the output of GLA07 for a specified time segment and the output of GLA08 and GLA09 are read and plotted on top of the image. Cloud and Aerosol optical depth would be useful mainly as a way to check the validity of the processing algorithms.

7 Development Plan

The development of the production algorithms for the lidar processing should be a team effort between the software development team under Jay Zwally and the atmospheric lidar group under Jim Spinhirne. The lidar group will work closely with the software development team to assist in the design, implementation, and testing of the atmospheric ATBD specified I-SIPS software components that will produce the level 1 and level 2 standard atmospheric data products (GLA02, GLA07, GLA08, GLA09, GLA10 and GLA11). Dr. Spinhirne's group will develop a set of working algorithms (protocode) and associated documentation for the lidar processing that will utilize their past experiences and the design of the I-SIPS software. The lidar group will consist of 3 to 5 senior research programmers, each of whom has ample experience in the processing and analysis of aircraft and ground-based lidar data. The development team during this period will be implementing the shell to provide the data and control into and from the lidar processing algorithms. During this protocode development period there will be working meetings between the teams to track progress, exchange designs and to insure that compatible systems are being developed. The lidar group protocode will be delivered to the software development team for use as examples, recode, or actual use in the I-SIPS software. The lidar group will work with the development team for

testing and verification of the I-SIPS production software, using simulated GLAS data sets produced by the lidar group. The objective of the testing and verification stage will be to produce the same results with the protocode and the final I-SIPS software. The development and turning over of the protocode should be accomplished during FY99. The implementation and test support should be FY00 with some small extension into FY01.

After launch the lidar group will ascertain the performance of the algorithms using the browse products defined in section 6 and the validation methods presented in section 8. Based on these assessments, the lidar group will work toward refinement of the I-SIPS production software by tweeking individual algorithms for peak performance. The protocode may be useful to the lidar group for this process or for special analysis. That work will not be part of the I-SIPS sustaining engineering efforts but is considered part of the lidar science team investigation. There will remain a need, as with all science team members, to work with the sustaining engineering team for the production software to correct errors and implement improved algorithms.

8 Validation Plan

8.1 Validation Criterion

8.1.1 Overall Approach

The validation program will consist of pre-launch and post-launch activities aimed at establishing the accuracy of the GLAS algorithms for retrieval of atmospheric parameters. Prior to launch, simulated GLAS data sets will be produced using the GLAS Atmospheric Lidar Simulator (GALS) program which uses data acquired by the Cloud and Aerosol Lidar System (CALS). We believe these simulations closely resemble the characteristics of actual GLAS data in terms of signal to noise ratio and atmospheric variability. The GLAS data analysis algorithms will be developed and tested using the simulated GLAS data sets as discussed in section 7. Additionally, we anticipate utilizing data acquired during the Lidar In-space Technology Experiment (LITE), which was flown aboard the shuttle in September, 1994. The signal to noise ratio of the nighttime LITE (532 nm) data is similar to what is expected for GLAS. Thus, the cloud, aerosol and boundary layer height algorithms could be exercised with LITE data, but because of a much greater sensitivity to multiple scattering, could not be used by the algorithms that compute cloud and aerosol extinction and optical depth. The output from these algorithms will be validated in a number of ways. For certain GLAS atmospheric products, (cloud top height, PBL height and aerosol layer height) validation is possible by using the lidar data itself. This is done by assembling the GLAS backscatter data into color images which show backscatter strength as a function of height and along track distance. The output from the cloud top, PBL top or aerosol layer height algorithms are overlaid onto the color backscatter image. If the cloud heights have been correctly retrieved, they will line up with the clouds easily discernable on the backscatter image. The same is true for aerosol layers and PBL height.

We are also working on the construction of an aerosol and cloud model that will produce fabricated cloud and aerosol layers of known height, thickness and optical properties. The model will be used to produce data sets with which to exercise the GLAS algorithm. The advantage to this approach is

that all the retrieved parameters (ie cloud, aerosol, boundary layer height optical depth, extinction, etc.) would have known values and could be compared with the various algorithm output.

After launch, validation efforts will focus on the deployment of a field mission specifically designed to collect validation measurements. This would include flying the NASA ER-2 with at least the CALS lidar and the MODIS Airborne Simulator (MAS). Missions of opportunity will also be exploited where field experiments, not necessarily related to EOS, are using aircraft which can accommodate a lidar system. Piggy-backing in this way will give us additional opportunities to acquire coincident data while keeping costs to a minimum. We also plan to involve the global ground based lidar community, giving them an opportunity to collect coincident data during times of GLAS overpasses.

8.1.2 Sampling Requirements and Tradeoffs

The major difficulty in obtaining validation measurements for the GLAS atmospheric products lies in the sampling coincidence requirements. The atmosphere has various length and time scales which determine how close in space and time a validation measurement must be to a GLAS observation in order for it to be useful. These scales depend on atmospheric state and the phenomena being measured, but are generally about 2 – 10 km and 10 – 30 minutes for the troposphere. For ground based validation measurements, this puts limits on both how close an overpass must come to the ground site, and how many GLAS profiles can be validated. GLAS travels at about 7 km/s and therefore will cover 10 km in about 1.4 seconds. Thus, a ground based measurement will be useful for validating no more than one and a half seconds of GLAS data. The situation improves considerably if a fast moving aircraft is used to collect the validation measurements. The NASA ER-2 travels at about 200 m/s and can be flown directly underneath the GLAS track. In 20 minutes, the ER-2 can travel 240 km and can thus be used to validate over 30 seconds of GLAS data. Obviously, to do a good job, aircraft measurements are required to validate the GLAS atmospheric data products. The ground based validation measurements will have to be carefully screened to eliminate cases where the atmosphere is highly variable (close to fronts), so that the horizontal averaging of the GLAS data (which may be required) does not render it unrepresentative of the ground based point measurement.

8.1.3 Measures of Success

Validation experiments are conducted to evaluate the accuracy of the GLAS retrieved atmospheric parameters. The validation measurements themselves will of course have errors associated with them. A very important part of the validation process is correctly assessing the magnitude of the validation measurement error. We will assume agreement when the error bar of the validation measurement overlaps with the estimated error bar of the GLAS retrieval.

8.2 Pre-launch Algorithm Test/Development Activities

8.2.1 Field Experiments and Studies

In most cases, algorithm validation will proceed hand-in-hand with the algorithm development cycle. Coding of the GLAS atmospheric channel algorithms requires the use of actual lidar data

sets with which to test the algorithm as it is being developed. Ongoing modeling efforts to provide simulated GLAS data with known optical characteristics will be the basis for algorithm testing and validation. Additionally, we will rely on the generation of GLAS simulated data sets using the GALS program as described in section 8.1.1. Since GALS uses actual lidar data acquired from prior field missions, and essentially adds noise to and degrades the data, the original aircraft lidar data can be used as input to an independent set of algorithms to retrieve a given GLAS atmospheric product. This retrieval, whether it be cloud top height, boundary layer height or optical depth, will be more accurate and much easier to retrieve than from the simulated GLAS data because of the much higher signal to noise ratio of the aircraft data.

Table II Prior ER-2 field experiments using CALS

Field Campaign	Principle Sensors	Primary Purpose
ASTEX	CALS, MAS, CAR, microphysics probes	Marine stratocumulus clouds over the ocean
TOGA-COARE	CALS, MAS, microphysics probes	Tropical cirrus clouds and multi layer clouds over the ocean
CEPEX	CALS, MAS	Tropical cirrus and radiation budget
MAST	CALS, MAS, microphysics probes	Marine stratocumulus clouds over the ocean
ARMCAS	CALS, MAS, CAR, AVIRIS, microphysics probes	Arctic stratus clouds over sea ice; multi- layer clouds; surface bidirectional reflectance
SCAR-B	CALS, MAS, CAR, AVIRIS, microphysics, aerosol properties, AERONET	Smoke, clouds and radiation from biomass burning
SUCCESS	CALS, MAS, HIS, AERI	Mid-latitude cirrus clouds over continents
WINCE	CALS, MAS, HIS,	Cloud detection and properties over snow and ice
FIRE III / ACE	CALS, MAS, HIS,	Arctic stratus clouds over sea ice

Additionally, during most of the aircraft missions, ancillary and in-situ data are available which can be used to verify and/or supplement the retrievals made from the aircraft lidar data sets. The retrievals made from the aircraft data sets as well as the in-situ observations (where available) will then be used to validate the retrievals made from the GLAS simulated data using the GLAS algorithms. It should be noted that the algorithms used to process the aircraft data to generate the validation data set will be similar to, but distinct from, the actual GLAS algorithms.

There is an extensive CALS data base archived at Goddard Space Flight Center which can be used to generate numerous GLAS simulations for algorithm development and testing. Table 2 lists the more recent experiments in which CALS has flown on the ER-2 in conjunction with other instruments.

8.2.2 Operational Surface Networks

Operational surface networks such as the AERONET sun-photometers and the ground-based, upward-looking Micro Pulse Lidars (MPLs) will be used whenever possible for the verification of aerosol optical thickness and cloud, aerosol and boundary layer height. There are already a number of MPL (8) systems deployed around the globe and by 2000, an additional 15 should be deployed. Further, we expect to fly the CALS on the NASA ER-2 to acquire data underneath the shuttle flight track. Data from other ground-based lidar sites around the world will also be utilized when possible. The retrieval of boundary layer height and in some cases cloud layer height (over land) can be verified using data from the NWS radiosonde network.

8.2.3 Existing Satellite Data

During the pre-launch algorithm development phase, satellite data are generally not required for validation.

8.3 Post-launch Activities

8.3.1 Planned Field Activities and Studies

The products from the GLAS atmospheric channel algorithms will be tested, verified, and validated to the fullest extent possible using available ground based radiation and cloud networks and flights of opportunity which may occur during the first year or so after launch. The ground networks cover five main catagories:

1) Atmospheric Radiation Measurement (ARM) Sites from DOE:

There are expected to be five sites around the world with micro pulse lidar (MPL) aerosol and cloud profilometers, MFRSR shadowband radiometers, and BBSS balloon sonde atmospheric sounders, all capable of long-term assessments of GLAS derived products. ARM site instrumentation will be involved in intercomparisons of cloud location (especially cloud bottom), attenuated backscatter cross section, aerosol extinction cross section, and optical thickness.

2) Aeronet Radiometer Sites from EOS:

Long term measurements from 60 sites around the world are providing optical ground based aerosol monitoring using automatic sun-sky scanning spectral radiometers. Some of the AERONET sites will be equipped with MPL's to measure vertical distributions of aerosol backscatter and extinction cross sections. The sunphotometer data will provide total column optical depth measurements. This will provide aerosol optical depth validation and possibly thin cloud optical depth validation as well.

3) MPLnet Lidar Sites from EOS:

As part of the general EOS validation scheme, 12 MPL's are now being shipped to various sites around the world to add to the aerosol and cloud database of the EOS ground validation network. They will be used for intercomparisons with GLAS products such as cloud location, aerosol and cloud backscatter cross sections, and optical thickness.

4) GLAS MPL sites:

To obtain better surface observations in the polar regions, it has been proposed to operate two to three full time MPL monitorng systems at the South Pole and possibly in Greenland as part of the GLAS validation program. These lidar systems will give extra cloud height and boundary layer height validation in climatic zones where ground monitoring is very sparse. If solarphotometer data are also available, optical properties will be validated.

5) Ground based lidar community

There are many ground based lidar systems in operation at universities and research institutes around the world. We plan to develop a GLAS correlative measurements group consisting of 10 to 20 lidar sites around the globe. We will keep updated tables posted on the world-wide-web which indicate when an overpass of GLAS will occur for each site. The lidar data collected during the overpass would then be analyzed for parameters such as cloud top and bottom, backscatter cross section, and cloud and aerosol optical depth. Ideally the analysis will take place at the foreign site, with the results being sent to the GLAS atmospheric science team at Goddard, where they will be archived.

An intense intercomparison period is scheduled during the first four months after launch. The GLAS satellite's orbit will be configured to enable an increase in overflights over targeted ground networks. Methodologies already developed by NASA/GSFC to generate cloud and aerosol products from MPL systems and MFRSR radiometers will be directly adaptable when comparing to the GLAS products. Less intense intercomparisons will be done after this period when the satellite will be in its normal orbit configuration. These will continue throughout the life of GLAS. We hope to take advantage of planned ER-2 field missions during this time, where one or more flights can be dedicated to flying under the GLAS ground track. The performance of the GLAS algorithms will be statistically evaluated and their accuracy within the different cloud and aerosol types will be classified. The goal of the intercomparison during the dedicated evaluation period will be to certify the GLAS algorithm accuracy to within a known range of tolerance.

8.3.2 New EOS-targeted Coordinated Field Campaigns

The products from the GLAS atmospheric channel algorithms will be extensively tested, verified, and validated by means of aircraft observations after the satellite has been launched into orbit. Since the algorithms were based upon many years of aircraft lidar remote sensing experiments, airborne validation procedures are evidently very appropriate for testing their efficacy and accuracy. Aircraft observations will be made at locations which are inaccessible to ground observations. Aircraft observations can be taken from a large geographical area in a short time compared to ground based observations. The NASA ER-2 aircraft has served as a platform for an atmospheric lidar during many experiments. It remains the best aircraft for this purpose because of its altitude, range, flight stability, and instrumentation capabilities.

During the post launch GLAS testing period, the ER-2 will be deployed for field operations dedicated to the validation of GLAS atmospheric channel algorithms. The aircraft will be stationed at a location where it is within range of several of the most significant cloud category situations so that the performance of GLAS can be evaluated in these situations. Examples of these categories are tropical tropopause cirrus, extra tropical synoptic scale frontal situations, and marine stratus. Each of these situations and others present characteristic difficulties in the analysis of lidar data. When the track of GLAS takes it over a certain type of atmospheric structure, the ER-2 will be launched to parallel the satellite's track during its overpass to gather data with its lidar and its other passive and active instrumentation. This suite of instrumentation permits the cloud parameters to be accurately measured. The parameters pertinent to GLAS are the vertical and horizontal locations of the cloud layers, the height of the earth's surface at atmospheric channel resolution, the backscatter and extinction coefficient profiles, the optical thickness of the cloud layers, and the vertical extent of the boundary layer aerosols. The aircraft data will be analyzed to produce the same set of products as those derived from GLAS. The results from the aircraft will be considered as ground truth and the GLAS results will be compared to these. Major discrepancies will require that the GLAS algorithms be reevaluated and modified. The performance of the GLAS algorithms will be statistically evaluated and their accuracy within the different cloud-complex types will be categorized to permit a classification of reliability for investigators. By the end of the dedicated evaluation period, the products of the GLAS algorithms will be certified to be accurate to within a known range of tolerance.

To assist in the verification of algorithm retrievals during the validation phase, we will deploy a number of ground-based, upward-looking Micro Pulse Lidars (MPLs) and sun-photometers to provide verification for cloud layer height, boundary layer height and aerosol optical depth. There are already a number of MPL (8) systems deployed around the globe and by the end of 1999, an additional 15 should be deployed. Further, we expect to fly the CALS on the NASA ER-2 to acquire data underneath the shuttle flight track. Data from other ground-based lidar sites around the world as well as sun photometer data from the AERONET global network of radiometers will be used as verification of aerosol optical thickness retrievals. The retrieval of boundary layer height (over land) can be verified using data from the NWS radiosonde network. Over ocean, radiosonde stations on small island can be used to verify boundary layer height for shuttle tracks which pass close to the island.

When the GLAS spacecraft assumes its nominal orbit, the performance of the GLAS algorithms will be reevaluated with ER-2 and other aircraft flights on an episodic basis. This will be done when a situation of opportunity arises for GLAS underflights during the many atmospheric aircraft experiments which typically take place within the planned lifetime of GLAS. During such experiments, it will often be possible to design one or more aircraft sorties to serve as a GLAS underflight. Depending upon the specific instrumentation of a given flight, the products of one or more of the GLAS algorithms will be evaluated. The performance of the instrument will be evaluated for degradation. Such degradation may require that the algorithms be modified. Also, the performance of the algorithms in additional categories of cloud situations will be analyzed and these results added to the performance catalog. A tentative list of future aircraft experiments which might serve as GLAS validation opportunities is presented in table III. The bulk of this this table is TBD.

The combination of dedicated aircraft lidar underflights immediately after the launch of GLAS and the episodic flights during its lifetime will give investigators a high degree of confidence in the reliability of its products when they are incorporated into atmospheric studies.

.

Table III. Future Field Campaigns which may provide GLAS validation data

Field Campaign	Principle Sensors	Primary Purpose
CRYSTAL – FY 2001	CALS, MAS, CARS	Tropical cirrus
TBD		
TBD		
TBD		

8.3.3 Need for other satellite data

The validation of GLAS atmospheric parameters does not require the use of coincident satellite measurements, but when such coincidences occur, we plan to take advantage of them. Of the GLAS products shown in table 1, satellite data are useful only for validating cloud and aerosol optical depth. The AM-1 and PM-1 EOS platforms as well as AVHRR can be used for this purpose. Additionally, the multispectral infrared radiometer data from any of these satellites can be used to increase the accuracy of the GLAS retrieved optical depth.

8.3.4 Measurement needs at calibration/validation sites

Intercomparison measurements at the validation sites rely heavily on ground and airborne lidar, sun-photometers and radiosonde. During the 3 month validation period immediately after launch we plan to organize a field campaign using the ER-2, portable lidars (MPL), sun-photometers and GPS receivers. Ideally, 3 or 4 MPL's and sun-photometers would be deployed at separate sites along the GLAS ground track separated by 50 to 100 km. The GPS receivers would give us precise knowledge of the validation measurement location. The ER-2 would carry CALS, MAS, a visible imager and possibly another lidar. A second plane might also be used to acquire in-situ cloud and aerosol particle samples. The most difficult aspect of this plan is in finding suitable places for the ground based MPL systems, since they must lie exactly along the GLAS flight track. Possible sites should be investigated.

8.3.5 Needs for instrument development

We have just recently been given approval to begin the development of the next generation ER-2 CALS system which is a high PRF, multiple wavelength/field of view depolarization instrument using photon counting detectors. The design removes multiple scattering, leading to direct optical thickness retrievals for transmissive clouds. Multiple annular FOV signals will give particle size. This instrument will be a significant advancement over the current CALS system and will be used in radiation and EOS field programs for the foreseeable future beginning with the SAFARI mission in late 2000. This system will be ideal for the validation of GLAS retrievals. Work is planned to continue on this upgrade, with the first flights of the system to occur in late FY 2000, during the SAFARI mission. By the time GLAS launches in 2001, this instrument should be well tested and ready to provide a central role in the validation of GLAS atmospheric data products.

8.3.6 Intercomparisons

The validation measurements will first be subjected to an error analysis to quantify the measurement accuracy. Only those measurements which were taken within a certain distance and time (as discussed in section 2.2) will be used. The comparison of cloud top height will be done using the ER-2 CALS data from the underflight when available. In other areas, ground based lidar and radiosonde data will be used. Cloud bottom will be validated from ground based lidar sites. Aerosol and thin cloud optical depth derived from the GLAS data will be compared with sunphotometer data, Raman lidar and data from the University of Wisconsin's High Spectral Resolution Lidar[4] (HSRL) ground based lidar system. Satellite data from AM-1, PM-1 and AVHRR will be used when possible for validation of aerosol optical depth.

8.4 Implementation of validation results in data production

8.4.1 Approach

During the first few weeks after launch, before field validation measurements have been compiled, we will monitor the performance of the cloud top height, aerosol layer height and PBL height algorithms by simply overlaying the results on height-distance images of lidar backscatter as discussed in section.2.1. Adjustments to the algorithms can be made quickly based on these visual inspections. After field validation measurements have been acquired, detailed comparisons between the output of the GLAS processing algorithms and the validation measurements will be performed here at Goddard Space Flight Center by the GLAS atmospheric algorithm development team. Problems and deficiencies in algorithm performance will be identified and corrected. The improved algorithms will be tested on the GLAS data from as many correlative measurement sites as possible to insure their increased accuracy. After an initial, intensive validation period lasting 3 to 4 months, the processing algorithms will be replaced with improved versions and all of the GLAS data acquired to that point will be re-processed. About one year later, additional improvements to the algorithms will require a second re-processing of the data.

9 Future Research

The level I and II data products discussed in this document form the basis for future research activities and the generation of level III data products. In general, level III data products require a level of analysis which precludes them from being produced routinely and continuously as are the level I and II data products. Level III products may involve inputs from other sensors and external models. They often will require a careful screening of the data and more user interaction and checking of the algorithm output.

In terms of the atmospheric measurements to be provided by the GLAS instrument, the basic height parameters provided in Level II can be expected to be robust and not require much further research beyond the improvements that will come out of algorithm development and testing. There are some exceptions. An example of a level III product would be lifting condensation level (LCL), derived from the output of GLA08. The more difficult parameters to obtain accurately from the lidar data are the optical depth and extinction cross sections for aerosol and cloud. It is expected that the accuracy and applicability of these can be significantly increased through Level III products and post processing. The two areas requiring further work for this are the use of data other than the lidar profile signal and improvements in multiple scattering corrections.

For cloud analysis, a desirable input would be simultaneous IR radiance measurements. With IR radiance obtained in sufficiently close time with the lidar profile it is possible to solve for the vertical profiles of IR absorption cross section (Spinhirne et al., 1990). Simultaneous IR radiance values should be available for a large fraction of the GLAS observations. At the time of the mission there will be over 20 spectral imagers with thermal IR channels in orbit. Since GLAS has a precessing orbit, the GLAS measurements will be within the swath width of the MODIS imagers for about two months of the year for example. The combination of the GLAS data with IR data will be a research topic for level III processing. An additional improvement of the cloud retrieval from GLAS data alone may also be possible from research and modeling on using the molecular and surface signals under thin cloud layers to improve optical depth calculations. The most significant improvement for cloud retrieval will likely come from research on the best approach for the multiple scattering correction. To first order, work is needed to develop the best possible corrections tables based on geographic location, cloud height and thickness and cloud structure. Another approach to be studied is to possibly make use of the below ground multiple scattering tail that should be observed by the GLAS ranging channel for a direct measure of the multiple scatter factor leading to improvement of correction tables.

For aerosol optical thickness and extinction cross section, multiple scattering corrections are less of an issue. The largest uncertainties would result likely from the value of extinction to backscatter ratio that is applied for the retrievals. An important factor for improving the retrievals for data time observations is to make use of the 532 and 1064 nm solar background signals. From these data alone, over oceans an optical thickness for aerosol could be obtained directly in the manner that AVHRR data are now used. Future research is needed to model the best approach for incorporating the solar background signals with the lidar return profiles. In addition the GLAS aerosol profiles can be combined with many other sensor data and retrievals. One example would be with AVHRR and MODIS aerosol retrievals. Again the precessing orbit of GLAS will provide large amount of coincident data that can be used to improve extinction to backscatter look up

tables for nighttime and other non-coincident GLAS observations. An especially important combination will be GLAS aerosol profiles with TOMS aerosol retrievals. Currently TOMS data are applied to retrieve absorbing aerosol in the atmosphere, but an assumption on the height profile of the aerosol is needed. For the large amount of coincident data with TOMS expected from the full GLAS mission, future research will enable improvements in the TOMS and GLAS aerosol data results.

The level III products will be produced by the atmospheric lidar group headed by Dr. James Spinhirne. They will be done on a case by case basis as opposed to a continuous processing as are the level I and II products. It may be possible, after enough experience has been gained, to automate certain level III data products.

Another area of future research is the development of methods to correct for the multiple scattering induced errors for surface ranging.

10 References

Ackermann, J., 1998: The Extinction-to-Backscatter Ratio of Tropospheric Aerosol: A Numerical Study, *J. Atmos. Oceanic Technol.*, **15**, 1043-1050.

Ansmann, A., U. Wandinger, M. Riebesell, C. Weitkamp and W. Michaelis, 1992: Independent measurements of extinction and backscatter profiles in cirrus clouds by using a combined Raman elastic-backscatter lidar, *Appl. Opt.*, **31**, 7113-7131.

Ansmann, A., J. Bosenberg, G. Brogniez, S. Elouragini, P. Flamant, K. Klapheck, H. Linn, L. Menenger, W. Michaelis, M. Riebesell, C. Senff, P. Thro, U. Wandinger and C. Weitkamp, 1993: Lidar Network Observations of Cirrus Morphological and Scattering Properties during the International Cirrus Experiment 1989: The 18 October 1989 Case Study and Statistical Analysis, *J. Appl. Meteor.*, **32**, 1608-1622.

Boers, R, E. W. Eloranta and R. L. Coulter, 1984: Lidar observations of mixed layer dynamics: tests of parameterized entrainment models of mixed layer growth rate. J*. Clim. Appl. Meteor*, **23**, 247-266.

Boers, R. and E. W. Eloranta, 1986: Lidar measurements of the atmospheric entrainment zone and the potential temperature jump across the top of the mixed layer. *Bound. Layer Meteor*., **34,** 357-375.

Boers, R., S.H. Melfi and S.P. Palm, 1991: Cold Air outbreak during GALE: Lidar observations and modeling of boundary layer dynamics. *Mon. Wea. Rev*., **119**, 1132-1150.

Congeduti, F., J. DeLuisi, T. DeFoor, and L. Thomason, 1998: Optical extinction properties of volcanic stratospheric aerosol derived from ground-based lidar and Sun photometer measurements, *J. Geophys. Res*., **103**, 13893-13902.

Duda, D. P., J. D. Spinhirne and E. W. Eloranta, 1999: Atmospheric Multiple Scattering Effects on Altimetry. Part I: Calculation of Single Pulse Bias. Submitted February, 1999

Duda, D. P., J. D. Spinhirne and E. W. Eloranta, 1999: Atmospheric Multiple Scattering Effects on Altimetry. Part II: Cloud Climatology Analysis of Expected Seasonal and Interannual Surface Altitude Errors. Submitted February, 1999

Eloranta, E. W., R. E. Kuehn and R. E. Holz, "Cirrus Cloud Backscatter Phase Functions Measured with the University of Wisconsin High Spectral Resolution Lidar" 10th Conference on Atmospheric Radiation, preprint, AMS, Madison, Wisconsin, 28 June–2 July, 1999.

Elouragini, S., 1995: Useful algorithms to derive the optical properties of clouds from a backscatter lidar return, *J. Modern. Opt.*, **42**, 1439-1446

Elouragini, S. and P. H. Flamant, 1996: Iterative method to determine an averaged backscatter-to-extinction ratio in cirrus clouds, *Appl. Opt.*, **35**, 1512-1518.

Gobbi, G. P., 1995: Lidar estimation of stratospheric aerosol properties: Surface, volume, and extinction to backscatter ratio, *J. Geophys. Res.*, **100**, 11219-11235.

Grund, C. J. and E. W. Eloranta, 1990: The 27-28 October 1986 FIRE IFO Cirrus Case Study: Cloud Optical Properties Determined by High Spectral Resolution Lidar, *Mon. Wea. Rev.*, **118**, 2344-2355.

Grund, C.J. and E. W. Eloranta, 1991: The University of Wisconsin High Spectral Resolution Lidar, *Optical Engineering*, **30**, 6-12.

Hlavka, D. L., J. D. Spinhirne, and J. R. Campbell, 1998: "Aerosol Analysis Techniques and Results form Micro Pulse Lidar", 19th International Laser Radar Conference, Annapolis, MD, July 6 - 10, 1998.

IPCC, 1995: Climate Change 1994. *Cambridge U. Press*.

Macke, A., 1993: Scattering of light by polyhedral ice crystals, *Appl. Opt*., **32**, 2780-2788.

Macke, A., P. N. Francis, G. M. McFarquhar and S. Kinne, 1998: The role of particle shapes and size distributions in the single scattering properties of cirrus clouds, *J. of Atmos. Sci.*, **55**, 2874-2883.

Marenco, F., V. Santacesaria, A. F. Bais, D. Balis, A. di Sarra, A. Papayannis, and C. Zerefas, 1997: Optical properties of tropospheric aerosols determined by lidar and spectrophotometric measurements (Photochemical Activity and Solar Ultraviolet Radiation campaign), *Appl. Opt.*, **36**, 6875-6886.

McCormick, M. P., H. M. Steele, W Chu, and T. Swissler, 1982: Polar Stratospheric Cloud Sightings by SAM II. *J. Atmos. Sci*., **39**, 1387-1397.

McCormick, M. P., P. Hamill and U. Farrukh, 1985: Characteristics of Polar Stratospheric Clouds as observed by SAM II, SAGE, and Lidar, *J. Meteor. Soc. Japan***, 63**, 267-276.

McFarquhar, G. M. and A. J. Heymsfield, 1997: Parameterization of Tropical Cirrus Ice Crystal Size Distributions and Implications for Radiative Transfer: Results from CEPEX, *J. Atmos. Sci.*, **54**, 2187-2200.

Melfi, S.H., J.D. Spinhirne, S.H. Chou and S. Palm, 1985: Lidar observations of vertically organized convection in the planetary boundary layer over the ocean. J*. Clim. Appl. Meteor*., **24**, 806-821.

Mishchenko, M. I., Wielaard, and B. E. Carlson, 1997: T-matrix computations of zenith-enhanced lidar backscatter from horizontally oriented ice plates, *Geophys. Res. Lett*., **24**, 771-774.

Nicolas, F., Bissonnette, L. R., and P. H. Flamant, 1997: Lidar effective multiple-scattering coefficients in cirrus clouds, *Appl. Opt*., **36**, 3458-3468.

Palm, S.P. and J.D. Spinhirne, 1987: Optimization of boundary layer height retrieval. Laser and Optical Remote Sensing of the Atmosphere, Volume **18**, 63-66, and presented at conference.

Palm, S.P. and J. Spinhirne, 1998: The detection of Clouds, Aerosol and Marine Atmospheric Boundary Layer Characteristics from Simulated GLAS Data. The 19th International Laser Radar Conference, Annapolis, Md, July 6-10, 1998.

Palm, S. P., D. Hagan, G. Schwemmer and S.H. Melfi, 1998: Inference of Marine Atmospheric Boundary Layer Moisture and Temperature Structure using Airborne Lidar and Infrared Radiometer Data, J*. Appl. Meteor*., **37**, 308-324.

Pinnick, R. G., J. M. Rosen and D. J. Hofmann, 1976: Stratospheric Aerosol Measurements III: Optical Model Calculations, *J. Atmos. Sci*., **33,** 304-314.

Pinnick, R. G., S. G. Jennings, P. Chylek, C. Ham and W. T. Grandy, 1983: Backscatter and Extinction in Water Clouds. *J. Geophys. Res*, **88**, 6787-6796.

Platt, C. M. R., 1979: Remote Sounding of High Clouds: I. Calculation of Visible and Infrared Optical Properties from Lidar and Radiometer Measurements, *J. Appl. Meteor.*, **18**, 1130-1143.

Platt, C. M. R., Reynolds, D. W., Abshire, N. L., 1980: Satellite and lidar observations of the albedo, emittance, and optical depth of cirrus compared to model calculations*. Mon. Wea. Rev*., **108,** 195-204

Platt, C. M. R., 1981: Remote sounding of high clouds. Part III: Monte Carlo calculations of multiple-scattered lidar returns, *J. Atmos. Sci*., **38**, 156-167.

Russell, P. B., T. J. Swissler, M. P. McCormick, W. P. Chu, J. M. Livingston and T. J. Pepin, 1981: Satellite and Correlative Measurements of the Stratospheric Aerosol. I: An Optical Model for Data Conversions, *J. Atmos. Sci*., **38**, 1279-1294.

Spinhirne, J. D., J. A. Reagan, and B. M. Herman, 1980: Vertical Distribution of Aerosol Extinction Cross Section and Inference of Aerosol Imaginary Index in the Troposphere by Lidar Technique,

J. Appl. Meteor., **19,** 426-438.

Spinhirne, J. D., 1982: Lidar clear atmosphere multiple scattering dependence on receiver range, *Appl. Opt*., **21**, 2467-2468.

Spinhirne, J. D., R. Boers and W. D. Hart, 1989: Cloud Top Liquid Water from lidar Observations of Marine Stratocumulus. *J. Appl. Meteor*., **28**, 81-90.

Spinhirne, J. D. and W. D. Hart, 1990: Cirrus structure and radiative parameters from airborne lidar and spectral radiometer observations: the 28 October 1986 FIRE study. *Mon. Wea. Rev,* **118**, 2329-2343

Spinhirne, J. D., W. D. Hart, D. L. Hlavka, 1996: Cirrus infrared parameters and shortwave reflectance relations from observations, *J. of Atmos. Sci*., **53**, 1438-1458.

Spinhirne, J. D. and S. P. Palm, 1996: Space Based Atmospheric Measurements by GLAS. Advances in Atmospheric Remote Sensing with Lidar. Selected Papers of the 18th International Laser Radar Conference, Berlin Germany. 213-216.

Spinhirne, J. D., Campbell, J. R., Hlavka, D. L., Ferrare, R. A., Turner, D. D., and Flynn, C. J., "Aerosol Retrieval Comparison During the SGP Summer '98 IOP from Multiple Lidar Probing", Poster Abstract, Atmospheric Radiation Measurement (ARM) Science Team Meeting, San Antonio, Texas, March 22-26, 1999.

Starkov, A. V., and C. Flesia, 1998: Correction of spaceborne lidar signal for multiple scattering from high clouds, Proc. of the 19th International Laser Radar Conference, July 6-10, Annapolis, MD.

Wielicki, B. A., B. Barkstrom, E. Harrison, R. Lee, G. Smith, and J. Cooper, 1996: Clouds and the Earth's radiant energy system (CERES): An Earth observing system experiment*. Bull. Amer. Meteor. Soc*., **77**

Wiscombe, W., 1977: Mie scattering calculations: Advances in technique and fast, vector-speed computer codes. NCAR Tech. Note TN140+STR. (Edited and revised 1996, available at ftp://climate.gsfc.nasa.gov/pub/wiscombe/Single_Scatt/Mie_Code/NCARMieReport.pdf

11 Acronyms

ACE	Arctic Clouds Experiment
AEROCE	Aerosol/Ocean Chemistry Experiment
AERONET	Aerosol Robotic Network
AIRS	Atmospheric Infrared Sounder

ARM	Atmospheric Radiation Measurement Program
ARMCAS	Arctic Radiation Measurements in Column Atmosphere-surface System (beaufort Sea, Alaska, June 1995)
ASTEX	Atlantic Stratocumulus Transition Experiment (Azores, June 1992)
AVHRR	Advanced Very High Resolution Radiometer
AVRIS	Airborne Visible / Infrared Imaging Spectrometer
CALS	Cloud and Aerosol Lidar System
CAR	Cloud Absorption Radiometer
CEPEX	Central Equatorial Pacific Experiment
CRYSTAL	
DAAC	Distributed Active Archive Center
DEM	Digital Elevation Model
EAL	Elevated Aerosol Layer
EOS	Earth Observing System
EOSDIS	EOS Data and Information System
FIRE	First ISCCP Regional Experiment
GLAS	Geoscience Laser Altimeter System
GLOBE	Global Backscatter Experiment
HSRL	High Spectral Resolution Lidar
ISCCP	International Satellite Cloud Climatology Project
LITE	Lidar In-space Technology Experiment
MAS	MODIS Airborne Simulator
MAST	Monterey Area Ship Tracks Experiment (Monterey California, June 1994)
MODIS	Moderate Resolution Imaging Spectroradiometer

PBL	Planetary Boundary Layer
SUCCESS	Subsonic Aircraft Contrail and Cloud effects Special Study (April – May, 1996)
WINCE	Winter Cloud Experiment